

Ex LIBRIS
UNIVERSITATIS
ALBERTAENSIS





Digitized by the Internet Archive
in 2019 with funding from
University of Alberta Libraries

<https://archive.org/details/Kulatunga1993>

UNIVERSITY OF ALBERTA

RELEASE FORM

NAME OF AUTHOR : CUMERASIRI RAWEENDRA KULATUNGA

TITLE OF THESIS : EVALUATION OF ^{153}Sm -BCPDA CONJUGATES FOR
APPLICATIONS IN RADIOIMMUNOTHERAPY

DEGREE : DOCTOR OF PHILOSOPHY

YEAR THIS DEGREE GRANTED : FALL 1993

Permission is hereby granted to the University of Alberta to reproduce single copies of this thesis and to lend or sell such copies for private, scholarly or scientific research purposes only.

The author reserves all other publication and other rights in association with the copyright in the thesis, and except as hereinbefore provided neither the thesis nor any substantial portion thereof may be printed or otherwise reproduced in any material form whatever without the author's prior written permission.

10, DAKSHINARAMA ROAD,
MOUNT LAVINIA, SRI LANKA

DATE : 13-5-93

UNIVERSITY OF ALBERTA

EVALUATION OF ^{153}Sm -BCPDA CONJUGATES FOR APPLICATIONS IN
RADIOIMMUNOTHERAPY

BY

C. R. KULATUNGA



A Thesis submitted to the Faculty of Graduate Studies and Research
in partial fulfillment of the requirements for the degree of Doctor of
Philosophy.

IN

PHARMACEUTICAL SCIENCES (BIONUCLEONICS)

FACULTY OF PHARMACY AND PHARMACEUTICAL SCIENCES

EDMONTON, ALBERTA

FALL 1993

UNIVERSITY OF ALBERTA
FACULTY OF GRADUATE STUDIES AND RESEARCH

The undersigned certify that they have read, and recommend to the Faculty of Graduate Studies and Research for acceptance, a thesis entitled EVALUATION OF ^{153}Sm -BCPDA CONJUGATES FOR APPLICATIONS IN RADIOIMMUNOTHERAPY submitted by C. R. KULATUNGA in partial fulfillment of the requirements for the degree of DOCTOR OF PHILOSOPHY in PHARMACEUTICAL SCIENCES (BIONUCLEONICS).

ABSTRACT

The goal of the present study was to radiolabel a monoclonal antibody (MAb B43) with ^{153}Sm via a bifunctional chelate 4,7-bis(chlorosulfohenyl)-1,10-phenanthroline-2,9-dicarboxylic acid (BCPDA), and to assess its radiochemical, biochemical, and biological properties with a view to utilizing this radiolabeled conjugate as a radioimmunotherapeutic agent.

BCPDA was synthesized according to the procedure given in the literature with some modifications. The stability constant of the Sm-BCPDA complex was determined fluorometrically to be 4.4×10^6 L/mole. Complexation yields of Sm-BCPDA and Sm-Diethylenetriaminepentaacetic acid (Sm-DTPA) were determined under different experimental conditions by cation exchange chromatography utilizing ^{153}Sm .

BCPDA was first conjugated to a model protein, human serum albumin (HSA) under various conditions. These conjugates which contained different number of chelates per mole of protein were purified by size exclusion chromatography, and their radiolabeling efficiencies were determined to be greater than 90% by cation exchange chromatography. BCPDA was next conjugated to the monoclonal antibody B-43. Radiolabeling efficiencies of these conjugates, as measured by cellulose TLC and cation exchange chromatography, were found to be close to 80%. It was also

determined by electrophoresis that the MAb sample contained a small protein fragment.

In vitro transchelation studies involving hydroxyapatite and HSA, indicated that BCPDA was unable to compete with hydroxyapatite for Sm, and that, at certain concentrations, BCPDA appears to interact with HSA in a non-covalent manner.

A biodistribution study of a Sm labeled MAB-BCPDA conjugate in mice revealed that Sm had transchelated or transcomplexed to some unknown component in the liver directly or indirectly within 6 hours.

ACKNOWLEDGEMENTS

I wish to thank my supervisor Dr. A. Noujaim and my co-supervisors Drs. M.R.Suresh and T.R.Sykes, for their guidance and support throughout the course of this work.

I would like to express my sincere appreciation to Drs. B.Kratochvil, J.A.Plambeck, R.G.Cavell, N.Dovich, J.Mercer, K.Noguchi F.Pasutto, Mr. J.Diakur, and Mr. D.Whyte for their help on certain aspects of this work. Their interest and helpful discussions are truly appreciated.

Finally, I am extremely grateful to my parents and thank them for their assistance and sacrifices that they have made for many years on my behalf.

(1.0) INTRODUCTION.....	1
(2.0) SURVEY OF THE LITERATURE.....	4
(2.1) Selection of Radioisotopes for Therapy.....	4
(2.1.1) Prospective Radionuclides	6
(2.1.2) Dosimetric Considerations.....	8
(2.1.3) Production of Therapeutic Radionuclides.....	13
(2.2) Radiolabeling Monoclonal Antibodies.....	14
(2.2.1) Radiochemical Studies.....	14
(2.2.2) Biochemical Studies.....	17
(2.2.3) Effect of Chelate to Antibody Ratio on Radiochemical Yield and Immunoreactivity	24
(2.2.4) Design Criteria of Chelate Ligands.....	24
(2.2.5) Some Examples of Bifunctional Chelating Agents Employed in Radioimmunotherapy.....	26
(2.3) In Vivo Stability of Metal Chelate Complexes.....	36
(2.4) Factors Affecting Antibody Targeting.....	37
(2.4.1) Physiological Factors.....	37

(2.4.2) Pharmacological Factors.....	37
(2.4.3) Immunological Factors.....	38
(2.5) Techniques of Antibody Targeting.....	38
(2.5.1) Pretargeting Techniques	38
(2.5.1 a) Bispecific Antibodies	38
(2.5.1.b) The Avidin-Biotin Delivery System.....	39
(2.5.2) Administration of Antibody Fragments.....	41
(2.5.3) Regional Injection of Radiolabeled Antibodies....	41
(2.5.4) Use of Chimeric Antibodies.....	42
(2.5.5) Site Specific Modification of Antibodies.....	44
(2.6) Properties of Samarium (Sm)	45
(2.6.1) Nuclear Properties of ^{153}Sm	45
(2.6.2) Chemical Properties.....	46
(2.6.3) Biological properties of Sm.....	48
(2.6.4) Radioimmunotherapeutic Studies of ^{153}Sm	49
(3.0) EXPERIMENTAL METHODS.....	50
(3.1) Synthesis of BCPDA.....	50

(3.2) Fluorometric Studies of BCPDA.....	54
(3.2.1) Determination of the Conditional Stability Constant of Hydrolysed BCPDA-Sm Complex	54
(3.3) Production of ^{153}Sm	55
(3.3.1) Low Specific Activity ^{153}Sm	55
(3.3.2) High Specific Activity ^{153}Sm	56
(3.4) Preparation of Sm Complexes.....	57
(3.5) Cation Exchange Chromatography.....	57
(3.6) Complexation of BCPDA as a Function of pH	58
(3.7) Determination of the Rate of Hydrolysis of BCPDA.....	58
(3.8) Size Exclusion Chromatography.....	59
(3.9) Thin Layer Chromatographic (TLC) Analysis of Sm^{3+} Complexes.....	60
(3.10) Conjugation of BCPDA to HSA	60
(3.11) Determination of the Degree of Conjugation.....	61
(3.12) Radiolabeling HSA-BCPDA Conjugates with ^{153}Sm	62
(3.13) Preparation of Monoclonal Antibody B43 (MAb B43) BCPDA Conjugates.....	63

(3.14) HPLC Analysis of MAb B43 Conjugates	63
(3.15) Determination of the Factors Affecting the Formation of Aggregates.....	64
(3.16) Iodination of MAb B43	65
(3.17) Purification of BCPDA-MAb B43 Conjugates by S-300 Chromatography	66
(3.18) Radioimmunoassay of Antibody Conjugates.....	67
(3.19) Radiolabeling MAb-BCPDA Conjugates.....	68
(3.20) Determination of Non-Specific Binding of MAb B43 to Teflon Vials.....	68
(3.21) Determination of Non-Specific Binding of ^{153}Sm to Teflon Vials.....	69
(3.22) Analysis of Antibodies by Electrophoresis.....	69
(3.22 a) Preparation of the Molecular Weight Standards.....	70
(3.22 b) Preparation of the Test Protein Samples	70
(3.23) Determination of Percent Non-Specific Binding of ^{153}Sm to MAb in the Presence of BCPDA.....	71
(3.24) Transchelation Studies.....	72

(3.24 a) The Effect of HSA	72
(3.24 b) The Effect of Hydroxyapatite	73
(3.24 c) MAb-BCPDA- ¹⁵³ Sm versus Teflon Vial.....	73
(3.25) Biodistribution Studies in Mice	74
(3.26) Counting of Radiolabeled Compounds.....	75
(3.27) Experimental Statistics.....	75
(4.0) RESULTS AND DISCUSSION.....	76
(4.1) Synthesis of BCPDA.....	76
(4.1.1) Preparations #1-#4	76
(4.1.2) TLC Studies of BCPDA (Hydrolysed)	86
(4.2) Fluorometric Studies of BCPDA and Sm-BCPDA Complexes.....	87
(4.2.1) Determination of the Conditional Stability Constant (K') of a 1 : 1 Sm-BCPDA (hydrolysed) Complex at pH 7.5.....	88
(4.2.2) Some Theoretical Calculations Based on the K _{stab.} of Sm-BCPDA.....	96
(4.3) Complexation Studies of Hydrolysed BCPDA with Sm ³⁺	98

(4.3.1) The Effect of pH on the % Complexation of BCPDA and Sm.....	103
(4.3.2) Radionuclidic Purity of Low and High Specific Activity Sm.....	104
(4.4) Rate of Hydrolysis of BCPDA.....	105
(4.5) Conjugation of BCPDA to HSA.....	106
(4.5.1) Radiolabeling HSA-BCPDA Conjugates.....	109
(4.6) Conjugation of MAb B43 to BCPDA.....	111
(4.6.1) Immunoreactivity of G-50 Purified Conjugates.....	114
(4.6.2) Factors Affecting the Percentage of Aggregates	116
(4.6.3) Purification of MAb-BCPDA Conjugates By Sephacryl S-300 Size Exclusion Chromatography	120
(4.6.4) Determination of the Degree of Conjugation of BCPDA to MAb B43	122
(4.6.5) Immunoreactivity of MAb B43-BCPDA Conjugates Purified by S-300 Chromatography ..	126

(4.6.6) Radiolabeling MAb-BCPDA Conjugates with ^{153}Sm	127
(4.6.7) Non-Specific Binding of Sm to MAb in the Presence of BCPDA	135
(4.7) Transchelation Experiments.....	143
(4.7.1) Sm-BCPDA and Sm-DTPA complexes versus HSA	143
(4.7.2) Interaction of Sm Complexes with Hydroxyapatite.	148
(4.8) Biodistribution Studies in Mice.....	151
(5.0) SUMMARY OF RESULTS.....	153
(6.0) CONCLUSION	156
REFERENCES.....	157
APPENDIX.....	167

Table 1	Equilibrium Absorbed Dose Constants.....	9
Table 2	Maximum Computed Specific Activities.....	11
Table 3	Absorbed Dose Calculations Utilizing Basic Model Assumptions (23).....	12
Table 4	Absorbed Dose Calculations.....	13
Table 5	A Summary of Radionuclide Production Methods.....	14
Table 6	Examples of various Bifunctional Chelates used For Radioimmunosintigraphy and Therapy.....	28
Table 7	Conjugation of HSA to BCPDA.....	61
Table 8	Conjugation of BCPDA to MAb B43	66
Table 9	Elemental Analysis of Compound (4).....	78
Table 10	Elemental Analysis of Compound (4) (Preparation #2).....	80
Table 11	Elemental analysis of Bathocuproine (Compound 1).....	81
Table 12	Elemental Analysis Of Compound (2)	82
Table 13	Elemental Analysis of Compound (3).....	82
Table 14	Elemental Analysis of Compound (3) Before Purification.....	84

Table 15 Elemental Analysis of Compound (3) After
 Purification.....85

Table 16 Elemental Analysis of Compound (4) (Preparation # 5)85

Table 17 TLC Results of Hydrolysed BCPDA.....86

Table 18 Relative Intensities of Uncomplexed BCPDA in Sm-
 BCPDA Mixtures90

Table 19 Calibration of [BCPDA] Vs. Relative Intensity.....90

Table 20 Complexation Yields of BCPDA and Sm.....101

Table 21 Complexation Yields of DTPA and Sm.....103

Table 22 pH versus % Complexation.....104

Table 23 Rate of Hydrolysis of BCPDA105

Table 24 Degree of Conjugation HSA : BCPDA.....108

Table 25 (a) Labeling of a Conjugate With 9 moles of
 BCPDA/Mole of HSA.....110

Table 25 (b) Labeling of a Conjugate With 4.5 moles of
 BCPDA/Mole of HSA.....110

Table 26 Percent Aggregates of Conjugates Purified by G-50.....113

Table 27 Immunoreactivity MAb B43 Conjugates Purified By
 G-50.....115

Table 28	Effect of Conjugation Ratio on the Crosslinking of HSA.....	117
Table 29	Effect of Conjugation Ratio on the Crosslinking of Human IgG.....	117
Table 30	Molar Absorptivity MAb B43	124
Table 31	IC-50 Values of the Purified Conjugates.....	127
Table 32	Labeling Efficiencies of Conjugates with Sm at 16 hours in Glass Vials.....	128
Table 33	Labeling Efficiencies of Conjugates at 16 hours With Sm in Teflon Vials.....	129
Table 34	Labeling Efficiencies Obtained for a 3:1 Conjugate in One Hour with Sm.....	131
Table 35	The Effect of Dilution On the Rate of Dissociation of the Radiolabeled MAb Conjugate	132
Table 36	Concentration of Iodinated MAb Versus % activity Bound to Vial.....	133
Table 37	Concentration of Sm Versus % activity Bound to Vial.....	134
Table 38	Analysis of a Solution Mixture of Sm, Chelate, and MAb B43 by G-50 Chromatography.....	136

Table 39 Analysis of a Solution Mixture of Sm, DTPA, and MAb
 B43 by Cellulose TLC..... 138

Table 40 Determination of Non Specific Binding of Sm With
 Purified Antibody..... 142

Table 41 Transchelation of Sm from Sm-BCPDA Complex to
 HSA..... 145

Table 42 Transchelation of Sm from Sm-DTPA Complex to HSA 146

Table 43 Transchelation of Sm from Sm-BCPDA Complex to
 Hydroxyapatite..... 149

Table 44 Transchelation of Sm from Sm-DTPA Complex to
 Hydroxyapatite..... 150

Table 45 Biodistribution Studies of MAb B43-BCPDA-Sm..... 152

Figure 1 Examples of Various Macrocyclic Chelators used for
 Radiolabeling Antibodies.....32

Figure 2 N₂S₂ Ligands35

Figure 3 N₃S Ligands.....35

Figure 4 N₂S₄ Ligands.....35

Figure 5 Chimeric Antibody43

Figure 6 Synthesis of BCPDA.....51

Figure 7 A Plot of [BCPDA] Vs. Relative Intensity.....91

Figure 8 Examples of Ligands Similar to BCPDA.....94

Figure 9 Theoretical Complexations of Sm and BCPDA97

Figure 10 Theoretical Percentages of Metal Transchelated to
 HSA99

Figure 11 A HPLC Chromatogram of MAb B43.....112

Figure 12 A HPLC Chromatogram of MAb-BCPDA Conjugate
 (1 : 1)112

Figure 13 A HPLC Chromatogram of IgG.....118

Figure 14 A HPLC Chromatogram of IgG and BCPDA at a 1 : 1
 Mole Ratio.....119

Figure 15	A HPLC Chromatogram of IgG and BCPDA at a 1 : 3 Mole Ratio.....	119
Figure 16	A S-300 Chromatogram of MAb-BCPDA Conjugate.....	122
Figure 17	A G-50 Chromatogram of MAb B43.....	137
Figure 18	A HPLC Chromatogram of MAb B43.....	138
Figure 19	Gel Electrophoresis (SDS-PAGE) Of Unpurified MAb B43.....	140
Figure 20	Gel Electrophoresis (SDS-PAGE) of Unpurified and Purified MAb B43.....	141

ABBREVIATIONS

(1) BCPDA	4,7-bis-(chlorosulfophenyl)-1,10-phenanthroline-2,9-dicarboxylic acid
(2) DOTA	1,4,7,10-tetraazacyclododecane-N,N',N'',N''', -tetraacetic acid
(3) DTPA	Diethylenetriaminepentaacetic acid
(4) EDTA	Ethylenediaminetetraacetic acid
(5) EDTMP	Ethylenediaminetetramethylenephosphonic acid
(6) Fab	Fragment antigen binding
(7) F _C	Fragment crystalline
(8) HAMA	Human antimurine antibodies
(9) HSA	Human serum albumin
(10) IgG	Immunoglobulin G
(11) LET	Linear energy transfer
(12) MT	Metallothionein
(13) NP	Non penetrating
(14) NT	Non target
(15) P	Penetrating
(16) RBE	Relative biologic effectiveness
(17) T	Target
(18) TETA	1,4,8,11-tetraazacyclotetradecane-N,N',N'',N'''-tetraacetic acid
(19) Tris	Tris(hydroxymethyl)aminomethane

(20) ПТНА

Triethylenetetraaminehexaacetic acid

(1.0) INTRODUCTION

Radiolabeled monoclonal antibodies are currently being investigated as potential radiopharmaceuticals for the diagnosis and treatment of cancer and other diseases such as cardiovascular dysfunctions. The three major components that constitute the process of radioimmunotherapy of cancer are monoclonal antibodies, radionuclides, and bifunctional chelates. Bifunctional chelates are compounds that have chelating groups containing two or more electron donating atoms that can coordinate to metal ions, and also organic functional groups that can react with specific functional groups of the protein. To obtain an optimum response from the above process one has to select the most appropriate item from each component and combine them under the most suitable conditions that are practically possible to form the radionuclide-antibody complex. The achievement of this goal depends on the scientific developments made in the areas of chemistry, bionucleonics, and immunology.

The bifunctional chelate acts as the link between the radionuclide and the monoclonal antibody. Techniques utilizing bifunctional chelates are most useful primarily due to the wider choice of radionuclides that can be employed, and the flexibility associated with the selection of methods of radiolabeling. Two important factors are to be considered with regard to the design of bifunctional chelates. (1) The functional group reacting with the antibody, and (2) the chelating groups forming the coordination

complex with the radiometal. This is in order to maintain maximum stability of the antibody-radionuclide complex and the biological activity of the antibody. The degree of conjugation between the antibody and the chelate is an important parameter to be considered. It has been observed that the biological activity of the antibody decreases, as the degree of conjugation increases (1).

A condition that is necessary for the radioisotope to be an effective therapeutic agent is that the tumor cells should be within the range of action of the beta (β^-) emitter. The selection of a radioisotope also depends on its physical/chemical properties such as the physical half life, energy of the beta particle, specific activity, the stability of the metal-ligand bond and on the biological properties such as the rate of uptake and clearance of the metal antibody complex. A knowledge of these properties could ensure the preparation of a radionuclide-antibody complex that would permit adequate accumulation at the tumor site in order for the radionuclide to deliver the maximum radiation dose. One of the major problems of utilizing radiolabeled antibodies for tumor therapy is the *in vivo* stability of the metal-ligand complex. Since some metals have greater affinities for serum proteins and other intracellular proteins than for the chelating group on the antibody, ligand replacement or transchelation reactions can occur *in vivo* resulting in the accumulation of the radionuclide in the liver and bone. The major advantage of using monoclonal antibodies as the mode of delivery of radioisotopes to the tumor site is that they can

be produced (1) : (a) in mass scale, (b) with high purity, (c) reproducibly and (d) as a homogeneous preparation.

The major objectives of our research programme were to (a) synthesise the bifunctional chelate, 4,7-bis-(chlorosulphophenyl)-1,10-phenanthroline-2,9-dicarboxylic acid (BCPDA) (2), (b) determine the stability of the Sm-BCPDA complex (fluorometrically), (c) conjugate this chelate to a model protein such as human serum albumin (HSA) and ultimately to a monoclonal antibody (MAb B43), (d) study the radiochemical properties of these conjugates, and (e) evaluate the biodistribution of the radiolabeled MAb B43 conjugate in mice with a view to utilizing ^{153}Sm labeled antibodies in radioimmunotherapy.

Since ^{153}Sm has not been extensively used as a radioimmunotherapeutic agent, relative to some other radioimmunotherapeutic agents such as ^{90}Y and ^{131}I , we decided to label MAb B43, an antibody that was readily available, via BCPDA. BCPDA has been previously utilised only in fluoroimmunoassays in the form of an Eu complex.

(2.0) SURVEY OF THE LITERATURE

(2.1) Selection of Radioisotopes for Therapy

When one contemplates the use of a radionuclide for radioimmunotherapy, the following factors have to be considered.

(a) The location of the nuclide with respect to the target. For example, whether the localization of the nuclide is outside the target cells or on the surface or is internalized (3).

(b) Degree of linear energy transfer (LET) and the relative biologic effectiveness (RBE). In this regard alpha (α) radiation has higher LET and RBE than beta radiation (Ref.4, p119). In fact, RBE of alpha particles is about 10 times greater than that of beta radiation. RBE is a relative measure of biological effectiveness of a specific type of a radiation in comparison to X- rays or gamma rays. On the other hand LET can be defined as the average energy released per unit length to the medium by the particulate radiation as it travels along its track (5). LET depends on the charge and velocity of the particle as well as on the density of the medium in which it travels. The larger the charge and lower the velocity of the particle, the greater is the LET. Since the alpha particle has a charge of +2 and a relatively low velocity as compared to a beta particle, due to its high mass it would have a larger LET than a beta particle, which has a high velocity and low charge (Ref.4, p119). The significance of LET

in radioimmunotherapy can be explained as follows. As the LET of a specific type of radiation increases, the latter's lethality also increases (Ref.4, p119).

(c) The physical half life of the radioisotope and its relationship to the pharmacokinetics of the antibody *in vivo* (6). That is if the half life is too short, most of the radioactivity would be lost when maximum antibody uptake by the tumor has occurred. On the other hand too long a half life would result in the exposure of normal tissues to unnecessary radiation.

(d) Specific activity of the radioisotope. Specific activity can be defined as the activity per milligram or millimole of the substance used. The specific activity of the isotope depends mainly on the method of production. Isotopes produced by a (n,γ) reaction normally have low specific activity due to the fact that the target material is not separated from the radioisotope product because they are chemically identical. In contrast to this method of production, accelerator or generator produced isotopes can generally be separated from the parent isotope since they have different chemical properties, and hence high specific activity is obtained. The major factor that could reduce the maximum achievable specific activity of these nuclides is the percent impurities contained in the target material, or introduced during the chemical separation (6).

(e) The stability of the metal ligand complex. This topic will be discussed in greater detail in section.(2.2.4).

(f) The method of labeling the antibodies with the radioisotope is another important consideration. One has to investigate the feasibility of direct labeling and indirect labeling techniques (7). In the same context it is necessary to determine whether any form of chemical pretreatment of the isotope is necessary, prior to labeling. The overall stability of the metal antibody attachment may depend to a large extent on the labeling techniques employed.

(g) The final factor that has to be considered in the selection of a radionuclide is the availability and the cost of production of the nuclide (6).

(2.1.1) Prospective Radionuclides

There are numerous methods in the literature for the classification of radionuclides used in therapy. I will present the classification of Humm (8) which is based on the range of the radiation emitted by the respective nuclides.

" (1) Alpha (α)-emitters

(2) Low range beta (β^-) emitters that have a mean range
< 200 μ m

(3) Medium range beta emitters that have a mean range of
200 μ m to 1mm

(4) High range beta emitters with a mean range >1mm".

Examples of radionuclides from each of the above categories will now be discussed.

(1) Alpha (α)-emitters : Some examples are (a) ^{211}At (b) ^{212}Bi . The main advantages of these nuclides are their high LET (80 $\text{KeV}/\mu\text{m}$) and low penetrability (9). Although the potential utility of ^{211}At as a radiotherapeutic agent is currently being studied, ^{212}Bi has less promise of being used due to its very short half life (1 hour). The disadvantage of α -emitters is that target cells need to be labeled for effective therapy (3).

(2) Low range beta emitters. Examples of this category are ^{33}P , ^{121}Sn , ^{177}Lu , ^{191}Os and ^{199}Au (8). Of these nuclides only Au-199 can be produced carrier-free. It also emits a gamma ray which is suitable for imaging.

(3) Medium range beta emitters. Some common radionuclides that can be included in this class are ^{47}Sc , ^{67}Cu , ^{109}Pd , ^{131}I and ^{186}Re (8). Of these ^{131}I is the most frequently used nuclide in radioimmunotherapy (10-13). The main disadvantage of ^{131}I is the dehalogenation of the protein *in vivo* (14).

(4) Long range beta emitters. Potential isotopes are ^{32}P , ^{90}Y , and ^{188}Re (8,15). Of these nuclides ^{90}Y , a pure β -emitter, is currently the most extensively studied isotope for radioimmunotherapy (16-20).

(2.1.2) Dosimetric Considerations.

What is important in radioimmunotherapy is the quantitation of the radiation dose to the tumor and to the normal tissues. The objective is to ensure that an adequate lethal dose of radiation is delivered to the tumor during therapy and the dose received by normal tissues is minimal. Although radioimmunotherapy has been performed for a number of years, most of the antibodies lack the required amount of specificity and stability between the antibody and the isotope to deliver an adequate amount of dose to the target site (21). This results in inaccurate and complex dosimetric calculations. Another complication is the absence of sufficient data about the localization of radiolabeled antibodies in tumors.

Dosimetric considerations generally involve (a) an estimate of the required lethal dose, (b) dose received by the normal tissues and (c) therapeutic effects of various radioisotopes.

Absorbed dose (D) can be defined as follows(4,p109)

$$D = \frac{A \times 1.44 \times T_e \times \sum \Delta_i \phi_i}{m} \text{ rads, where}$$

$$\phi_i = \text{absorbed fraction} = \frac{\text{energy absorbed}}{\text{energy emitted by source}}$$

$$\Delta_i = \text{equilibrium absorbed dose constant of } i \text{ type of radiation}$$

$$= 2.13 \times \text{fraction of quanta emitted per disintegration} \times \text{energy of the emitted quanta} = \text{g-rad} / \mu\text{Ci-hr.}$$

A = activity in μCi , T_e = effective half life in hrs
 m = mass of organ in grams.

The equilibrium absorbed dose constant can be used as a first approximation to compare the suitability of radionuclides for radioimmunotherapy, if all other factors are assumed to be equal for these nuclides. For example, if a monoclonal antibody is labeled separately with different β^- emitting nuclides, since $\phi=1$ and if one assumes they have similar LET values, *in vivo* stabilities and biological properties, the nuclide with the highest Δ_i would be the obvious candidate to be selected. Δ_i values of some nuclides used in radioimmunotherapy are given in the following Table 1 (22).

Table 1 Equilibrium Absorbed Dose Constants

RADIONUCLIDE	DECAY MODE	g-rad $\mu\text{Ci}^{-1} \text{ h}^{-1}$
I-131	5 betas	0.39
Y-90	1 beta	1.99
Re-188	7 betas	1.63
At-211	alpha	5.21
Bi-212	alpha	3.25
^{153}Sm	3 betas	0.56

The factor that is as important as the total absorbed dose, is

the dose rate (21). As stated earlier, even though one needs to know the total dose for the treatment, the time in which this dose is supplied will determine the effectiveness of the therapy. This is due to the fact that if sufficient time is allowed for the repair mechanisms in tumor cells to proceed, it would counteract the damage caused to it by the radiation.

If one examines the relationship between the specific activity and the physical half life $T_{1/2}$ (physical) of a radioisotope it is quite apparent that the shorter the $T_{1/2}$ (physical) is, the higher is the maximum theoretical specific activity. One then can conclude that under these conditions, the nuclide with the higher specific activity would deliver a higher dose rate if all other properties of the nuclides are assumed to be similar. The favourable influence of a high dose rate on radiotherapy could be offset by a relatively short biological half life of the radiolabeled antibody. Maximum theoretical specific activities of various radionuclides commonly used in radioimmunotherapy are given in the following Table 2 (23).

Table 2 Maximum Computed Specific Activities

NUCLIDE	GBq/mM
^{67}Cu	1.99×10^6
^{90}Y	1.82×10^6
^{131}I	6.03×10^5
^{153}Sm	2.48×10^6

Wessels and Rogus (23) have reported theoretical absorbed dose values in various organs for a number of radionuclides. They have made the following assumptions in the computation of these values. A radiolabeled antibody with an activity of 3.7×10^9 Bq was injected into a 70 Kg patient who has a 500g solid tumor in a 1833g normal liver. The total body is considered to be the "non target organ". "The time-dependent averaged target-to-non-target uptake ratios (T/NT) have been idealized to be 3, 5, 8 and 10 for post-injection time intervals 0-12, 12-24, 24-48, and 48- ∞ hrs respectively" (23). Additional details and assumptions on which these calculations were made are listed in reference (23). Tables (3) and (4) attempt to depict the effectiveness of a number of radionuclides in radioimmunotherapy by the comparison of various dose related parameters calculated by the above authors based on the above mentioned assumptions. Dose ratio equals tumor dose/whole body dose. One important factor that is normally

considered in the selection of a radionuclide is the ratio of non-penetrating to penetrating radiation. It is quite apparent that ^{90}Y is far superior to other nuclides listed in this regard.

Table 3 Absorbed Dose Calculations Utilizing Basic Model
Assumptions (23)

NUCLIDE	DOSE RATIO	NP/P
Cu-67	7.8	1.41
Y-90	8.5	>1000
I-131	6.3	0.56
Re-186	8.5	17.2
At-211	4.0	152

NP/P=non penetrating/penetrating

Table 4 (23) shows the same dose related parameters calculated for the different nuclides as before but with an additional consideration in that these values are calculated for 1 nMole of antibody with 1 label per mole of antibody. In this instance ^{90}Y , due to its higher specific activity and a high % yield of β^- delivers a much higher dose than for example, ^{186}Re . Similarly ^{211}At gives a higher dose than (even higher than ^{90}Y) ^{186}Re . These

values are very helpful in determining the optimum number of labels needed for efficient therapy without any significant loss of immunoreactivity of the antibody.

Table 4 Absorbed Dose Calculations

Nuclide	Dose Tumor (CGy)	Dose Whole Body (CGy)
Cu-67	160	21
Y-90	810	98
I-131	120	19
Re-186	290	34
At-211	2900	750

(2.1.3) Production of Therapeutic Radionuclides

A brief summary of production methods of therapeutic radionuclides is given in Table 5.

Table 5 A Summary of Radionuclide Production Methods

Type of Radionuclide	Radionuclide	A Typical Method of Production	Reference
Alpha emitter	^{211}At	$^{209}\text{Bi}(\alpha, 2n)^{211}\text{At}$	24
Alpha emitter	^{212}Bi	$^{228}\text{Th}/^{212}\text{Bi}$ generator	24
Beta emitter	^{188}Re	$^{188}\text{W}/^{188}\text{Re}$ generator	6, 24
Beta emitter	^{90}Y	$^{90}\text{Sr}/^{90}\text{Y}$ generator	6
Beta emitter	^{67}Cu	$^{68}\text{Zn}(p, 2p)^{67}\text{Cu}$ accelerator	6
Beta emitter	^{131}I	$\text{U}(n, f)^{131}\text{I}$	6
Beta emitter	^{153}Sm	$^{152}\text{Sm}(n, \gamma)^{153}\text{Sm}$	6
Beta emitter	^{109}Pd	$^{108}\text{Pd}(n, \gamma)^{109}\text{Pd}$	6

(2.2) Radiolabeling Monoclonal Antibodies

(2.2.1) Radiochemical Studies

There are basically 2 methods of radiolabeling antibodies. They

are the indirect and direct methods, where the antibody is labeled with or without a bifunctional chelate, respectively.

(a) Direct Labeling; The only examples of radioisotopes that have been observed to be chemically suitable and utilized mostly for direct labeling of antibodies are the isotopes used for diagnostic purposes such as ^{99m}Tc , radioiodines and to a lesser extent the rhenium isotope, ^{186}Re (7,25). The chemical pretreatment of isotopes to the forms required for direct labeling may damage the antibody if performed in the presence of such an antibody. Some of these pretreatment methods used, for example in the direct labeling of Tc to thiol groups of antibodies, can be summarised as follows (7). Since Tc in the +7 oxidation state does not bind to proteins, it is first reduced to a lower oxidation state before labeling. Several reducing agents such as stannous ions, electrolytic methods, and sodium azide/conc.HCl have been used for this purpose (7). In order to improve this process of labeling, the disulfide bonds of the antibody are also reduced to the sulphydryl groups by dithiothreitol (DTT) or by ascorbic acid (7). F(ab')_2 fragments have been reduced by stannous ions (pretinning) prior to labeling with Tc(7). A disadvantage of the direct labeling method is that most often the metal-protein bond formed may not be very stable (26). Therefore due to the above limitations direct labeling of proteins generally results in a narrow choice of isotopes.

(b) Indirect Labeling. This entails the use of bifunctional

chelates and provides the user with a wide choice of radioisotopes.(27).

The two main strategies employed during indirect labeling can be described as follows.

(a) Initially the metal is allowed to complex with the bifunctional chelate and then the metal chelate complex is conjugated to the protein. Normally the concentration of chelate is in excess of the metal concentration in order to complex most of the radiometal. The advantages of this method are that it prevents non-specific binding of metal to the antibody. Also if chemical pretreatment of the metal is needed for complexation, the pretreated metal can first be reacted with the chelate and purified, before the conjugation reaction with the protein and hence avoid the possibility of damaging the antibody. The disadvantage of this method is that the purification procedures may involve considerable amount of time which may lead to a loss in specific activity. Additionally, if the functional group on the chelate which is used in the conjugation reaction with the protein is unstable in an aqueous medium, it could lose its reactivity towards the protein during the chelating step.

(b) In situations where no such chemical pretreatment of the radioisotope is needed, the preferred strategy of labeling antibodies is as follows. During the first stage, the protein is allowed to react with the chelate to form the stable antibody-chelate conjugate. The

second step involves the reaction of the metal ion with the chelate. In this method too, the concentration of the conjugated chelate is in excess of the added metal ion concentration. In this procedure the chemical reaction between the protein and the chelate is separate from the labeling step. The protein chelate conjugate can first be synthesized purified and characterized. The metal ion could then be introduced just prior to using the antibody. The antibody-metal complex thus formed, is generally stable (27, 28).

In either strategy, the chelates should possess the following properties (29) : (1) their binding should not influence the specificity or the affinity of the antibody to the tumor, (2) they should not affect the rate of metabolism or the biodistribution of the antibody, (3) the metal-chelate bond should be strong in order to prevent the dissociation of the metal from the antibody chelate complex, and (4) it should facilitate the clearance of the radiometal once the metal antibody complex has been catabolized.

(2.2.2) Biochemical Studies

(a)Conjugation of Bifunctional Chelates to Antibodies

The linking arm of the bifunctional chelate will specify the group of the protein that it will react with (1). The reaction between a chelate and a protein depends primarily on the following: (30,

Ref.31, p10-14):

(1) Nucleophilicity of the protein functional group under consideration. Normally conjugation reactions are nucleophilic, where the protein functional group is the nucleophile that attacks the chelate functional group, that results in the displacement of a leaving group. Therefore, the higher the nucleophilicity of the protein group and the ease of displacement of the leaving group, the greater is the rate of the conjugation reaction.

(2) pH of the medium. The nucleophilicity depends on the extent of protonation of the nucleophile, which in turn is a function of the pK_a of the nucleophile. As the pH of the medium is increased to a value above its pK_a , an increasing amount of the nucleophile will be in the free or the deprotonated form. This will result in an increase in the nucleophilicity of the group.

(3) Steric hindrance The specified functional group of the protein reacting with the chelate may be affected by the steric hindrance of other groups in the vicinity.

The three most common functional groups (30, Ref.31, p30-40) of a protein that are utilised in conjugation reactions are : (1) amino groups ($-NH_2$) of lysine, (2) carboxyl groups ($-COOH$) of glutamic and aspartic acids, and (3) thiol groups ($-SH$) of cysteine.

Bifunctional chelates that have been synthesized with specific groups, designed to react selectively with each of the above

functional groups are described as follows (30, Ref.31, p30-40).

(1) Groups specific to thiols.

The thiolate anion is considered to be the most reactive group of a protein, and has the ability to react very rapidly and selectively with certain functional groups, more than any other group of a protein. Examples of such reactive groups are : (a) haloacetyl groups, such as bromo and iodoacetamides are the most commonly used class of compounds which react easily with thiol groups at neutral pH and at room temperature. One should note that the acetamides can also react with amines and therefore they are not specific reagents to thiols. (b) N-maleimides. The selectivity of maleimides towards thiols arises due to their ability to react at neutral or low pH values when most other reactive groups of proteins are predominantly in the protonated forms. A disadvantage of maleimides is that they tend to undergo hydrolysis above pH 8.

(2) Groups specific to amines.

These are the most abundant class of functional groups present in a protein. The reactivity of amino groups is at an optimum only at high pHs, due to the high pK_a value of the $-NH_3^+$ ion. The two major categories of reactions of the amino groups are (a) alkylations and (b) acylations. Examples of alkylating reagents are the above mentioned haloacetyls, maleimide derivatives, aryl halides and carbonyl compounds. Examples of acylating reagents are isocyanates,

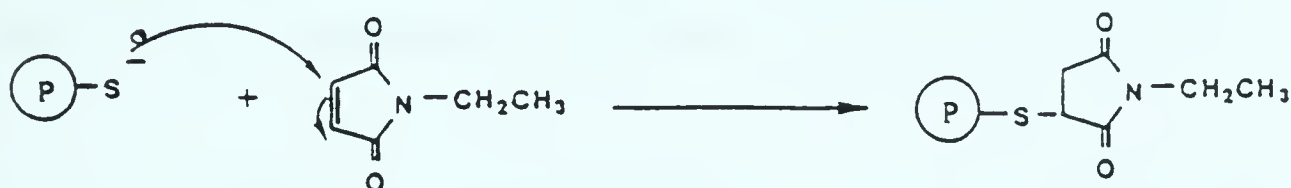
isothiocyanates, imidoesters, N-hydroxysuccinimidyl esters, p-nitrophenyl esters, acyl chlorides, and sulfonyl chlorides.

(3) Groups specific to carboxylates. The most common method of conjugating proteins utilizing this functionality, is by reacting it with an amino group, after the carboxylate has been activated by a carbodiimide. The end result of this reaction is the formation of an amide bond. Carbodiimides can also react with alcohols, water and other nucleophiles.

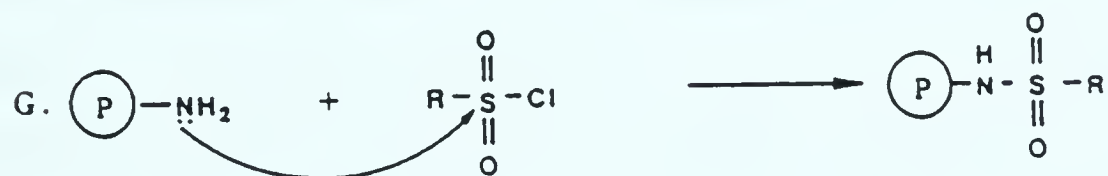
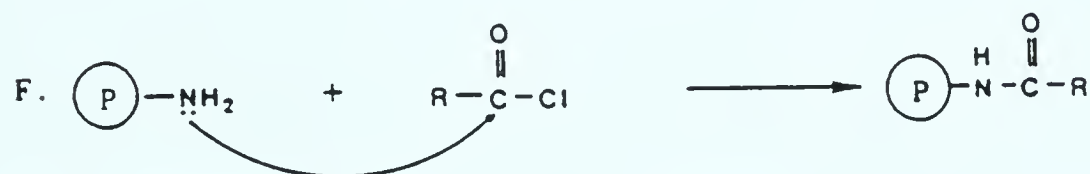
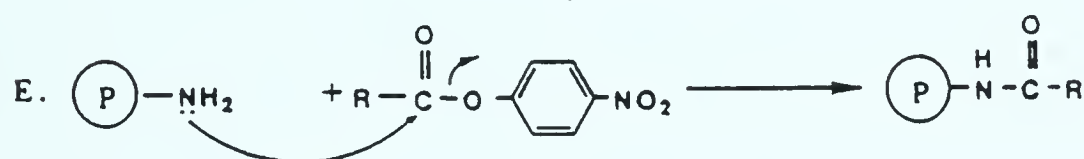
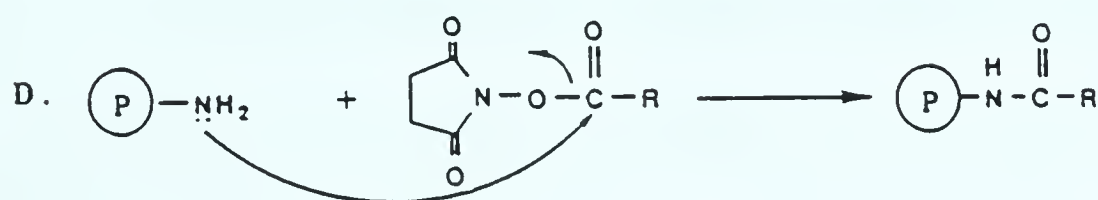
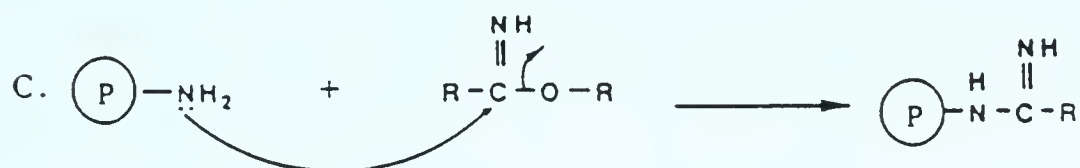
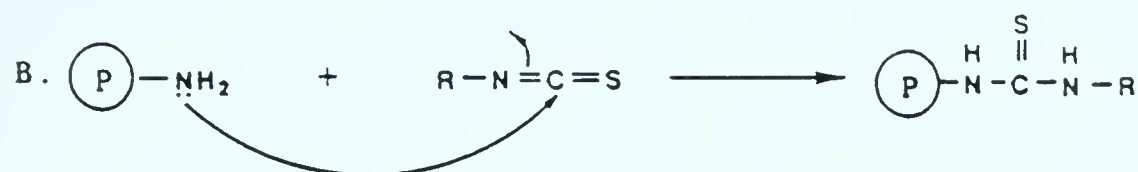
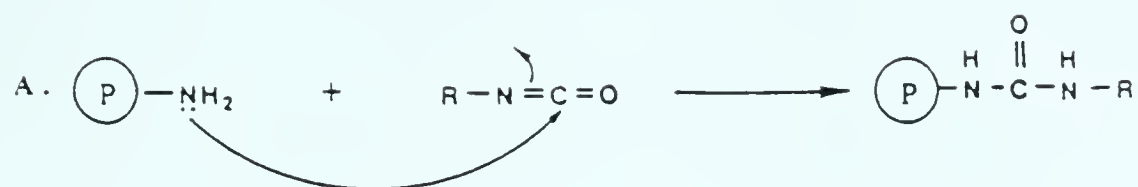
The important aspect of conjugation is to maximize the number of chelates per antibody molecule while maintaining optimum immunoreactivity of the antibody. The following examples summarize the above discussed reactions.



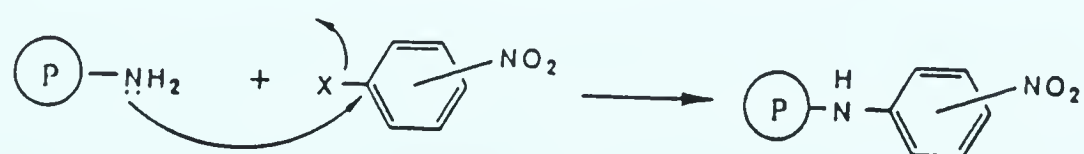
Reaction of iodoacetamide with protein thiol group (Ref.31, p32)



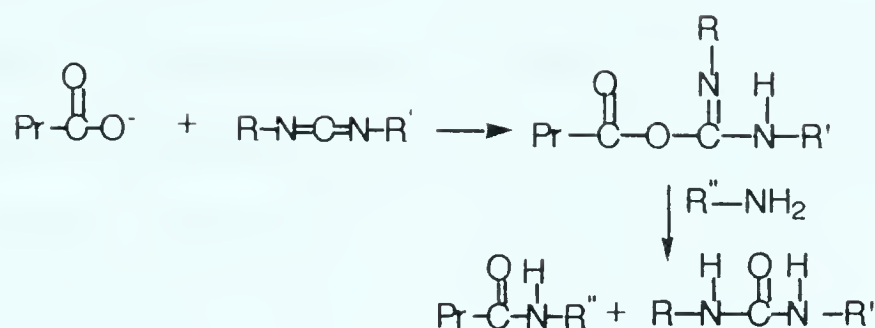
Reaction of N-ethyl maleimide with protein thiol group
(Ref.31, p32)



Acylation of protein amino groups : (A) isocyanate, (B) isothiocyanate, (C) imidoesters, (D) N-hydroxysuccinimidyl ester, (E) p-nitrophenyl ester, (F) acyl chloride, (G) sulfonyl chloride (Ref.31, p38).



Reaction of aryl halides with amino groups (Ref.31, p36)



Reaction of carboxyl group with amino group via carbodiimide
(Ref.31, p40)

(b) Determination of Chelate to Antibody Ratio

A number of methods are available for the determination of the number of chelates conjugated to an antibody. These include fluorescent, UV and radioactive methods (32,27,33,34,35,36). A fluorescence and a UV method to determine the number of chelates on a protein have been described by Diamandis and Evangelista (2,33). In their studies, the characteristic metal ion emissions that occur when the metal is complexed to the chelate and the absorbance of the conjugated chelate which is distinct from the protein absorbance, are used respectively to quantitate the concentration of the chelate bonded to the protein. Detailed descriptions of UV methods and a radioactive method I have used are in the results and discussion section of this thesis. A brief description of other methods that have been employed will now be given.

The chelate can first be complexed with the radioisotope ensuring that all of the radioisotope is complexed. Then the labeled chelate of known activity can now be allowed to react with the

protein. By using a chromatographic procedure to separate the protein from the unreacted chelate, and measuring the activity in the protein fraction, the degree of conjugation can be calculated if the initial reacting ratio of the protein and the chelate is known. A modification of this method consists of carrying out the conjugation reaction between known concentrations of protein and unlabeled chelate. Once the conjugation reaction is complete the protein chelate conjugate is separated. To this purified conjugate, a radioactive metal ion of known concentration and activity is added in excess of the conjugated chelate concentration. By measuring the % activity of the conjugate, one can then determine the number of chelates per protein molecule. Two important assumptions have to be made when one employs the above radioactive methods of determining the degree of conjugation : (1) that the affinity of the conjugated and unconjugated chelate for the metal ion is the same, and (2) that non-specific binding of metal to protein is minimal (36).

It should be noted that there could be a significant amount of dissociation of the metal chelate complex during these separation procedures if the stability of the complex is low. Others have used ^{14}C and ^3H labeled chelates to determine the degree of conjugation (1,9).

(2.2.3) Effect of Chelate to Antibody Ratio on Radiochemical Yield and Immunoreactivity

As the number of chelating groups on an antibody increases a loss in immunoreactivity is observed. This has significant consequences in radioimmunotherapy as well as in immunoscintigraphy. The decrease in immunoreactivity of antibodies with high chelate to protein ratios (9,36) could be due to the fact that some chelates may also react with antigen binding sites of the antibody. As the number of chelates on an antibody increase, the probability that these chelates may also bind at antigen binding sites of the antibody increases. This would result in a decrease of antigen binding ability of the conjugate.

On the other hand, lower chelate to antibody ratios would mean that conjugates may not be labeled with the desired specific activity. This is specially disadvantageous when labeled conjugates are used for therapeutic purposes. Therefore, in order to obtain a conjugate with sufficiently high immunoreactivity and the desired specific activity for therapeutic applications, one should determine the optimum concentrations of the protein and chelate and also the reaction mole ratio between the two reagents.

(2.2.4) Design Criteria of Chelate Ligands

An important factor in the design of a chelate is the stability

of the metal chelate complex under *in vivo* conditions. The stability or the formation constant (K) for a metal ligand complex can be defined as follows.



$$K = \frac{[ML]^{n-m}}{[M^{n+}][L^{m-}]}$$

where :

$[M^{n+}]$ = metal ion concentration at equilibrium

$[L^{m-}]$ = ligand concentration at equilibrium

$[ML]^{n-m}$ = concentration of the metal ligand complex at equilibrium.

A few common parameters that affect the value of K are discussed below.

(1) Steric Effects : A requirement for complexation is that the functional groups of the ligand are able to complex the metal with the least amount of steric hindrance or strain. Therefore the objective would be to design a chelate which is sterically favourable to react selectively with the metal of interest (37, Ref.38, p9).

(2) Chelate Effect; Normally a ligand that forms a ring structure upon complexation with a metal has a higher stability than a complex that is similar but lacks some or all of the ring structures. The greater the number of rings of a chelate, the higher is the stability of the complex (37,39).

(3) Ring Size; Stability constants of metal ligand complexes decrease as the size of the ring increases. As the number of carbon atoms bridging the coordinating atoms increase, the distance between the coordinating atoms increase. Thus, it becomes more difficult for the atoms to be brought together from a greater distance (Ref.38, p67).

(4) pH of Medium; Although the pH does not affect the thermodynamic stability constant, the conditional stability constant is a function of the pH of the medium (40).

(5) Hard and Soft Metals and Bases (Ligands) (37, Ref.38, p32,). Metal ions are considered to act as Lewis acids, and ligands as Lewis bases. Generally the most stable complexes are formed by the reaction between hard acids and hard bases or between soft acids and soft bases.

(6) Examples of some other parameters that influence the stability of a complex are the ionic size, coordination number and the oxidation state of the metal ion (Ref.38, p32).

(2.2.5) Some Examples of Bifunctional Chelating Agents Employed in Radioimmunotherapy

(1) Polyaminopolycarboxylic acids

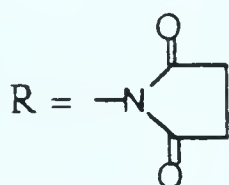
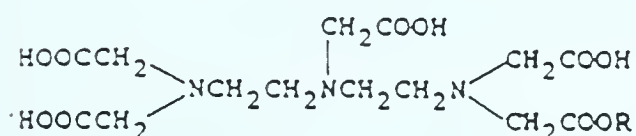
The original bifunctional chelates prepared by Yeh and

Sundberg (28) for immunoscintigraphy were the polyaminocarboxylic acid derivatives. The metal complexing group of these chelates is the polyaminocarboxylic moiety and the conjugation to proteins occurs via one of the following : diazonium ions, bromoacetyls, isothiocyanates and carboxyl groups. Examples of this class of chelates are the EDTA, DTPA, and TTHA derivatives. Of these chelates, the most extensively used in the radiolabeling of antibodies are the DTPA derivatives such as the bicyclic anhydride and the p-isothiocyanatobenzyl DTPA which have generally been determined to have much higher stabilities than the EDTA derivatives with metals utilised in the radiolabeling of proteins. The disadvantage of the bicyclic anhydride derivative of DTPA as compared to the isothiocyanato derivative is that in the former, one potential metal coordinating carboxylic group is utilised in the conjugation of this chelate to proteins (41). The conjugation of the latter chelate to proteins is made via the isothiocyanate group, which makes all the carboxyl groups available for coordination with metal ions. Although it was presumed originally that TTHA chelates, due to their additional carboxyl group would be a better chelator than even DTPA, it was observed from biodistribution studies, that TTHA did not form more stable complexes with, for example, ^{111}In than DTPA (9). Some examples of radiotherapeutic metals that have been complexed by these ligands are, : Re-186, Bi-212, Pd-109, Sc-46, and Y-90 (9,42,43). Structural examples of various polyaminocarboxylic acid chelators are given in Table 6.

Table 6 Examples of various Bifunctional Chelates used
For Radioimmunoscentigraphy and Therapy

(a) DTPA Derivatives (9)

Chelate Structure



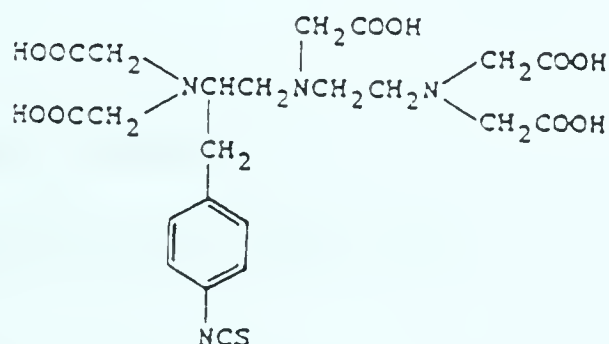
N-hydroxysuccinimide
monoester of DTPA.

Antibody Reactive Moiety

Antibody conjugation via N-hydroxy
succinimide activated monoester of DTPA

Table 6 continued

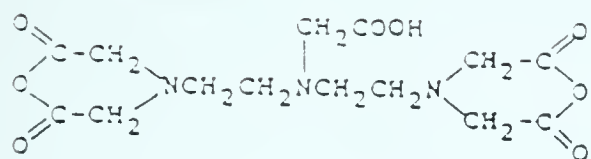
Chelate Structure



Antibody Reactive
Moiety

-NCS group

1-(p-isothiocyanatobenzyl) DTPA

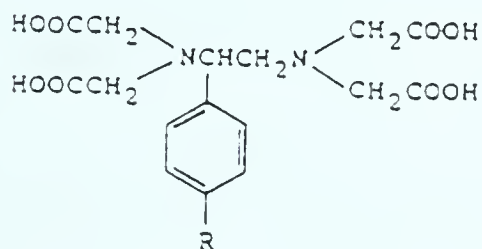


Anhydride group

Bicyclic anhydride of DTPA

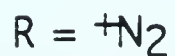
(b) EDTA Derivatives (9)

Chelate Structure

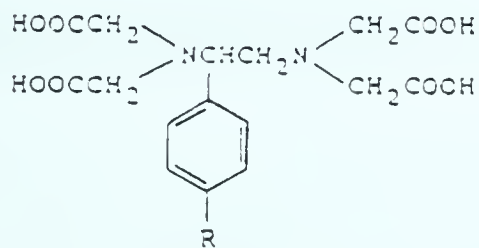


Antibody Reactive
Moiety

Diazonium ion

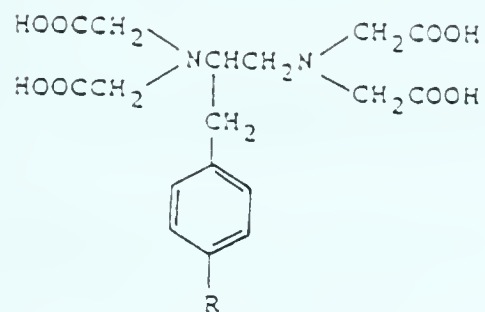


1-(p-benzenediazonium) EDTA



Bromoacetamide group

1-(p-bromoacetamidophenyl) EDTA.



-NCS group

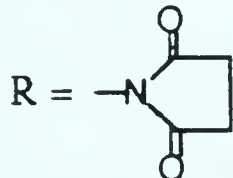
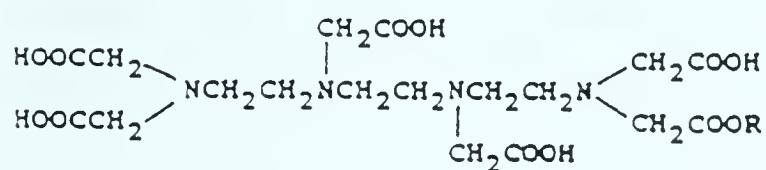
R = -NCS

1-(p-isothiocyanatobenzyl) EDTA

(c) Triethylenetetraaminehexaacetic Acid

(TTHA) Derivatives (9)

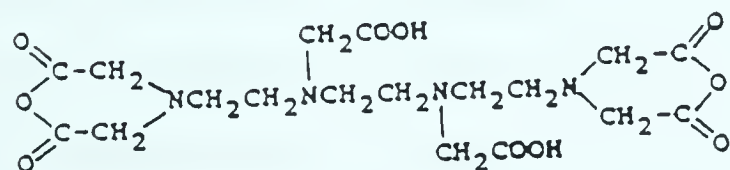
Chelate Structure



N-hydroxysuccinimide monoester of TTHA.

Antibody Reactive Moiety

Antibody conjugation via N-hydroxysuccinimide activated monoester of TTHA



Anhydride group

Bicyclic anhydride of TTHA.

(2) Phenolic Aminocarboxylic Acid Derivatives

Although most chelates in this category have been extensively used to complex radiometals such as gallium (Ga) and Indium (In), that are employed in immunoscintigraphy (9), no data have yet been published with regard to the *in vivo* or *in vitro* stabilities of these ligands with radiotherapeutic metals.

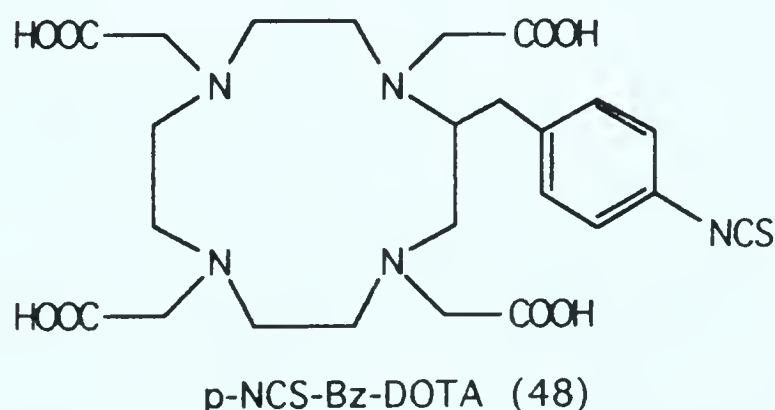
(3) Macrocyclic Amine Derivatives.

The need to change the design of chelates from the more widely used polyaminocarboxylic acid derivatives arose from the fact that some radiometals used in radioimmunotherapy, such as Cu(11) were observed to be very unstable *in vivo* when complexed to DTPA or EDTA derivatives. One of the first successful macrocyclic chelates synthesised by Moi (44), was a 14 membered cyclic ring, named 6-(p-bromoacetamidobenzyl) - 1,4,8,11-tetraazacyclotetradecane - N, N', N'', N'''-tetraacetic acid (TETA), that was used in the radiolabeling of an antibody with Cu-67. If one compares the thermodynamic stabilities of Cu-DTPA and Cu-TETA complexes, with the stabilities of these complexes in human serum, although the thermodynamic stability of Cu-DTPA is much higher than the Cu-TETA complex (44), the dissociation of the Cu-TETA complex in human serum was much slower (about 1% per day) than the Cu-DTPA complex. It has also been suggested that (9), in order to prevent steric hindrance by the protein, which in turn would reduce the

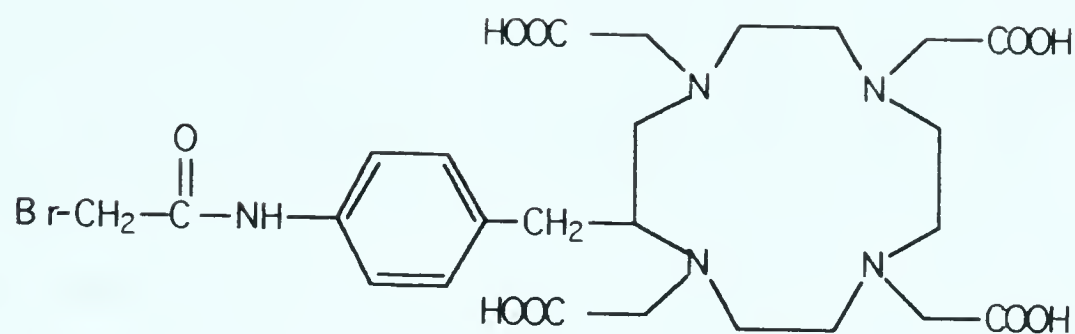
complexation yields when radiolabeling TETA conjugated antibodies, the metal should be first complexed with the chelate, TETA, before the conjugation reaction between the chelate and the antibody. Crystallographic studies (45) of the Cu-TETA complex have determined that two of the carboxylate groups and all of the nitrogens of the TETA ligand are coordinated to the metal ion. The second macrocyclic chelate that has been utilised in complexing a radiometal for therapeutic purposes is the 12 -membered 1,4,7,10-tetraazacyclododecane N,N',N'',N'''-tetraacetate (DOTA). Some potential radiotherapeutic metals that have been labeled to antibodies via these chelates are Cu and Y (44-47). Figure 1 outlines some of the DOTA and TETA derivatives commonly proposed for radiometal chelation.

Figure 1 Examples of Various Macrocyclic Chelators used for Radiolabeling Antibodies

(A)

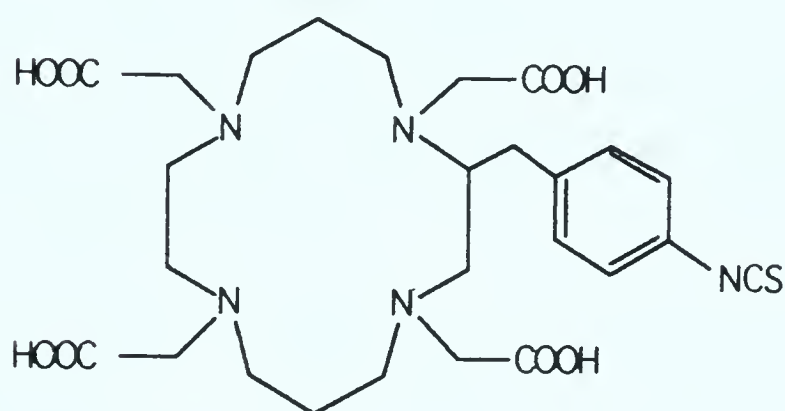


(B)



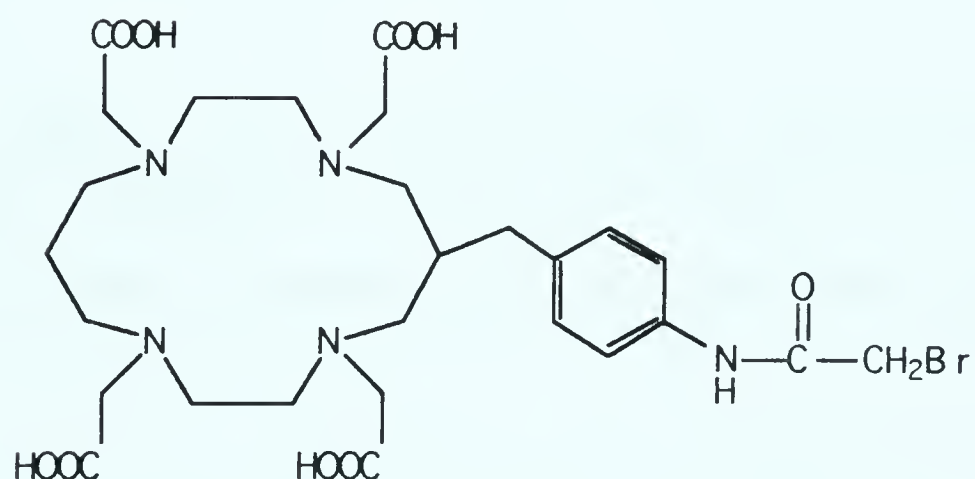
p-bromoacetamidobenzyl-DOTA (46)

(C)



p-NCS-Bz-TETA (48)

(D)



6-(p-bromoacetamido-benzyl)-1,4,8,11-tetraazacyclotetradecane-N, N', N'', N'''-tetraacetic acid (9)

(4) Sulfur Ligands

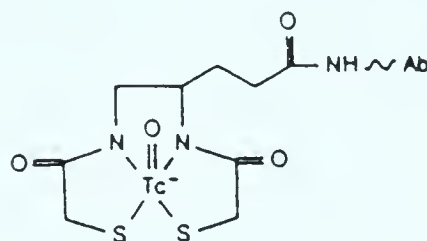
Since sulfur is considered to be a soft base, these ligand systems were primarily designed to complex soft acids like $^{99m}\text{Tc}(9)$. Since the chemistry of Tc and Re are very similar, each of the following chelates have been used to radiolabel antibodies with Tc as well as Re.

(a) N_2S_2 ligands : An example of a (Tc- N_2S_2) complex is shown in Figure 2 (49,50,). *In vivo* studies performed by Fritzberg and co-workers, of antibodies labeled with Re and Tc via this ligand, have indicated high *in vivo* stabilities and very similar biodistribution patterns for these antibodies (50).

(b) N_3S ligand system. : The bifunctional chelate in this class, that has been specifically used with ^{186}Re is the "tetrafluorophenyl ester derivative of mercaptoacetylglycyl-gamma-aminobutyrate ($\text{MAG}_2\text{-GABA}$)" (51). An example of an (Re N_3S) complex is shown in Figure 3.

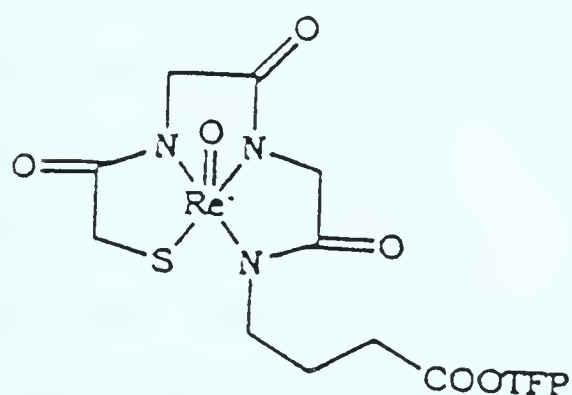
(c) N_2S_4 ligand. : The N, N', N'', N'''-tetrakis (2-mercaptoethyl)-ethylenediamine, synthesized by Najafi and co-workers (52), has been utilized to label antibodies with ^{99m}Tc and ^{186}Re (Figure 4)

Figure 2 N₂S₂ Ligands



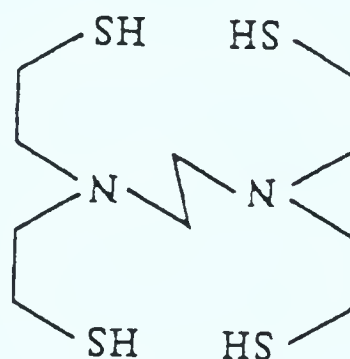
Tc-4,5-bis(thioacetamido) pentanoate (50)

Figure 3 N₃S Ligands



Re-Tetrafluorophenyl ester of
mercaptoacetylglycyl-gamma-
aminobutyrate (51)

Figure 4 N₂S₄ Ligands



N,N',N'',N'''-tetrakis(2mercaptoethyl)-
ethylene diamine (52)

(5) Natural Bioligands

One possible advantage of utilizing these large bioligands is that one of these molecules can complex a number of radiometal

ions. Some examples of these ligands are metallothionein (MT) and desferrioxamine (DFA) (53,54,55). It has been reported that one molecule of MT has the ability to complex up to 20 metal ions (53). Since MT is a "cysteine-rich" protein, it forms stable complexes with soft acids such as Tc and Au (9,56). MT is normally conjugated to proteins via the lysine amino groups of MT (53). DFA on the other hand, has been mainly used to label human immunoglobulins with ^{67}Ga (9,54).

(2.3) *In Vivo* Stability of Metal Chelate Complexes

The *in vivo* stability of a radiolabeled protein conjugate depends primarily on two factors (1) Absolute stability of the radiometal ligand complex, and (2) the relative stabilities between the above metal ligand complex, and other ligands (e.g. serum proteins), with the metal under discussion. The transfer of the metal from the chelate (ligand) that was originally used in the complexation, to a serum protein, is commonly known as a transchelation or a transcomplexation.

Another possible method of dissociation of the metal from the antibody is the cleavage of the bond between the chelate and the antibody. Generally this form of dissociation depends on the design and the chemical nature of the "linking arm" of the chelate, which determines whether it is a "metabolizable" bond (9,57).

The dominant contributor to the *in vivo* instability of radiolabeled antibodies is the competition from other proteins for the metal. Therefore, it is always necessary to perform *in vitro* transchelation experiments to obtain an estimate of the relative stability of the metal-ligand complex of interest.

(2.4) Factors Affecting Antibody Targeting

Although considerable advances have been made in the production of highly specific and stable radiolabeled antibodies, current experimental data depict a very low uptake by tumors during *in vivo* experiments relative to what has been achieved under *in vitro* conditions. This could be related to certain physiological, pharmacological and immunological factors which have been reviewed by Sands (58), Yuanfang (9), and by Buchbaum (59). Some of these are mentioned briefly.

(2.4.1) Physiological Factors

(a) Blood flow, (b) Size and location of tumors, (c) Vascular permeability of tumors, (d) Metabolism of antibodies and (e) Nature of tumor.

(2.4.2) Pharmacological Factors

(a) Dose of antibody, (b) Method of administration, (c) Form of antibody, and (d) Type of radiolabel.

(2.4.3) Immunological Factors

(a) Circulating antigens, (b) Antimurine response, (c) Antigen modulation, and (d) Affinity and specificity of antibodies.

(2.5) Techniques of Antibody Targeting

The efficiency of treatment of tumors by radioimmunotherapy depends mainly on the ability to optimize the localization of the radiolabeled antibody at the target site while minimizing the background activity (24). In order to improve the target to non-target ratio, a number of strategies are currently being adopted. Some of these strategies are discussed below.

(2.5.1) Pretargeting Techniques

The major problem of radioimmunotherapy has been the low uptake of the radiolabeled antibody by the tumor and the localization of radioactivity in normal tissues resulting in unwanted exposure of the latter to radiation. One method of overcoming this problem was to develop pretargeting approaches.

(2.5.1 a) Bispecific Antibodies (60,61,62)

Here, the tumor site is targeted first with non-radiolabeled antibody which is bispecific or bifunctional. That is, one arm can attach itself to the tumor antigen and the other arm can subsequently bind to a radiometal ligand complex. This procedure has

enabled the delivery of high concentrations of unlabeled antibodies to the tumor site and remain at that site for a considerable amount of time. This would provide adequate time for the elimination of the unbound antibody. If the antibody also has a high affinity for the metal ligand complex, it would lead to a rapid uptake of the complex by the tumor target, via the already bound antibody.

(2.5.1.b) The Avidin-Biotin Delivery System

The above system originated as a modification of the concept known as "tumor pretargeting" (57). It is well known that prelabeled antibodies directed towards tumor targets require considerable amount of time to localize at the required target site (63). This delay has often resulted in high non-target to target ratios and ligand exchange reactions (64). The avidin-biotin system has been adopted to eliminate or minimize such effects (64-71).

Avidins are a class of proteins which have a high affinity and specificity for biotin (64). Two main pretargeting procedures have been studied using the avidin-biotin system (72,73). These are the (a) "two-step" and (b) the "three-step" methods. In both these systems the underlying principle is allowing sufficient time for the unlabeled antibody to localize at the target site and then administering the radiotherapeutic agent that can bind rapidly with the antibody that is already bound to the tumor. The unbound radiotherapeutic agent, being of low molecular weight, would be

cleared from circulation within a short period of time.

(a) Two-Step Method

Here, the antibody can either be conjugated to a molecule of streptavidin or can be biotinylated. The modified antibody is then injected intraperitoneally or intravenously. This would be the first step. After two or three days biotin or avidin, radiolabeled via a bifunctional chelating agents such as cyclic anhydride of DTPA, is injected when the antibody uptake by the tumor is at a maximum and the unbound antibody concentration has reached its minimum level.

(b) Three-Step Method

The first step is similar to that of the two step method. For example a biotinylated antibody can first be administered, and as a second step this can be followed by an injection of excess unlabeled avidin. This has two main functions.(1) To eliminate the unbound biotinylated antibody from circulation, and (2) to complex with the biotinylated antibody that is prelocalized in the tumor. As the third step, radiolabeled biotin is injected in a manner similar to the second step in the two-step method. The major advantage of this method is that, since avidin is a multivalent molecule it can in theory produce an antibody that contains more radiolabeled biotin molecules than the two step method.

(2.5.2) Administration of Antibody Fragments

There have been a number of studies performed to determine the relative and absolute uptake of radiolabeled antibodies and their fragments ($F(ab')_2$ and Fab') by tumors (59,24,74). The advantage of these fragments, compared to the intact IgG molecules is that the fragments, due to their small size, are cleared at a faster rate from the circulation than intact IgG molecules (22)- fastest being Fab' and then $F(ab')_2$ (75). This would result in higher target to non-target ratios for the fragments compared to the ratios obtained for whole antibody molecules. Another possible advantage of using fragments is that they have been found to be less immunogenic than whole antibodies (22). This may be due to the fact that these fragments lack the F_C portion of the antibody. The disadvantages of fragments are the reduced absolute uptake of fragments by tumors when compared to whole antibodies (59), probably due to the rapid clearance of these fragments from circulation and the observation that on some occasions fragments accumulate in the kidneys (59). Certain reports (9) indicate that the localization of intact antibodies in tumors has been 3 to 24 times greater with fragments. On one occasion however, equal amounts of fragments and whole IgG had localized in tumors (24).

(2.5.3) Regional Injection of Radiolabeled Antibodies

Another possible means of improving the target to non-target

ratio is local or regional radioimmunotherapy (57,72,76-82). Some tumors in humans are restricted to particular areas of the body. Examples of such are ovarian, bladder, pancreatic and gastrointestinal carcinomas. For example ovarian cancer which is confined in most cases to the peritoneal cavity, has been targeted for treatment by intraperitoneal injection of radiolabeled antibodies (72). However results obtained showed no significant improvement in the treatment of this cancer. In another study (77) where the treatment of an ovarian cancer, performed either by intravenous or intraperitoneal administration was compared, the antibody uptake by tumors when treated intravenously was higher than when treated intraperitoneally.

A comparative study (76) of intraperitoneal versus intravenous treatments of a colon cancer showed no difference in the tumor to non-tumor ratio between the two methods, even after 24 hours.

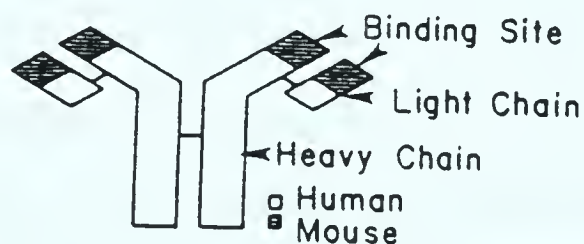
(2.5.4) Use of Chimeric Antibodies

Since most antibodies used in radioimmunotherapy are murine, the occurrence of an immune response in humans as a result of repeated injections of these proteins is not surprising (83). The host antibodies produced against these foreign proteins can react with the injected murine antibodies. This results in reduced uptake of the radiolabeled antibodies by tumors, a rapid clearance of the administered antibodies from circulation, and an accumulation in the

reticuloendothelial system (73). The host antibodies raised against the murine antibodies are known as Human Antimurine Antibodies (HAMA).

One possible technique of minimizing the HAMA response is the injection of chimeric antibodies (73,75). Since it is believed that the Fc portion of the murine antibody generates the majority of the HAMA responses (76), antibodies of murine origin where the Fc portion has been substituted by a human Fc portion, known as chimeric antibodies, are now being investigated. Studies conducted involving either chimeric or "humanised" antibodies, where substitution occurred only in the hypervariable region of the antibody, have not indicated an increase in tumor localisation but have shown reduced localisation in the reticuloendothelial system (73). Figure 5 depicts the structure of a typical chimeric antibody.

Figure 5 Chimeric Antibody (Ref. 59)



Another technique of eliminating the HAMA response would be to use human antibodies (59). These antibodies have been used in mice containing human colon cancer xenografts as well as in humans (59). It was observed that the patients did not generate any

antibodies against the administered radiolabeled antibodies (59).

(2.5.5) Site Specific Modification of Antibodies

A frequently encountered problem associated with radioimmunotherapy or immunoscintigraphy is the loss in immunoreactivity of the monoclonal antibody due to the chemical reactions between the antibody binding site and the free ligands or metal ligand complexes. A covalent bond is formed as a result of this reaction. Generally, the ligands react with certain functional groups of the protein located throughout the protein molecule. The loss of immunoreactivity can easily result from chemical reactions at sites near the antigen binding positions in the variable region of the antibody. The consequence of this would be a loss in the ability of the conjugated antibodies to bind to antigens.

One possible method of minimizing this problem of loss in immunoreactivity is to attach ligands at a position that would create minimum disruption at antigen binding sites. One method that has been studied (84,9) is the reaction of ligands with the carbohydrate section of the protein. The carbohydrate section is generally located in the Fc portion of the protein which is distal to the antigen binding site. The ligand that has been mostly used in these studies is DTPA and the radionuclides used were In-111 for immunoscintigraphy and Bi-212 and Y-90 for radioimmunotherapy (84). These studies indicate that higher conjugation ratios of ligand

to antibody were possible with no loss in immunoreactivity when compared to chelate attachment to amino acid residues of antibodies (84). An additional advantage of the above method is the production of antibodies with uniform immunoreactivities.

(2.6) Properties of Samarium (Sm)

(2.6.1) Nuclear Properties of ^{153}Sm

Samarium-153 (^{153}Sm) is generally produced by the bombardment of enriched $^{152}\text{Sm}_2\text{O}_3$ with thermal neutrons through the reaction of $^{152}\text{Sm}(n, \gamma)^{153}\text{Sm}$. Samarium-153 has a half life of 1.95 days, and the decay product is Eu-153. The major emissions of ^{153}Sm are shown below (Ref.85,p 20);

(1) β^- (E_{max}) = 640 KeV (30%), 710 KeV (50%), 810 KeV (20%)

(2) gamma (γ) = 103 KeV (28%)

^{153}Sm could be classified as a "high range" β^- emitter, according to Humm's classification (8) of β^- emitters, because of the penetration range of 2.0 mm (86) of its β^- particles. This falls between the penetration ranges of ^{131}I (0.99 mm) and ^{90}Y (5.9 mm). The two day half-life enables the administration of ^{153}Sm as a single dose or as fractionated doses. The 103 KeV γ emission can be utilized to monitor radiolabel distribution scintigraphically, as well as for dosimetric calculations. Its fairly short half life makes

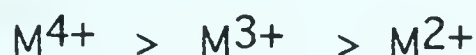
possible the production of ^{153}Sm with moderately high specific activity. These features would make ^{153}Sm a potential candidate for radioimmunotherapy.

(2.6.2) Chemical Properties

Samarium belongs to a group of elements known as the lanthanides. This series consists of the elements lanthanum (La) to lutetium (Lu) (Ref.87, p 6). The term rare earths is also sometimes used to identify these elements (Ref.87, p 6) but has one additional element added to the above series. This element is Y. The unique feature of the electronic configurations of these lanthanides is that, after lanthanum, the 4f orbitals begin to fill up in preference to the 5d orbital. As a consequence some scientists prefer to name this series as the "4f transition elements" (Ref.87, p 6). The most common or "characteristic" oxidation state of these elements is +3 (Ref.88, p 16). Other oxidation states such as Eu^{2+} , Yb^{2+} , Sm^{2+} , Pr^{4+} , and Tb^{4+} have also been observed (Ref.88, p 17). The lanthanides are easily oxidized to the +3 state under acidic or basic conditions (Ref.88, p 39). Therefore these metals are considered to be strong reducing agents under the same conditions.

Since the 4f electrons of the lanthanides are well shielded, their involvement in chemical interactions with ligands are minimal (Ref.88, p 53). Therefore, one can conclude that the nature of the bonding between the lanthanides and ligands is predominantly ionic

or electrostatic (Ref.88, p 53). As a result, the ability of a lanthanide cation to form complexes with a particular ligand would be expected to decrease as follows:



If one looks at the ionic radii for the +3 lanthanide ion it is quite apparent that the values are much larger than most other tripositive cations (89). A consequence of this would be a low ionic potential (charge/radius). This in turn would mean decreased polarizing power (89). The ionic nature of the bonding is greatly enhanced by this feature. Therefore these ions are classified as hard acids. Hard acids generally form very stable bonds with hard bases such as molecules containing oxygen and nitrogen (90). It is generally observed that complexes formed between lanthanides, and ligands containing carboxylate groups, to be the most stable and widely used (89). Another unique feature of the lanthanides is their large coordination numbers (91). Sm for example has a maximum coordination number of 8 (89). This enables Sm to complex with compounds such as diethylenetriamine pentaacetic acid (DTPA), which is an octadentate ligand (89).

It is known that certain lanthanide metal complexes, when excited by UV radiation, fluoresce with characteristic metal ion emissions (92-96). The proposed mechanism of fluorescence (93,95) briefly is as follows. At the first stage, UV radiation is absorbed by the ligand of the complex. Then the absorbed energy is transferred

from the ligand to the complexed metal ion. The excited metal ion can now dissipate its energy, resulting in the characteristic metal ion fluorescence. The intensity of the emission depends on the efficiency of energy transfer from ligand to the metal ion. Of the lanthanides studied only europium and terbium have been extensively used as fluorescent probes (2,32,33).

(2.6.3) Biological properties of Sm

Lanthanides are normally regarded as being of low toxicity (97). The toxicity in most cases depends on the route of administration (97). The common symptoms of toxicity are writhing, ataxia, labored respiration and sedation (97). The LD₅₀ (mg/kg) of samarium chloride for the following animals (97) are : frog =150 (subcutaneous), mouse =585 (intraperitoneal), mouse > 200 (oral), and guinea pig = 750-1000 (subcutaneous). The values for samarium nitrate (97) are as follows: Frog =1600 (subcutaneous), mouse (male) =315 (intraperitoneal), guinea pig = 500 (subcutaneous), and rat (female) = 2900 (oral).

A number of biodistribution studies have been performed to indicate the general metabolic pattern of lanthanides (97). When ¹⁶⁷Tm-EDTA was administered to rabbits, 70% of the metal localised in the skeleton. When Eu was administered intravenously to rats, the metal localised mainly in the liver, kidney and bone. Studies involving ¹⁴⁰La, ¹⁴⁴Ce, ¹⁴³Pr show the major organ of

localization to be the liver. ^{160}Tb and ^{169}Yb localized mainly in the bone (50%) and kidney (25%). When SmCl_3 was administered intravenously into rats, the biodistribution depicted that 50% of the dose localized in the liver and 25% in the skeleton (Ref.85, p 23).

(2.6.4) Radioimmunotherapeutic Studies of ^{153}Sm

Literature indicates only a limited number of studies that have employed ^{153}Sm in radioimmunotherapy (86, 98-101). Cyclic DTPA anhydride and p-isothiocyanatobenzylmethyl DTPA are the only two chelates that have been used to radiolabel antibodies with ^{153}Sm . These studies suggest that the antibody radiolabeled with Sm via p-isothiocyanatobenzylmethyl DTPA had a higher *in vivo* stability, due to the low bone activity, than when it was radiolabeled via the cyclic DTPA anhydride. Comparable high liver activities were observed with both chelates.

In addition to the above mentioned radioimmunotherapeutic studies of ^{153}Sm , several Sm phosphonate ligand complexes alone have been investigated as potential radiotherapeutic compounds for bone therapy. Some examples of such ligands are ethylenediamine-tetramethylenephosphonic acid (EDTMP), nitrilotrimethylene-phosphonic acid (NTMP), and diethylenetriaminepentamethylene-phosphonic acid (DTPMP) (102-107). Of these, ^{153}Sm -EDTMP has shown to be the most promising complex due to high uptake of

activity by bone and minimal localisation of activity in blood and liver, when this complex was used (102,107).

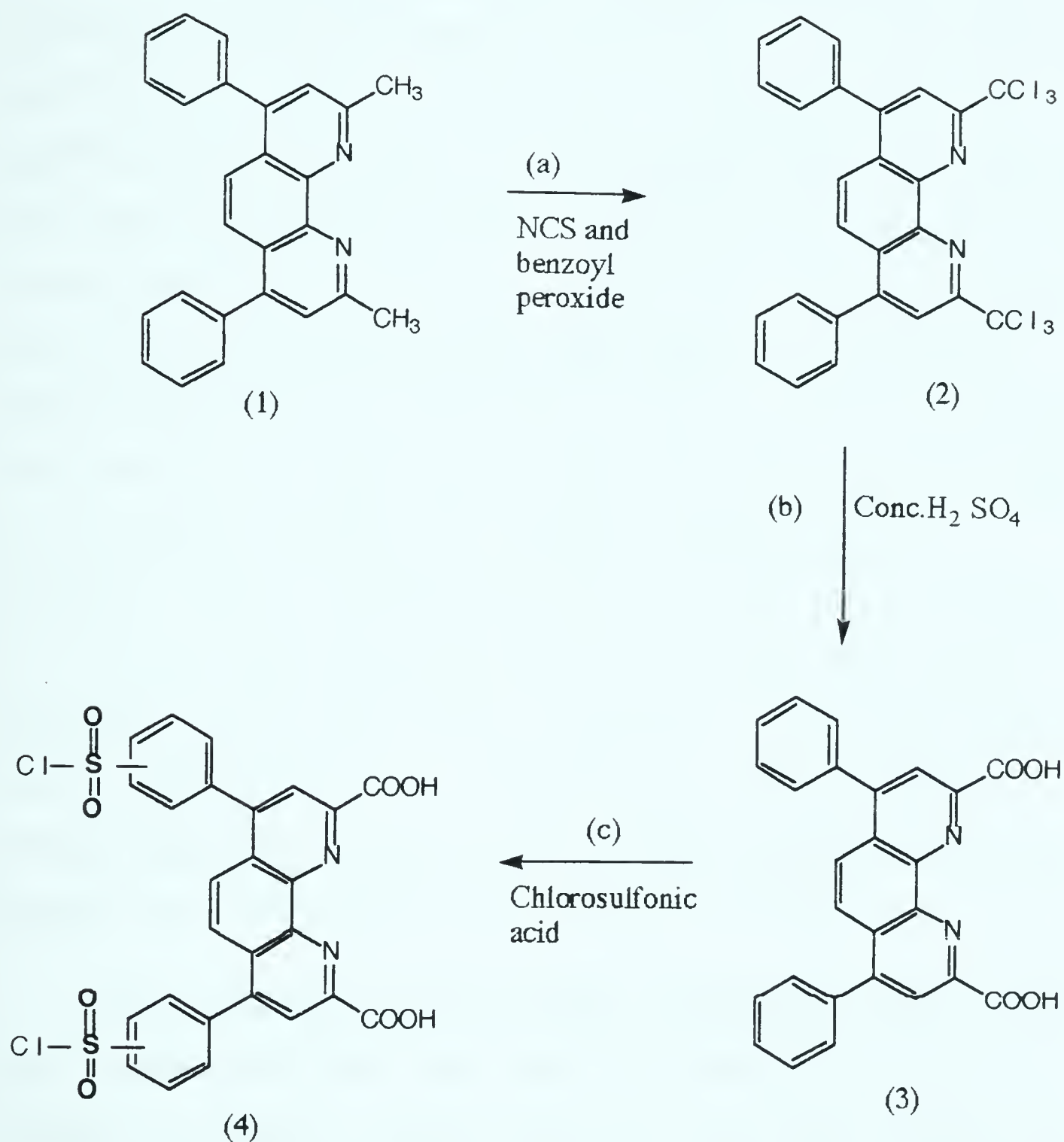
(3.0) EXPERIMENTAL METHODS

All glassware and Teflon vials were first acid washed and rinsed with distilled deionised water. Solvents and chemicals (analytical reagent grade or A.C.S. certified) were used as received from the suppliers. Buffer solutions were initially eluted through Chelex-100 column to remove trace metal impurities. Trizma Base (reagent grade, purity 99.9%) was obtained from Sigma Chemical Company. A spectrophotofluorometer made by the American Instrument Company was used in fluorometric studies. A Hewlett Packard Diode Array Spectrophotometer (model 8452A) was used for UV absorbance measurements. Protein-chelate conjugates were analysed by a Tracor high pressure liquid chromatograph (model 970A) at 280 nm.

(3.1) Synthesis of BCPDA

A schematic representation of the synthetic procedure is shown in Figure 6 (2).

Figure 6 Synthesis of BCPDA



The synthetic method established by R.A. Evangelista (2) was followed. Step (a) : 4 g of bathocuproine (1), 9.8 g of N-chlorosuccinimide, and 0.011 g of benzoyl peroxide were added to 100 mL of carbon tetrachloride. This mixture was refluxed while

stirring for 6 hours. At the end of this time period, the mixture was allowed to cool and the succinimide removed by filtration. The remaining residue, after solvent removal by vacuum evaporation, was dissolved in 100 mL of chloroform. A saturated solution of Na_2CO_3 (100mL) was used to wash the organic phase. This phase was then dried using anhydrous MgSO_4 . Compound (2) was obtained by the vacuum evaporation of the solvent. Step (b) : To 1.5 g of compound (2), 6.5 mL of concentrated H_2SO_4 was added and the resulting mixture was heated in an oil bath for 2 hours at 80°C while stirring. Once the reaction mixture was cooled, it was slowly added to 100 mL of ice water in order for the product, compound (3), to precipitate. Step (c) : 0.42 g of compound (3) was added in aliquots to 2.1 mL of cold chlorosulfonic acid with stirring. This solution was heated at 80°C for 4 hours. The solution mixture was cooled and was added slowly to 80 mL of ice water. The precipitated product was filtered through a sintered glass funnel, washed with distilled water, and dried for 12 hours under vacuum.

Certain deviations from the above established method of the direct synthesis of BCPDA were made during steps (a) and (b). Although the literature claimed that only 6 hours were needed to complete the synthesis of compound (2), a minimum of 12 hours were needed in the present synthesis to complete this step. This was established by the analysis of NMR spectra of the product at various time intervals. Also, after several attempts, a direct synthesis of a pure compound of (3) from compound (2) was not

possible. Since compound (3), as obtained by a direct synthesis was found to be impure, a purification procedure as described below, was adopted prior to the synthesis of compound (4).

0.2 g of unpurified compound (3), obtained directly from compound (2) was allowed to stir in an aqueous solution of NaHCO_3 (8.0 g.in 100 mL) containing 50 mL of MeOH, for 3 hours. As this compound was being dissolved, a white precipitate of the sodium salt of compound (3) appeared in the solution. This solution was then washed with 50 mL of diethyl ether to remove any non polar organic impurities. The aqueous solution was then acidified with conc. HCl until the acidity of the medium reached a pH of 2. This solution was allowed to stir overnight. The yellow precipitate of the diacid was recovered from the solution by centrifugation. A NMR spectrum was obtained and an elemental analysis performed on this compound.

This purified compound (3) was then utilised to prepare compound (4) as described in the literature. An elemental analysis and the following spectra of this compound were obtained : IR, UV, and NMR. A FAB-MS spectrum was also obtained using an AEI/Kratos MS 9 double focussing mass spectrometer equipped with a FAB gun. The FAB gun was operated with xenon as the bombarding species. The FAB-MS spectrum was provided by Dr. A Hogg of the Department of Chemistry, University of Alberta.

(3.2) Fluorometric Studies of BCPDA

A spectrophotofluorometer made by the American Instrument Company (model # J4-8912) was used. Excitation source was a xenon lamp. The sample cells consisted of Suprasil quartz cells which have a light path of 1 cm. The excitation wavelength was 320 nm. Slitwidths of 0.1 mm were used for the detection of free ligand and 0.5mm, for the detection of metal ion fluorescence respectively. The sample volume was 1.0 mL.

A fluorescence spectrum of a free hydrolysed sample of BCPDA was first obtained. BCPDA was hydrolysed by heating a water suspension of BCPDA at about 70 °C for about 2 hours, after which a clear solution was obtained.

(3.2.1) Determination of the Conditional Stability Constant of Hydrolysed BCPDA-Sm Complex

Required concentrations of hydrolysed BCPDA and Sm^{3+} were dissolved in 0.05 M Tris buffer of pH 7.5. The ionic strength of the solution at this pH and concentration of Tris-HCl (0.04 M), was calculated to be 0.04. Emission intensities of the free ligand at 410 nm were measured by determining the relative intensities. This is a measure of the intensity of emission detected by the photomultiplier tube relative to the blank. Initially, a plot of the relative intensities versus various concentrations of the free ligand

was made to generate a calibration curve. The emission intensity of a sample buffer containing no BCPDA ($[BCPDA]=0$), was determined by measuring the intensity of this sample after zeroing the relative intensity meter with the same sample buffer. The zeroing procedure used in all cases was the same. The concentration of each sample of the free ligand prepared in duplicate were determined by measuring the UV absorbance at 324 nm and using the molar absorptivity value of the ligand given in the literature (2).

The following concentrations of $SmCl_3$ and BCPDA were mixed in duplicate samples. Final concentrations of Sm and BCPDA were 1×10^{-5} M and 0.89×10^{-5} M respectively. The total volume of each mixture was 2.6 mL. The relative intensity of the free ligand (uncomplexed) emission was measured at 410 nm. The emission spectrum of a pure $SmCl_3$ solution showed no peaks at 410 nm. A scan was also made from 500 nm to 750 nm to observe the metal ion fluorescence.

(3.3) Production of ^{153}Sm .

(3.3.1) Low Specific Activity ^{153}Sm

Generally, 1 mg of enriched $^{152}Sm_2O_3$ obtained from the Oak Ridge National Laboratory, specified as 99.06% pure was irradiated at the University of Alberta SLOWPOKE facility, for 4 hours at a flux of $10^{12}n/cm^2sec$. The required quantity of Sm_2O_3 was first weighed in a small plastic vial and closed tightly. This small vial

was then inserted into a bigger plastic vial and heat sealed. The samples were transferred to and out of the irradiation site via a rabbit tube utilising compressed air. The specific activity obtained under these conditions was about 1mCi/mg of Sm_2O_3 . $^{153}\text{Sm}_2\text{O}_3$ was then dissolved in 2 mL of 1N HCl (analytical reagent grade BDH).

Radionuclidic purity of a sample of Sm_2O_3 was determined after it was irradiated for 5 minutes at a flux of $10^{12}\text{n/cm}^2/\text{sec}$, allowed to decay for a further 5 minutes and counted for 10 minutes using a hyper-pure germanium detector. The gamma spectrum of this sample was then plotted with intensity (counts) of the peaks as the Y axis and energy (KeV) as the X axis. The sample irradiation and the production of spectral data were performed by Mr. John Duke of the SLOWPOKE facility.

(3.3.2) High Specific Activity ^{153}Sm

Specific activities of about 1Ci/mg Sm_2O_3 were obtained from Nordion International Incorporated in the form of SmCl_3/HCl . For each experiment a small aliquot of the SmCl_3 was dissolved in the desired buffer, which was run through a Chelex-100 (iminodiacetate in the sodium form, obtained from Biorad) column with dimensions of 3.7 cm X 15 cm to remove trace metal impurities. A gamma spectrum indicating the radionuclidic purity of this sample was obtained as described before, after counting this sample for 10 minutes.

(3.4) Preparation of Sm Complexes

In each experiment the metal and the ligand were dissolved in specific buffers at the required concentrations. The desired volumes from each solution were mixed in acid washed 5 mL conical Teflon vials (Teflon PFA, obtained from Cole Parmer Instrument Co.). All buffers were eluted through the above mentioned Chelex column to remove trace metal impurities prior to use. The buffers used in these experiments were acetate buffer (0.1M) for pH 4, 5, and 6 and Tris buffer (0.1M) for pH 7.5.

(3.5) Cation Exchange Chromatography

Sephadex carboxymethyl (CM) C-25, cation exchange resin in the sodium form was obtained from Sigma Chemical Company. In a typical experiment, 0.5 mL of the resin was used with isotonic saline as the mobile phase (102,103). In each experiment 10 mL of saline were used to elute the sample. The percent recoveries of BCPDA, HSA, and MAb were determined by measuring the UV absorbance before and after elution of these samples through the column. The wavelengths used in these determinations were 280 nm for proteins, and 324 nm for BCPDA. This technique was used to determine the % complexation of Sm-BCPDA, Sm-DTPA, Sm-BCPDA-antibody conjugate, and Sm-HSA.

(3.6) Complexation of BCPDA as a Function of pH

The concentration of BCPDA used for the above purpose was 10^{-4} M and at a mole ratio of 10 : 1 between BCPDA and low specific activity Sm. The pH values utilized were 4, 5, 6, and 7.5. The reactions were performed in acid washed glass vials for 16 hours. The mixtures were then analysed by cation exchange chromatography. The radioactivities of the column and the wash were measured in order to determine the % complexation. In all experiments the residual radioactivity of each vial was also measured.

(3.7) Determination of the Rate of Hydrolysis of BCPDA

The rate of hydrolysis was determined by measuring the ability of BCPDA to conjugate to HSA. Initially BCPDA was allowed to remain in a solution of ethanol for various time periods, before adding the required volumes to a solution of HSA. The protein fraction of this mixture was separated from the unconjugated BCPDA by G-50 size exclusion chromatography. A UV spectrum of the protein fraction was then obtained for each sample. The following concentrations and volumes of BCPDA and HSA were used in each experiment.

(1) Control experiment - 10 μ L of BCPDA in ethanol (95 % v/v) at a concentration of 1mg /mL was mixed immediately with a 100

μL solution of HSA (1mg/mL) in carbonate buffer of pH 9.

(2) A 10 μL solution of BCPDA in ethanol was allowed to remain in solution for 20 minutes before the addition of 100 μL of HSA at the same concentrations as above.

(3) A 10 μL solution of BCPDA in ethanol was allowed to remain in solution for 40 minutes before the addition of 100 μL of HSA as previously described.

All samples were allowed to react for about 2 hours before the protein fractions were purified from the unconjugated chelate.

(3.8) Size Exclusion Chromatography

Sephadex G-50 and Sephacryl S-300 (superfine) gels, obtained from the Sigma Chemical Company and Pharmacia respectively, were used. The column dimensions for Sephadex G-50 were 1.0 cm X 15.0 cm and the eluting buffer was acetate buffer (pH = 6, 0.1M). The column used for Sephacryl S-300 was 1.0 cm.X 45 cm, and the eluting buffer was also an acetate buffer of pH 6. This technique was mainly used to purify conjugates from free chelates (G-50) and from aggregated protein molecules (S-300).

(3.9) Thin Layer Chromatographic (TLC) Analysis of Sm^{3+} Complexes

Cellulose (Merck-5577) TLC plates were used in this study (108). The length and width of each plate were 7cm and 0.5cm respectively. The solvent system consisted of a mixture of MeOH/0.1N HCl (70 : 30 V/V) (108). After developing the Sm complexes on the TLC, the plate was cut into two portions 0.5cm above the origin. Both sections were then counted to obtain the percentage complexation or labeling. Complexes of Sm analysed by this method were, (1) Sm-BCPDA, (2) Sm-DTPA, (3) Sm-BCPDA-antibody conjugate, and (4) Sm-HSA.

(3.10) Conjugation of BCPDA to HSA

The method used for the conjugation of BCPDA to HSA is identical to that which was reported by Evangelista (2). Briefly, the procedure is as follows : The protein was first dissolved in an appropriate buffer. The BCPDA was dissolved in 95% (v/v) ethanol. The desired concentrations and mole ratios of the protein and the chelate were mixed for the required amounts of time. The percentage of ethanol in the final reaction mixture was equal to or less than 10%. Table 7 depicts the concentrations, reaction ratios, times and pH that were used. The conjugated protein was purified from the free chelate by Sephadex G-50 size exclusion chromatography.

Table 7 Conjugation of HSA to BCPDA

final concentration of HSA [M]	final concentration of BCPDA [M]	mole ratio of HSA:BCPDA	pH of medium	time of reaction
(A) 1.3×10^{-5}	1.4×10^{-5}	1:1	7.2	1/2 hr.
(B) 1.3×10^{-5}	1.4×10^{-4}	1:10	9.0	15 hr.
(C) 1.3×10^{-5}	1.4×10^{-4}	1:10	7.2	1/2 hr.
(D) 1.6×10^{-5}	7.6×10^{-5}	1:5	7.2	1/2 hr.
(E) 1.3×10^{-6}	1.5×10^{-4}	1:100	7.2	1/2 hr.

(3.11) Determination of the Degree of Conjugation

Two methods were used for the measurement of the degree of conjugation of BCPDA to the protein. (a) UV spectrophotometric method, proposed by Evangelista (2) and (b) a radioactive method.

(1) UV method

Once the protein conjugate was purified by G-50 size exclusion chromatography, the concentration of the chelate conjugated to the protein was determined by measuring the UV absorbance at 324 nm. Molar absorptivity at 325 nm is given as $1.52 \times 10^4 \text{ mol}^{-1} \text{L.cm}^{-1}$ (2). Since the concentration of the protein is known and the concentration of the chelate can be determined from the above data, the number of chelates per mole of protein can be determined.

(2) Radioactive method

Once the ligand - protein reaction was complete, radioactive $^{153}\text{SmCl}_3$ (low specific activity) in acetate buffer of pH 6, was added to the mixture containing the protein and the ligand. The moles of Sm added was less than the total number of moles of ligand in the mixture. The radiolabeled conjugate was separated from the radiolabeled free ligand. Activities of both species were determined and % radioactivity in each component was calculated. Since the concentrations and the reaction ratios of the protein and the ligand are known, the number of ligands per mole of protein could also be calculated.

(3.12) Radiolabeling HSA-BCPDA Conjugates with ^{153}Sm

HSA conjugates with 4.5 and 9.0 moles of BCPDA per mole of protein were labeled with low specific activity $^{153}\text{SmCl}_3$ in 0.1M acetate buffer of pH 6. Mole ratios of 10 : 1, 40 : 1, and 100 : 1 between BCPDA and Sm were used. Complexation yields were determined by cation exchange chromatography. As a control experiment, pure HSA at a concentration equivalent to that of the conjugates was complexed with Sm for the same period of time and analysed by cation exchange chromatography.

(3.13) Preparation of Monoclonal Antibody B43 (MAb B43) BCPDA Conjugates.

Monoclonal antibody B43, an antibody raised against the CA125 ovarian cancer antigen, generously supplied by Biomira Inc., at an original concentration of 6mg/mL in phosphate buffered saline (PBS) pH = 7.4, was used as a model compound. The antibody (2mg/mL in PBS pH=7.4) and BCPDA (1mg/mL in ethanol) were reacted for 60 minutes at the following mole ratios of protein to BCPDA : 1 : 1, 1 : 5 and 1 : 10 respectively. The % of ethanol in the final reaction mixture was equal to or less than 10%.

Since the last preparation (1 : 10) appeared cloudy at the end of reaction, it was first centrifuged for about 5 minutes. The supernatant of this solution, as well as preparations 1 : 1 and 1 : 5 were purified by G-50 size exclusion chromatography. The protein fraction of each of these solutions was analyzed for aggregates by HPLC.

(3.14) HPLC Analysis of MAb B43 Conjugates

A high pressure liquid chromatograph (Tracor model # 970A) and a Spectra Physics integrator (SP4290) system was used for the analysis of MAb B43-BCPDA conjugates. The analyses were performed at a wavelength of 280 nm. Sample volume used in each experiment was 20 μ L. The column was a TSK G-3000SW (Toso Haas) (7.5X300mm.) which has a separation range of MW 1,000-300,000.

The mobile phase utilised was TSK buffer of pH 7.2, at a flow rate of 1 mL/min. The % of aggregates in the MAb B43 -BCPDA conjugates was determined by dividing the integrated areas of the aggregate peaks by the total integrated peak areas of the aggregates and the conjugate monomer peaks.

(3.15) Determination of the Factors Affecting the Formation of Aggregates.

In order to determine some of the factors which might affect the degree of aggregate formation as a result of conjugation, the influence of the following three variables on aggregate formation was studied.

(1) Nature of proteins used (immunoglobulins versus albumin).

In this case, a HSA solution (1 mg/mL in PBS pH=7.4) and human gamma globulin (IgG) solution at a concentration of 0.5 mg/mL in PBS were conjugated with a BCPDA solution (1 mg/mL in ethanol) at various ratios. The extent of aggregation as a result of this reaction was measured by HPLC as described before.

(2) The Influence of the Rate of Addition of BCPDA to the MAb B43 Sample.

To 1 mL of the MAb B43 solution (2 mg/mL PBS), 50 microlitres of a BCPDA solution (1 mg/mL ethanol) were added slowly over a

period of 10 minutes to obtain a mole ratio of 5 : 1 between the chelate and the antibody. After 2 hours the resulting solution was analysed by HPLC for aggregates.

(3) The Effect of Concentration of the MAb B43 on the Formation of Aggregates.

The effect of MAb concentration on the formation of aggregates was measured by using three sequential dilutions of the antibody (2mg/mL, 1mg/mL, and 0.5mg/mL). These MAb samples were then allowed to react with a BCPDA solution (1mg/mL) at mole ratios of 5 : 1. Once the reaction was complete, the samples were analysed by HPLC for % aggregate formation.

(3.16) Iodination of MAb B43

Ten microlitres of a solution of iodogen in CHCl_3 (1mg /4mL) were transferred into two tubes. The CHCl_3 was then evaporated using a stream of air. Three hundred microlitres of a MAb B43 solution (1mg/mL) in PBS of pH 7.2 were mixed with 10 μL of no-carrier-added Na^{125}I (specific activity of this sample was 4 GBq/mL which was obtained from the Edmonton Radiopharmaceutical Centre) and transferred to the iodogen coated test tubes. The iodination of the protein was then allowed to proceed for 5 minutes. At the end of 5 minutes, the content of each of these tubes was added to tubes containing 10 μL of 1M Na^{127}I solution. This mixture

was then applied to a 3mL PD-10 (Sephadex GM-25) column. Five hundred microlitres of PBS were used to elute the iodinated protein. Each of the above iodinated protein samples was then analyzed for radiochemical purity by developing them on ITLC (61886) obtained from Gelman Sciences Inc. with a solvent mixture consisting of methanol : water (85 : 15 v/v) as the mobile phase. The ITLC plates were then cut into two pieces, 0.5 cm above the origin. Each piece was then counted as described in section (3.26).

(3.17) Purification of BCPDA-MAb B43 Conjugates by S-300 Chromatography

Initially, the following mole ratios of the antibody and the chelate, as shown in Table 8, were mixed for 90 minutes.

Table 8 Conjugation of BCPDA to MAb B43

Sample	MAb B43 2mg/mL in PBS pH =7.2	BCPDA 1mg/mL in ethanol	Mole ratio
1	2 mL	20 μ L	1 : 1
2	2 mL	100 μ L	1 : 5
3	2 mL	200 μ L	1 : 10

Sample #(3) turned cloudy as soon as the two components were mixed. This sample was first centrifuged for about 5 minutes, and the supernatant was collected. The supernatant of this solution, together with samples (1) and (2) were then eluted on the S-300 column, using acetate buffer of pH 6.

(3.18) Radioimmunoassay of Antibody Conjugates

To determine the immunoreactivity of the MAb B43-BCPDA conjugates, a competitive inhibition radioimmunoassay developed by Biomira Inc. was utilised. These experiments were performed by Ms. Heidi Erb.

Procedure : The following concentrations of the standard MAb B43 were made in phosphate buffered saline (PBS), containing 1% BSA : 48, 24, 12, 6, and 3 ng/ 50 μ L of buffer. Conjugated MAb B43 test samples having approximately the same concentrations as the above samples, were also prepared in PBS. Several test tubes were coated with the "catcher" antibody, anti CA-125 (MAb B-27.1) that reacts with a distinct epitope of the ovarian cancer antigen (OV antigen) CA 125. To these test tubes 50 μ L of the standard and the test MAb B43 samples that would react with a different epitope of the same OV antigen were added. To each of these test tubes, 50 μ L of the OV antigen and 150 μ L of 125 I-MAb B43 tracer were then added. Three separate control test tubes were made by adding 50 μ L of buffer, 50 μ L of the OV antigen and 150 μ L of 125 I-MAb B43 to

anti CA-125 coated test tubes. All test tubes were shaken for a few minutes and incubated at room temperature overnight. Next, the contents of all the test tubes were aspirated, washed twice with water and counted. A plot of % inhibition versus concentration of antibody, is made and the concentration at which the binding of the tracer is inhibited by 50% (IC_{50}) is calculated.

(3.19) Radiolabeling MAb-BCPDA Conjugates

The three conjugate preparations described in section (3.17) which were purified by the S-300 column, were labeled with high and low specific activity $^{153}Sm^{3+}$ in acetate buffer at a pH of 6, for various time periods, in Teflon and glass vials. Aliquots of the resulting mixture were analysed at specific time intervals by cation exchange chromatography and by cellulose TLC. In the case of cation exchange chromatography, the radioactivities of the column, wash, and of the vial were determined, while in the TLC method, the radioactivities of both the sections were determined.

(3.20) Determination of Non-Specific Binding of MAb B43 to Teflon Vials

In order to determine the percentage of the antibody concentration that may not be recovered at the end of experiments performed in Teflon vials due to the adsorption of the MAb on to the vial, the following experiment was conducted utilising the tracer

^{125}I labeled MAb B43. Constant volumes of MAb B43 containing the tracer in Tris buffer of pH 7.2, with known radioactivities at various concentrations, were allowed to shake for 24 hours in Teflon vials. The MAb solutions were then removed from the vials, and the radioactivity of the unwashed empty vials was determined.

(3.21) Determination of Non-Specific Binding of ^{153}Sm to Teflon Vials.

The objective of this experiment was to investigate whether the non-specific binding of ^{153}Sm to the vial was a function of the metal ion concentration. Various concentrations of ^{153}Sm in acetate buffer at a pH of 6, were allowed to shake for 12 hours in Teflon vials. The solutions were then removed and the radioactivities of the empty vials determined, after washing them with 1 mL of buffer. (high specific activity ^{153}Sm was used in the above experiments).

(3.22) Analysis of Antibodies by Electrophoresis

The system used was the Pharmacia PHAST SYSTEM, that consists of a separation unit (B459532) and a development unit (B459533). The test samples were analysed under nonreducing conditions, using polyacrylamide gel electrophoresis in the presence of sodium dodecyl sulphate (SDS-PAGE). Homogeneous PhastGels were used in all analyses. These gels contain constant concentrations of polyacrylamide. The buffer system of the gel

consisted of 0.112M acetate, 0.112 M Tris, of pH 6.5. The PhastGel SDS buffer strips consists of 0.2M tricine, 0.2M Tris, and 0.55% SDS at a pH of 8.1. Separation was performed for 20 minutes at 250 volts (70Vh).

(3.22 a) Preparation of the Molecular Weight Standards

Low molecular weight calibration kit vial containing a mixture of 6 proteins, with a molecular weight range of 14,400-94,000, and each at a concentration approximately of 100 μ g per vial, obtained from Pharmacia, were utilized. The standard protein mixture was dissolved in 100 μ L of distilled water containing 2.5% sodium dodecyl sulfate (SDS) and 5% β - mercaptoethanol and heated in a water bath at 100 °C for about 5 minutes to reduce and denature the proteins. Sufficient amount of the tracking dye, 1% bromophenol blue solution, was added to this mixture.

(3.22 b) Preparation of the Test Protein Samples

To 100 μ L solutions of MAb B43, SDS and bromophenol blue were added at the same concentrations as above. The samples were then centrifuged prior to application on the gel. One microlitre of each of the samples was added onto the applicator. At the end of the separation, the gel was developed using the following staining, destaining, and preserving solutions to depict the various protein

bands. Staining solution : Coomassie Blue R 250 staining solution, containing 30% MeOH, and 10% acetic acid. Destaining solution : distilled water containing 30% MeOH and 10% acetic acid. Preserving solution : Water containing 5% glycerol and 10% acetic acid. The developing time was 36 minutes.

(3.23) Determination of Percent Non-Specific Binding of ^{153}Sm to MAb in the Presence of BCPDA

When a MAb-BCPDA conjugate is labeled with Sm, a certain percentage of the Sm may bind non-specifically to the antibody while the rest of the Sm binds to the chelate. This will depend to a great extent on the relative affinities of the antibody and the chelate for the Sm. In order to determine these relative affinities, the following experiment was conducted using the undermentioned concentrations of MAb and hydrolysed BCPDA to simulate their concentrations in a conjugate containing three BCPDA molecules per MAb molecule.

To 500 μL of a MAb solution (3×10^{-6} M) in Tris buffer of pH 7.5, was added 170 μL of hydrolysed BCPDA solution (2×10^{-5} M) also in Tris buffer. To this mixture 40 μL of high specific activity $^{153}\text{SmCl}_3$ in Tris buffer (2×10^{-5} M) were added. The above mixtures were analysed by G-50 size exclusion chromatography and by cellulose TLC. In each method, the activities of the protein fraction and the chelate fraction were determined.

(3.24) Transchelation Studies

The two major species *in vivo* that have the potential of competing for Sm, when Sm labeled antibodies are administered into a patient are, HSA and bone material. Therefore, two separate experiments were performed utilising HSA and hydroxyapatite, the dominant component in the bone, to measure the competition of these two for Sm that was complexed to BCPDA.

(3.24 a) The Effect of HSA

(1) Sm-BCPDA versus HSA

(2) Sm-DTPA versus HSA

Initially the metal ligand complexes were prepared at a concentration of 10^{-5} M using a 10:1 ligand : metal ratio, in Tris buffer of pH 7.5. After sufficient time was allowed for this reaction to reach equilibrium, various amounts of HSA (see Tables 41 and 42) in Tris buffer were added to the metal ligand complex. The resulting mixture was then analysed at various time intervals by cellulose TLC, using the same conditions stated in section (3.9). As a control experiment free Sm was reacted with HSA for the same periods of time under the same conditions.

(3.24 b) The Effect of Hydroxyapatite

(1) Sm-BCPDA versus hydroxyapatite

(2) Sm-DTPA versus hydroxyapatite

Metal ligand complexes at concentrations of 10^{-5}M with a 10:1 ligand to metal ratio were first made in Tris buffer of pH 7.5. Various amounts of hydroxyapatite (calcium phosphate hydroxide) type 1 which is approximately a 25% solid suspension in 0.001M phosphate buffer of pH 6.8, obtained from the Sigma Chemical Company, were mixed with differing concentrations of the metal ligand complexes (see Tables 43 and 44) for 15 and 30 minutes. The mixtures were then centrifuged for 2 minutes at a speed of 1500 rpm. The radioactivities of the supernatant and the solid phase were determined.

(3.24 c) MAb-BCPDA- ^{153}Sm versus Teflon Vial

To measure the competition of the vial material for the BCPDA complexed Sm, the following experiment was performed. Various concentrations of MAb-BCPDA conjugates in Tris buffer of pH 7.5 containing 3 chelates per mole of MAb were allowed to react with ^{153}Sm for various time intervals in teflon vials. At the end of each time period, the mixture was removed from the vial and the latter was washed with 1 mL of Tris buffer. The resulting residual radioactivity of each vial was determined.

(3.25) Biodistribution Studies in Mice

In this study, injection of radiolabeled antibody solutions in acetate buffer of pH 6 and the dissection of animals were performed by Dr. Z Peng. The method adopted was similar to the standard operating procedure provided by Biomira Inc. Initially high specific activity ^{153}Sm was reacted for 1 hour with 1.5 mL of the MAb B43 conjugate that contained 3 chelates per protein molecule. The resulting mixture was diluted with acetate buffer to obtain a total volume of 2.5 mL. The final solution contained approximately 20 μg of antibody and 2.96×10^5 Bq of ^{153}Sm radioactivity per 100 μL . Twelve Balb C mice were injected, each with 100 μL of sample using a tail vein. The syringes were weighed before and after injection to obtain the weight of dose injected.

Four mice at each of the following time periods of 6 hours and 24 hours, and three mice at the end of 48 hours were sacrificed. The mice were then dissected and various organs were removed, weighed, and counted for their radioactive content.

One hundred microlitres of the residual sample was weighed and diluted in 10 mL of acetate buffer. One hundred microlitre, two hundred microlitre, and three hundred microlitre aliquots of this solution were counted in triplicate. The radioactivities of these solutions served as the dose standards for each time period.

(3.26) Counting of Radiolabeled Compounds

All radioactive compounds were counted for two minutes either in a Beckman 8000 or a Packard 5530 multi-sample gamma counter that contains a NaI (TI) detector. ^{153}Sm labeled compounds were counted within an energy range of 60 KeV to 250 KeV and ^{125}I labeled compounds in the range of 15 KeV to 80 keV. The radioactivity was expressed as counts per minute (CPM).

(3.27) Experimental Statistics

All experiments were performed in duplicate, (n=2) unless otherwise indicated. The average or the mean results of these duplicate experiments are reported. Labeling of MAb-BCPDA conjugates with high specific activity ^{153}Sm was performed in triplicate (n=3) and the biodistribution studies were conducted in quadruplicate (n=4) at each time interval.

(4.0) RESULTS AND DISCUSSION

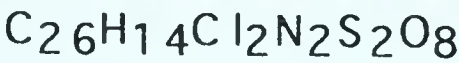
(4.1) Synthesis of BCPDA

(4.1.1) Preparations #1-#4

In preparation #1, the NMR of the product obtained, after step (a) had proceeded for 6 hours, (2) indicated the presence of methyl protons by the appearance of a peak at $\delta = 3.0$. When a portion of this compound was further reacted for an additional 5 hours, with more NCS and benzoyl peroxide, the methyl proton peak still appeared in the ^1H NMR spectrum. Another 5 hours of refluxing with more NCS and benzoyl peroxide ensured complete reaction, by the disappearance of the methyl protons. Compound (2) has the following NMR peaks. $\delta = 7.5$ (m, 10H), $\delta = 8.0$ (s, 2H), and $\delta = 8.3$ (s, 2H). These were comparable to the results obtained by Evangelista (2). Compound (2) was reacted with H_2SO_4 to obtain compound (3) as indicated in the experimental section. The melting point was observed to be about 200°C . The melting point range reported in the literature (2) was 202°C - 208°C . The percent yield for this step was 83 %. When compound (3) was reacted with chlorosulfonic acid for about 4 hours as specified in the literature, a dark brown product which had a melting point greater than 290°C was obtained. The IR spectrum (KBr disk) for this compound is depicted in spectrum 1, Appendix 1. The major peaks depicted in this spectrum are at 2900 cm^{-1} to 3700 cm^{-1} (-OH of carboxylic groups) 1700 cm^{-1} ($\text{C}=\text{O}$)

1300, cm^{-1} and 1100 cm^{-1} ($\text{O}=\text{S}$). ^1H NMR of this compound in $(\text{CD}_3)_2\text{SO}$ consisted of the following peaks-: $\delta = 7.65$ (m, 4H), $\delta = 7.85$ (m, 4H), $\delta = 8.05$ (m, 2H), $\delta = 8.3$ (m, 2H). These peaks pertain to the aromatic protons. The broad peak seen at $\delta = 7$ is due to the rapid exchange of the carboxylic protons of BCPDA with water. When a small quantity of D_2O was added to this sample, the peak at $\delta = 7$, moved to $\delta = 4$. This experiment proves the presence of exchangeable protons, namely the carboxylic protons in compound (4). NMR and IR data reported in the literature (2) are as follows. IR KBr disk 2800 to 3600, 2500 (shoulder), 1730, 1620, 1595, 1510, 1480, 1450, 1310, 1220, 1180, 1030, 895, 840, and 695 cm^{-1} . ^1H NMR in $(\text{CD}_3)_2\text{SO}$ δ 7.61 to 7.67 (m, 4H), 7.83 to 7.87 (m, 4H), 8.02 to 8.13 (m, 2H), 8.30 to 8.33 (m, 2H). The literature claims that the final product, compound (4), has a light yellow colour. The results of an elemental analysis of my product are shown below in Table 9.

Table 9 Elemental Analysis of Compound (4)



(Preparation #1)

Element	Theoretical %	Experimental %
C	50.58	22.26
H	2.28	1.11
N	4.54	1.86
Cl	11.48	4.49
S	10.38	11.80
O	20.74	9.06
C : N	11.14	11.96
C : H	22.18	20.05
C : S	4.87	1.89
C : Cl	4.41	4.95

One can see that although the spectral data imply that compound (4) is pure, the elemental analysis indicates otherwise. It appeared that significant amount of impurities were present in this compound mixture. It was also evident that the experimental value of C : S ratio was significantly smaller than the theoretical value, which could have meant that the impurity was predominantly a sulfur containing material.

In preparation # 2, the unused portion of the incompletely reacted compound (2) was used in the preparation of compound (4), under the same conditions as before. The melting point and the NMR data of the final compound in this preparation conformed to the data given in the literature. The results of the elemental analysis (Table 10), have shown that the % C was slightly lower and % Cl was slightly higher than the theoretical and literature values. This is reflected in the C : Cl ratio where the experimental value is much lower than the theoretical value. The point that could be made at this stage, considering the results of these two preparations, is that the nature of the impurity may still be inorganic but the composition has changed from a predominantly sulfur containing compound to a chlorine containing compound.

Table 10 Elemental Analysis of Compound (4)
(Preparation #2)

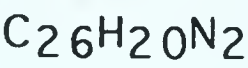
Element	Theoretical %	Experimental %
C	50.58	48.07
H	2.28	2.48
N	4.54	4.36
O	20.74	20.44
Cl	11.48	13.37
S	10.38	10.45
C : N	11.14	11.03
C : Cl	4.40	3.48
C : H	22.18	19.38
C : O	2.44	2.35
C : S	4.87	4.60

The next preparation (#3) of compound (4) resulted in a black powder. It was then decided to perform elemental analyses of the starting material and of the intermediate compounds (2) and (3) at the end of each step to determine which of these compounds is impure, and to purify that compound prior to proceeding with the next step of the synthesis. The results of the elemental analyses of the compounds in this preparation (#4) are given below in Tables 11

to 13.

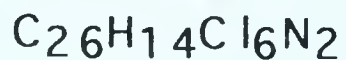
Table 11 Elemental analysis of Bathocuproine

(Compound 1)

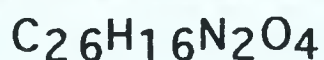


Element	Theoretical %	Experimental %
C	86.6	84.0
H	5.6	5.6
N	7.8	7.5
C : N	10.9	11.2
C : H	17.4	15.1

The lower % of C, and C : H values were assumed to be due to moisture present in bathocuproine.

Table 12 Elemental Analysis Of Compound (2)

Element	Theoretical %	Experimental %
C	55.06	52.06
H	2.49	2.43
N	4.94	4.59
Cl	37.51	38.80
C : N	11.14	11.34
C : H	22.11	21.42
C : Cl	1.47	1.34

Table 13 Elemental Analysis of Compound (3)(Preparation # 4)

Element	Theoretical %	Experimental %
C	74.0	53.13
H	3.8	3.77
N	6.6	4.75

Compound (3) has the following NMR peaks. $\delta = 7.7(\text{m}, 10\text{H})$,

8.1(s, 2H), 8.35(s, 2H). These results were comparable to those reported in the literature (2). It was also observed that compound (3) contained a certain amount of black material. The above results clearly demonstrate the presence of a significant concentration of impurities in compound (3.). Therefore, it was believed necessary to purify compound (3) according to the procedure outlined in the experimental section before proceeding with the final step of the synthesis in order to prepare compound (4) with adequate purity. This is contradictory to what is reported in the literature (2) which claims a direct synthesis of BCPDA was possible without the need of any purification steps.

In the final preparation of BCPDA (preparation #5), a percentage yield of 42.3% was obtained for compound (2). This product was then used to synthesize compound (3). The NMR of this compound was comparable to that reported in the literature (2), and Table 14 shows the results of the elemental analysis.

The above results confirm that the predominant element that constitute the impurity is sulfur. This compound was then purified according to the method described in the experimental section. A total of 260 mg of the purified compound was isolated. This represents a yield of 35% in the preparation of compound (3) from compound (2). The results of the elemental analysis of this compound after purification are shown in Table 15.

Compound (4) i.e. BCPDA was synthesized from this purified

product with a yield of 66%. See attached IR, NMR, UV, and FABMS spectra of this compound (4) (spectra 2- 5, Appendix 1). The IR and the NMR spectra were similar to those obtained at the end of preparation #1. The UV spectrum depicts two absorption maxima at 292 nm and at 324 nm. The $[M H]^+$ peak that is normally associated with FAB mass spectra is seen in spectrum # 5, at $m/e = 617 = [BCPDA H]^+$. The results of an elemental analysis of this compound are depicted in Table 16.

Table 14 Elemental Analysis of Compound (3) Before Purification

Element	Theoretical %	Literature % (1 H ₂ O)	Experimental %
C	74.0	71.73	60.06
H	3.8	4.14	4.06
N	6.6	6.39	5.37
S	-	-	3.81
Cl	-	-	0.0

Table 15 Elemental Analysis of Compound (3) After
Purification

Element	Theoretical %	Literature % (1 H ₂ O)	Experimental % Batch # 1	Experimental % Batch # 2
C	74.0	71.73%	69.96	69.78
H	3.8	4.49	4.07	4.04
N	6.6	6.29	6.19	6.20
O	15.6	not determined	15.05	17.76

Table 16 Elemental Analysis of Compound (4)
(Preparation # 5)

Element	Theoretical %	Literature %	Experimental %
C	50.58	50.27	50.22
H	2.28	2.39	2.81
N	4.54	4.26	3.97
Cl	11.48	11.67	11.24
S	10.38	10.51	10.44

Percentage of oxygen is not included in the above Table, because the previous analyses have produced inconsistent results and also the literature does not provide the oxygen %.

(4.1.2) TLC Studies of BCPDA (Hydrolysed)

As we were unable to develop a TLC system to analyse unhydrolysed BCPDA, the following systems were developed for the hydrolysed sample, one of these being a system reported in the literature (2). One spot was seen under all systems. Table 17 summarizes the R_f values obtained for the hydrolysed BCPDA, using various solvent systems.

Table 17 TLC Results of Hydrolysed BCPDA

TLC	Solvent system	R_f
Silica gel 60F 254	MeOH/CH ₃ NO ₂ /NH ₄ OH (50%/30%/20%)	0.47
As above	MeOH/Isopropanol/ NH ₄ OH (50%/30%/20%)	0.50
Reversed phase* KC18F	MeOH/CH ₃ NO ₂	0.60

* (Reference 2)

(4.2) Fluorometric Studies of BCPDA and Sm-BCPDA Complexes.

Fluorescence of BCPDA was observed when the molecule was excited by the absorption of UV radiation. The excitation wavelength was 320nm. The emission wavelength was determined to be about 410 nm. When energy is absorbed by a molecule in the ground state, it will be excited to higher energy states, commonly known as excited states. The molecule then relaxes or deactivates to its original ground state by the emission of photons (93). Normally, fluorescence of a molecule occurs quite rapidly upon reaching the excited state, and is defined as the emission of energy from the lowest level of the excited singlet state to the singlet ground state, without changing the spin of the excited electron (109). The intensity of emission is proportional to the concentration of the species, and therefore a plot of concentration versus the intensity of emission can be used as a mode of calibration in the determination of unknown concentrations of a species of known emission intensity.

When the ligand is complexed to a metal, the excited molecule can transfer its energy, via its triplet state to the metal ion. The metal ion can then undergo a radiative deactivation, which will lead to the metal ion fluorescence, characteristic to the particular metal ion (93). The major Sm^{3+} emissions are reported as (1) 560nm (2) 600nm and (3) 648 nm. These are strong to medium peaks (92). It has

also been observed that the complexing ligand did not significantly change the wavelengths at which metal ion emissions occurred (92). When Sm^{3+} was complexed to BCPDA, only emissions at 570nm, and 610nm were clearly observed (spectrum 6, Appendix 1). Since no fluorescence emissions were observed at these wavelengths, for free Sm^{3+} , the above results provide distinct proof to the fact that the Sm ion complexes to BCPDA under the experimental conditions employed.

(4.2.1) Determination of the Conditional Stability Constant (K') of a 1 : 1 Sm-BCPDA (hydrolysed) Complex at pH 7.5

Previous studies of Eu-BCPDA complexes by Diamandis (33) indicate that when the ligand is in excess, relative to the metal ion, complexes such as $\text{M}-(\text{BCPDA})_2$ and $\text{M}-(\text{BCPDA})_3$ are formed. As the metal ion concentration was increased, these complexes formed the 1 : 1 complex, M-BCPDA. Therefore, in the determination of K' , excess Sm ions were used to ensure the formation of Sm-BCPDA complex.

The residual concentration of uncomplexed BCPDA in sample mixture was determined using the calibration curve of [BCPDA] versus fluorescence emission intensity (see Table 19 and Figure 7). Tris buffer was used since it is believed to have minimal interactions with metals. A pH of 7.5 was selected since it

represents the physiological pH at which stabilities of metal ligand complexes should be measured to ensure that during *in vivo* experiments, if all other factors remain constant, stability of the metal ligand complex will remain unaffected. The fluorescence intensities of the uncomplexed BCPDA of duplicate sample mixtures of Sm and hydrolysed BCPDA, each at concentration of $1 \times 10^{-5} \text{M}$ and $0.89 \times 10^{-5} \text{M}$ respectively are shown in Table 18.

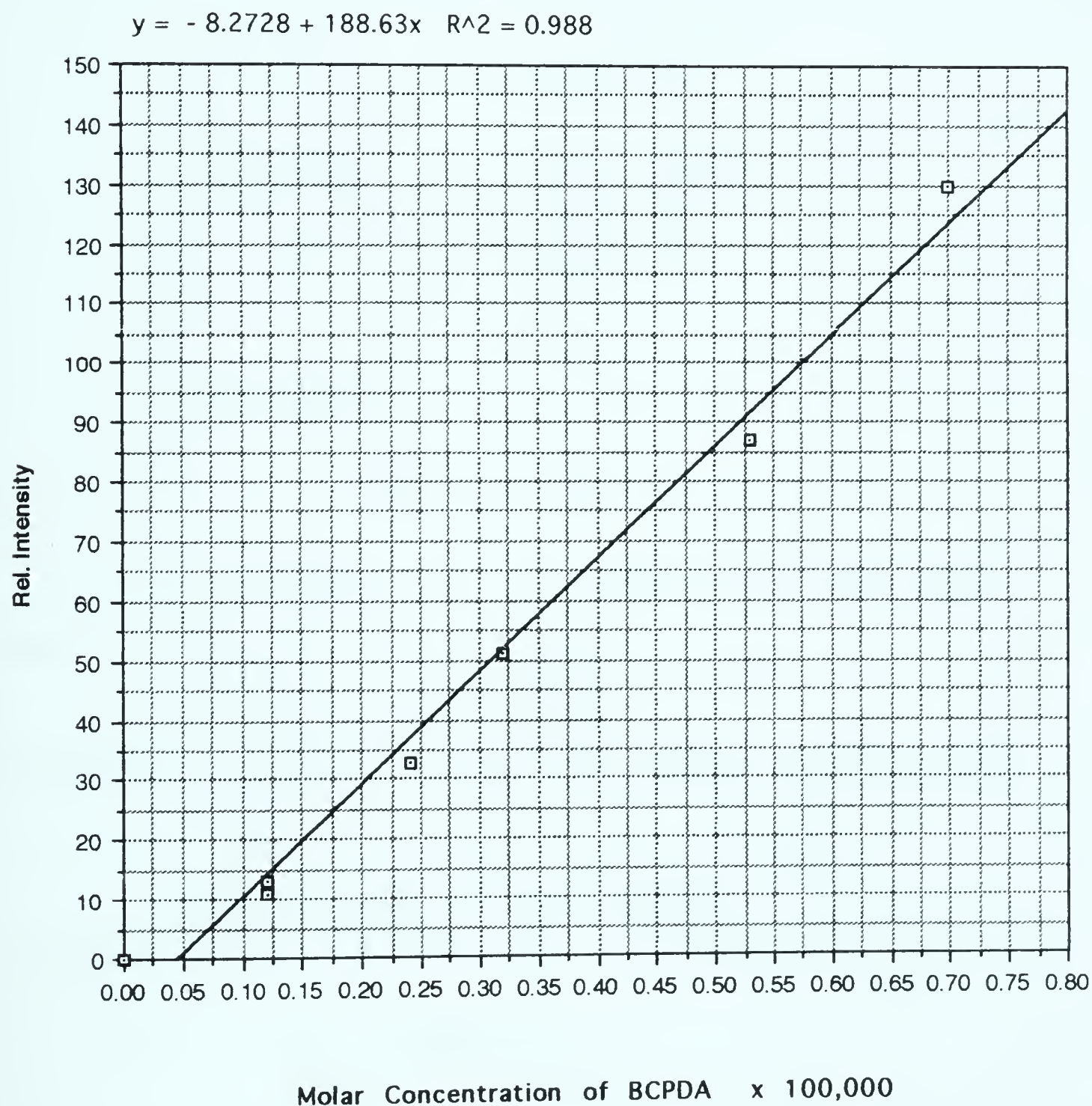
Table 18 Relative Intensities of Uncomplexed BCPDA in
Sm-BCPDA Mixtures

Mixture #	Relative Intensity
1	9
2	10

Table 19 Calibration of [BCPDA] Vs. Relative Intensity

Sample #	[BCPDA] M	Relative Intensity
1	1.2×10^{-6}	11
2	1.2×10^{-6}	13
3	0.24×10^{-5}	33
4	0.32×10^{-5}	51
5	0.53×10^{-5}	87
6	0.70×10^{-5}	130
7	0	0

Figure 7 A Plot of [BCPDA] Vs. Relative Intensity



Calculation of Uncomplexed [BCPDA]

From graph (Figure 7) $y = -8.27 + 188.63x$

$$x = [\text{BCPDA}]$$

$$\text{Mixture (1), } 9 = -8.27 + 188.63x$$

$$x = 1.0 \times 10^{-6} \text{M}$$

$$\text{Mixture (2), } 10 = -8.27 + 188.63x$$

$$x = 1.0 \times 10^{-6} \text{M}$$

Calculation of K'



A typical calculation of K' of mixture (1) is shown below.

$$\text{Start } M_{\text{total}}(T) = 2.6 \times 10^{-8} \text{ moles}$$

$$L_{\text{total}}(T) = 2.3 \times 10^{-8} \text{ moles}$$

$$\text{at equilibrium } [L_{\text{eq}}] = 10^{-6} \text{ M} = 2.6 \times 10^{-9} \text{ moles (from figure 7)}$$

$$ML_{\text{eq}} = 2.04 \times 10^{-8} \text{ moles} = L_T - L_{\text{eq}}$$

$$M_{\text{eq. moles}} = M_T - ML_{\text{eq}} = 5.6 \times 10^{-9}$$

$$\text{At equilibrium, } [M] = 2.2 \times 10^{-6} \text{M}, [L] = 1 \times 10^{-6} \text{M}, [ML] = 0.78 \times 10^{-6} \text{M}$$

$$K' = \frac{0.78 \times 10^{-6}}{0.22 \times 10^{-5} \times 1 \times 10^{-6}}$$

$$= 3.5 \times 10^6 \text{ M}^{-1}$$

$$\log K' = 6.54$$

Similarly for mixture (2), $K' = 3.5 \times 10^6 \text{ L/moles}$

$$\log K' = 6.54$$

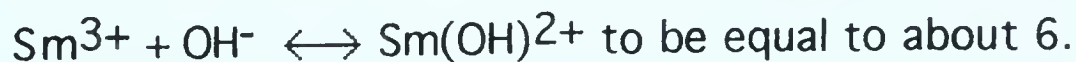
An attempt was made to estimate the stability constant ($K_{stab.}$) of this complex, under the conditions specified in the experimental methods section, utilizing the following assumptions.

(1) The pK_a of quinoline-2-carboxylic acid is 4.97 (Ref.110, p175). Since the chemical environment of $-COOH$ groups of BCPDA is similar to that of quinoline-2-carboxylic acid, it can be concluded that at pH 7.5, both the $-COOH$ groups are fully ionized, as long as the ionization of one $-COOH$ group does not affect the ionization of the other $-COOH$ group. If this is true, the $[L]_{eq}$ determined above would be $[L^{4-}]_{eq.}$. Therefore $\alpha_L = 1$.

(2) It has been reported (111), that $\log K$ for the following reactions are-:



Therefore one can assume that $\log K$ for the reaction,



$$\text{Therefore } \alpha_M = \frac{1}{1 + K[OH^-]} = 0.8$$

$$K_{stab} = \frac{K_{cond.}}{\alpha_L \alpha_M}$$

$$K_{stab.} = \frac{3.5 \times 10^6}{1 \times 0.8} = 4.4 \times 10^6 \text{ L/mole, at an ionic strength}$$

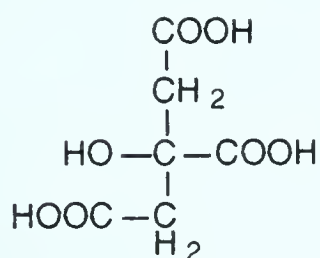
of 0.04 and at a temperature of 25 °C.

The stability constants of the following Sm^{3+} complexes with ligands containing similar functional groups to those of BCPDA, will now be considered.

Figure 8 Examples of Ligands Similar to BCPDA

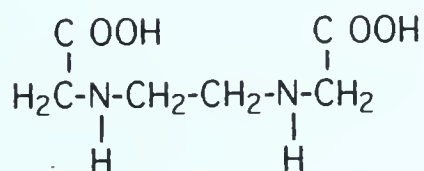
(a)

$K_{\text{stab.}} = 10^8 \text{ L/mole}$ (Ref. 110, p162, Ref. 112, p162.)



Citric Acid

(b)

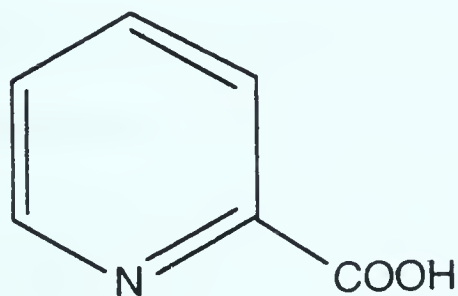


$K_{\text{stab.}} = 10^{8.3} \text{ L/mole}$
(Ref. 87, p70)

N' N'-Ethylene diamine diacetic acid

(c)

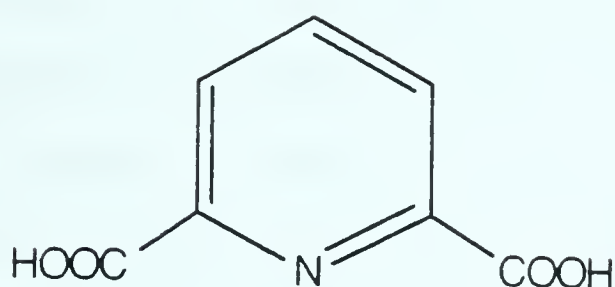
$K_{\text{stab.}} = 10^{4.3} \text{ L/mole}$
(Ref. 110, p172)



Picolinic Acid

(d)

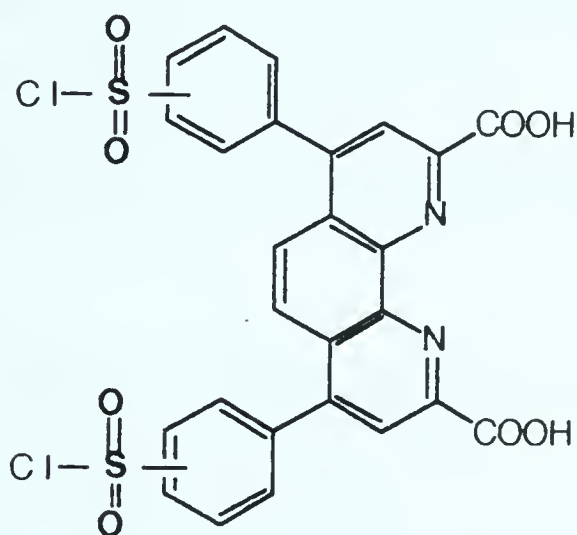
$K_{\text{stab.}} = 10^{8.7} \text{ L/mole}$
(Ref. 110, p174)



Dipicolinic Acid

(e)

$K_{\text{stab.}} = 10^7 \text{ L/mole}$
(approx.)



BCPDA

Of these compounds, EDDA, although it does not contain an aromatic backbone, contains all of the coordinating atoms of BCPDA that have the potential of interacting with the metal ion. The only difference being, EDDA due to the lack of an aromatic back bone, possesses extra flexibility to complex. The stability constant of EDDA is about one order of magnitude higher than the experimentally

obtained $K_{stab.}$ value of BCPDA. If one considers picolinic and dipicolinic acids, they both have aromatic nitrogen and also the former has one adjacent $-COOH$ group where as the latter has two $-COOH$ groups on either side of the nitrogen. As expected, dipicolinic acid has a much higher $K_{stab.}$ value than picolinic acid. It also appears to have a higher $K_{stab.}$ value than BCPDA.

If one considers all of the above facts, it may be suggested that either Sm complexes only with the two $-COOH$ groups of BCPDA or that the two nitrogens and one $-COOH$ group interacts with Sm. To obtain definitive proof of the Sm-BCPDA structure, crystallographic or molecular mechanical studies would have to be pursued.

(4.2.2) Some Theoretical Calculations Based on the $K_{stab.}$ of Sm-BCPDA

(a) Percent Complexation of Sm and BCPDA at Varying Equimolar Reacting Concentrations.

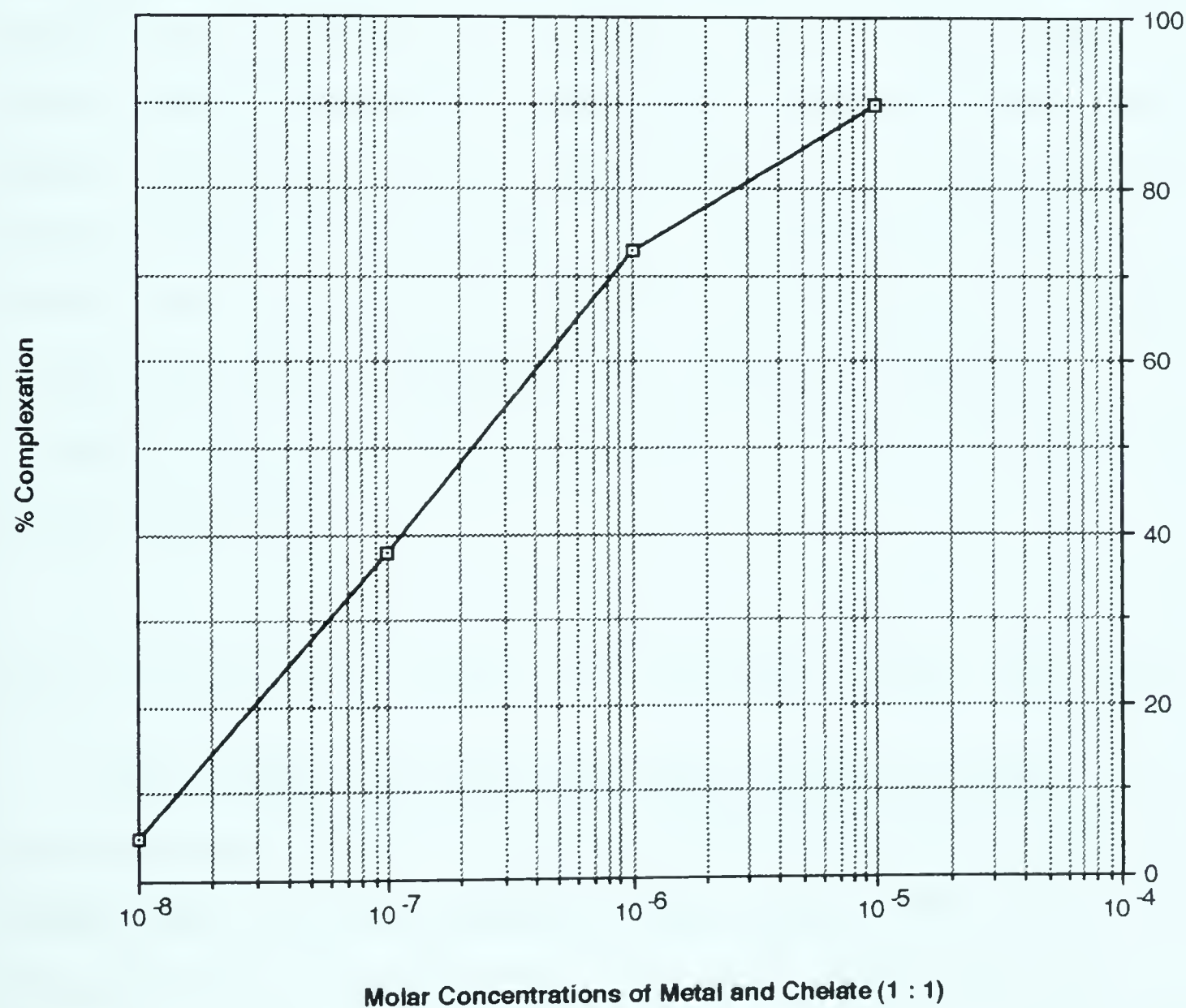
For example, if an equal number of moles of BCPDA and Sm^{3+} are added together, each at a final concentration of $10^{-5}M$, the % complexed would be 90%. A plot of % complexation versus the final reacting concentration of metal and ligand at a 1 : 1 mole ratio is given in Figure 9.

If one attempts to make a 1 : 1 Sm-BCPDA complex, where the metal and ligand is each at a final concentration of $10^{-8}M$, before

complexation, the % complexation according to the graph would be less than 10%. As the concentration of metal and ligand increase, the % complexation also increases.

Figure 9 Theoretical Complexations of Sm and BCPDA

Concentrations of Metal and Chelate vs. % Complexation



(b) Percentage of Metal Transchelated to Human Serum
Albumin (HSA) From Different Metal-BCPDA (1:1)
Complexes with Varying K

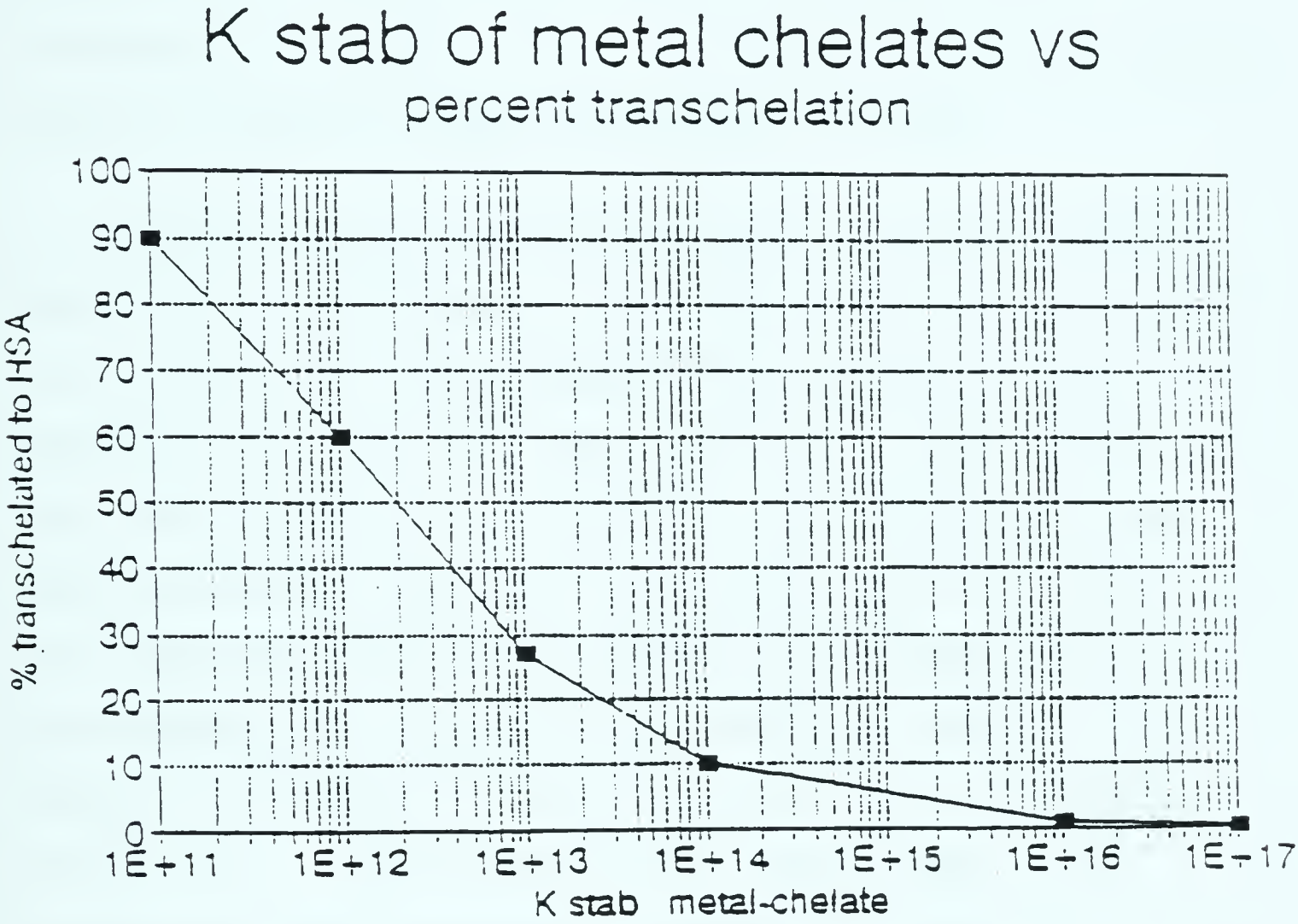
It has been reported by Schomacker(113) that the K' value of HSA and Eu to be 10^6 L/moles at a pH of 7.4. It can be assumed that the K' value of Sm-HSA would be very similar to the above value. In a typical *in vivo* experiment, if 1mg of an antibody which contains 3 metal complexed chelates is injected into a patient, the final metal chelate concentration *in vivo* would be about 10^{-9} M, assuming the volume of blood is 5 litres. The *in vivo* concentration of HSA is 10^{-3} M. Under these conditions the % metal transchelated to HSA, for various metal chelate complexes with differing K' values, are calculated and a plot of % transchelation as function of K' values is given in Figure 10.

(4.3) Complexation Studies of Hydrolysed BCPDA with Sm^{3+}

These studies were conducted using a cation exchange chromatographic method reported by Goeckler (102,103). In this method free Sm^{3+} and insoluble $\text{Sm}(\text{OH})_3$ remain on the cation exchange column, while complexed Sm will be eluted from the column. When ^{153}Sm is complexed with a ligand and eluted from the column, the % activity in the eluate represents the % complexation. The full recovery of the complex depends on the net charge of the

complex.

Figure 10 Theoretical Percentages of Metal Transchelated to HSA



If the complex is anionic, it can be eluted from the column quite easily. Since each hydrolysed BCPDA molecule has two sulphonate groups which are fully ionised at a pH of 7.5, and if a minimum of 2 : 1 mole ratio of BCPDA : Sm is used during complexation, an anionic complex would result even if one considers only the 4 negative charges of the sulphonate groups.

The first study we conducted using this technique was to measure the % complexation of hydrolysed BCPDA and Sm at various concentrations of metal and ligand. These results were then compared to the theoretical values obtained for approximately the same concentrations of Sm and BCPDA using the experimentally determined stability constant at the same pH (see Table 20). If a good correlation was obtained between the theoretical and the experimental values, it could provide additional evidence to the validity of the stability constant determined. Due to the reasons discussed, a 2 : 1 mole ratio of BCPDA : Sm was used. It was assumed that the % complexation between a 2 : 1 ratio and a 1 : 1 ratio are similar. The % recovery of BCPDA from the column was determined by measuring the UV absorbance at 324nm of a Sm-BCPDA complex before and after elution from the column. The recovery was determined to be 100%. The activity of a 100 μ L ^{153}Sm solution (10^{-5}M), a quantity of Sm that can be considered to be a maximum in these experiments, was observed to be fully retained on the column. The latter two experiments were the control

experiments with regard to the validity of using cation exchange chromatography to determine the degree of metal ligand complexations.

Table 20 Complexation Yields of BCPDA and Sm

Final Conc. of BCPDA	Final Conc. of Sm ³⁺	% Complexation (Experimental) (n=2)	% Complexation (Theoretical 1:1) (n=2)
(1)1.33x10 ⁻⁵ M	0.7x10 ⁻⁵ M	90±0	90
(2) 2x10 ⁻⁶ M	1x10 ⁻⁶ M	68±5	73
(3) 1x10 ⁻⁶ M	5x10 ⁻⁷ M	60±9.	60
(4) 2x10 ⁻⁷ M	1x10 ⁻⁷ M	55±6.	38

It is quite evident from these results that the experimental and the theoretical values are very similar. It should be noted that when samples (1) and (2) were analysed, a minimal amount of Sm remained in the vial. Residual Sm activities of the vials were not measured after samples (3) and (4) were analysed. Discrepancies between the experimental and the theoretical values in sample (4) could be due to the unaccounted activities remaining in the vials. The similarities between the experimental and the theoretical

values would mean that the experimentally determined conditional stability constant at this pH is fairly accurate, assuming that the metal ligand complex is quite inert and hence the equilibrium between the metal and the ligand is not disrupted to any great extent during the short separation time on the column. Another factor that could underestimate the experimental % complexation is the presence of the protonated forms of the complex which could give rise to cationic complexes. These cationic complexes could be retained on the cation exchange column, and result in lower observed activity in the wash. Since a ratio of 2 : 1 of hydrolysed BCPDA : Sm was being used, the contribution from a protonated species of the complex, to the % activity on the column could be considered to be negligible.

A similar experiment using DTPA and Sm was performed under the same conditions. The results indicate (see Table 21) that even at very low concentrations of metal and ligand almost complete complexation has occurred. If, for example, one compares the % complexation between Sm and BCPDA at a ligand concentration of 10^{-6}M and % complexation between DTPA and Sm at the same concentration of ligand, it is quite evident that the % complexation of the former is much lower than that of the latter complex. The only conclusion that can be made is that the stability of the DTPA-Sm complex is much greater than the stability of the BCPDA-Sm complex.

Table 21 Complexation Yields of DTPA and Sm

Final Concentration of DTPA	Final Concentration of Sm	% Complexation (n=2)
$1.3 \times 10^{-5} \text{M}$	$0.7 \times 10^{-5} \text{M}$	98 ± 2
$2 \times 10^{-6} \text{M}$	$1 \times 10^{-6} \text{M}$	98 ± 1
$1 \times 10^{-6} \text{M}$	$5 \times 10^{-7} \text{M}$	96 ± 0

(4.3.1) The Effect of pH on the % Complexation of BCPDA and Sm

An important factor that influences the % complexation of a metal ligand system, is the $[\text{H}^+]$ or the pH of the medium and depends on the competition between the metal ion and the H^+ for the binding sites of the ligand. The following results in Table 22 depict the variation of the % complexation with pH.

It appears that at a ligand concentration of 10^{-4}M and at a mole ratio of 10:1 between BCPDA and Sm, no significant change in the % complexation has occurred in the pH range of 4-7.5. Although the different conditional stability constants of a metal ligand system determine the % complexations at each pH, it appears that the observed complexation yields in this experiment were not significantly affected by the H^+ concentration of the medium, under the above experimental conditions.

Table 22 pH versus % Complexation

pH	Ligand Concentration M	BCPDA : Sm Mole Ratio	% Complexation (n=2)
4	10^{-4}	10 : 1	92 ± 0
5	10^{-4}	10 : 1	95 ± 0
6	10^{-4}	10 : 1	92 ± 1
7.5	10^{-4}	10 : 1	95 ± 2

(4.3.2) Radionuclidic Purity of Low and High Specific Activity Sm.

The gamma spectra of all samples of ^{153}Sm indicate that the % of radionuclidic impurities (short and long lived) in these samples are insignificant. Spectrum 7 (Appendix 1) is a gamma spectrum of a batch of enriched $^{152}\text{Sm}_2\text{O}_3$ after it was irradiated for about 5 minutes. As one can see the two most intense peaks are those associated with ^{153}Sm (70 KeV and 103 KeV). Spectra 8 and 9 (Appendix 1) are gamma spectra of new (1 week after the end of bombardment E.O.B.) and old (1 month E.O.B.) samples respectively, of $^{153}\text{SmCl}_3$ obtained from Nordion International Incorporation. The only difference between these two spectra, is the relative increase in intensity of the long lived ^{154}Eu in the spectrum of the old sample of $^{153}\text{SmCl}_3$.

(4.4) Rate of Hydrolysis of BCPDA

It has already been shown that the two absorption maxima of BCPDA, occur at 324nm and 294nm. The measurement and comparison of the absorbances at these wavelengths at various time periods during an experiment, would give an indication to the absolute concentration and to the rate of increase or decrease of the concentration of BCPDA. Since the ability of BCPDA to conjugate to HSA is measured by this experiment, the absorbance of HSA at 280nm should have minimal contribution to the absorbance at 324nm in order to achieve accurate results by this method. It has been reported in the literature (2, 33) and demonstrated by experiment (see spectrum 10 Appendix 1) that the contribution from 280nm to the 324nm is insignificant. Therefore the absorbance at 324nm at various time intervals was measured and the values at different times were compared. The results of this experiment are indicated in Table 23.

Table 23 Rate of Hydrolysis of BCPDA

Time (minutes)	Absorbance (A.U.) at 324nm
0	2.8×10^{-2}
20	1.5×10^{-2}
40	mostly absorbing at 280nm

It is quite apparent from the results shown in the above Table, that the rate of hydrolysis of BCPDA in an aqueous medium is rapid. The sulfonyl chloride groups are well known to undergo rapid hydrolysis when exposed to moisture. These results further confirm the necessity for BCPDA to be conjugated to the protein as quickly as possible prior to any significant loss in the concentration of the sulfonyl chloride groups.

(4.5) Conjugation of BCPDA to HSA

As stated in the experimental method section (Table 7), BCPDA was conjugated to HSA under different conditions to obtain the optimum conditions convenient for future conjugation and labeling experiments. G-50 size exclusion chromatography was observed to be quite satisfactory in the purification of protein conjugates from the unreacted BCPDA under the employed experimental conditions. Baseline separation was observed between the two species that enabled the collection of the two peaks with no apparent contamination of one from the other. Typical calculations in the determination of the degree of conjugation based on a UV method (2) and a radioactive method are given below.

UV Method

$$\text{moles HSA} = 1.47 \times 10^{-8}$$

$$\text{moles BCPDA} = 1.62 \times 10^{-8}$$

approximate mole ratio = 1: 1

pH = 7.3

total volume = 1.01mL

volume of protein fraction after elution = 6 mL

absorbance at 324nm = 0.04

$$\begin{aligned}\text{concentration of conjugated BCPDA} &= \frac{0.04}{1.52 \times 10^{-4}} \\ &= 0.026 \times 10^{-4} \text{ M}\end{aligned}$$

moles of BCPDA in 6mL = 1.57×10^{-8}

moles HSA = 1.47×10^{-8}

HSA : BCPDA = 1: 1

Radioactive method

activity in protein fraction = 138607 cpm

total activity eluted from column = 160676 cpm

% activity in protein fraction = 86%

$$\begin{aligned}\text{moles BCPDA conjugated} &= 86\% \text{ of } 1.62 \times 10^{-8} \\ &= 1.39 \times 10^{-8}\end{aligned}$$

moles of HSA = 1.47×10^{-8}

HSA : BCPDA = 1 : 1

Table 24 Degree of Conjugation HSA : BCPDA

Sample	Number of Chelates per Mole of Protein (UV Method) (n=2)	Number of Chelates per Mole of Protein (Radioactive Method) (n=2)
A	1.0±0.1	0.88±0.03
B	8.0±0	9.0±0.3
C	7.0±0.6	9.0±0.3
D	3.4±0.3	4.5±0
E	16.5±3.5	17.0±0

Please refer to Table 7 for concentrations, ratios and other reaction conditions employed in samples (A) to (E). Results in Table 24 appear to indicate that a good correlation exists in the values obtained for the degree of conjugation by the two methods utilized (UV and radioactive). The two methods are independent of each other and rely on different principles, namely in one method on the molar absorptivities and in the other method on the affinities of the ligands to Sm. The fact that the results obtained by the two methods are very similar, would tend to indicate that the molar absorptivities and the affinity for Sm of the conjugated and the unconjugated BCPDA are similar. Another factor that is clear from these experiments is that non-specific binding of Sm to HSA is

negligible at the concentrations used in these experiments. This assumption has also been proven in a later experiment. It can be seen that, when the reacting conjugation ratio between the BCPDA and HSA is low the degree of conjugation is very high (90%). But when the reacting ratio is increased, a dramatic decrease in the degree of conjugation is shown (19%). This is true for the results obtained by either of the methods (UV or radioactive) employed in the calculation of the degree of conjugation. Diamandis (33) has attributed several reasons for this phenomenon. (1) Since BCPDA has two sulfonyl chloride groups, two protein molecules may react with one BCPDA molecule, and (2) although HSA has 59 amino groups available to react with the ligand, some of these groups may not be readily exposed to the incoming ligands due to steric hindrance. These factors could lead to a level of saturation of the number of reactive and available amino groups. The results also appear to indicate that optimum % of conjugation can be achieved at a pH of 7 in 1/2 hour. Although the number of free amino groups increase as the pH is increased, the hydrolysis of the sulfonyl chloride groups also increases. This may explain the similar values obtained for the degree of conjugation at pH 7 and pH 9.

(4.5.1) Radiolabeling HSA-BCPDA Conjugates

Two separate labeling experiments were conducted utilizing HSA-BCPDA conjugates, where the molar ratios of BCPDA to HSA were 9 : 1 and 4.5 : 1 consecutively. The results of these

experiments are given in Tables 25 (a) and 25 (b).

Table 25 (a) Labeling of a Conjugate With 9 moles of BCPDA/Mole of HSA

Final Concentration of BCPDA	Mole Ratio of BCPDA:Sm	% Labeling (Complexation) (n=2)
3.8 X 10 ⁻⁵ M	100:1	93±0
3.6 X 10 ⁻⁵ M	40 :1	93±1
2.8 X 10 ⁻⁵ M	10:1	97±0

Table 25 (b) Labeling of a Conjugate With 4.5 moles of BCPDA/MOLE HSA

Final Concentration of BCPDA	Mole Ratio of BCPDA:Sm	% Labeling (Complexation) (n=3)
2.3X10 ⁻⁵ M	100:1	96±3
2.2x10 ⁻⁵ M	40:1	95±2
2.0X10 ⁻⁵ M	10:1	96±2

It is quite evident that the labeling efficiency depends on the concentrations of the ligand and not on the number of ligands attached to the protein. Therefore, one could conclude that additional stability is not conferred upon the metal ligand complex by the presence of a higher number of ligands in the conjugate, relative to a conjugate with lesser number of ligands but having the same ligand concentration as before. It is also apparent that a mole ratio of 10:1 between the ligand and the metal ion is adequate to obtain maximum complexation. The acetate buffer of pH=6 used for the labeling experiment appears to provide a suitable medium for this purpose. Finally when Sm is allowed to react with free HSA at a concentration similar to that of a HSA-BCPDA conjugate used in the above experiments, only about 4% of the activity is associated with HSA. These results confirm that non-specific binding of Sm to HSA is minimal at these concentrations.

(4.6) Conjugation of MAb B43 to BCPDA

MAb B43 conjugates, prepared under various conjugation ratios and purified by G-50 size exclusion chromatography were analysed by HPLC to determine the % of aggregates. Typical chromatograms of pure MAb B43 and of a MAb B43-BCPDA conjugate which was prepared at a mole ratio of 1 : 1 are given in Figures 11 to 12.

Figure 11 A HPLC Chromatogram of MAb B43

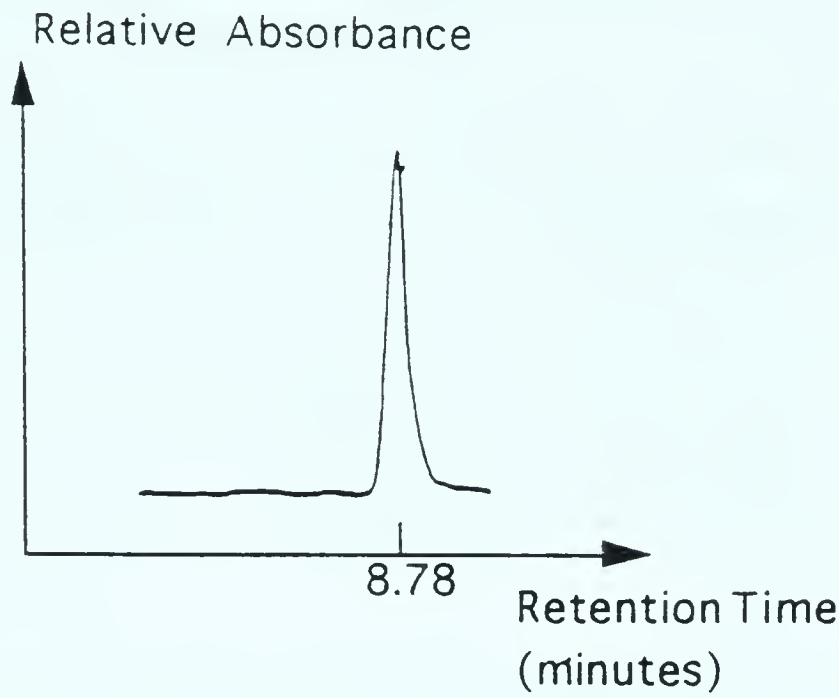


Figure 12 A HPLC Chromatogram of MAb-BCPDA Conjugate (1 : 1)

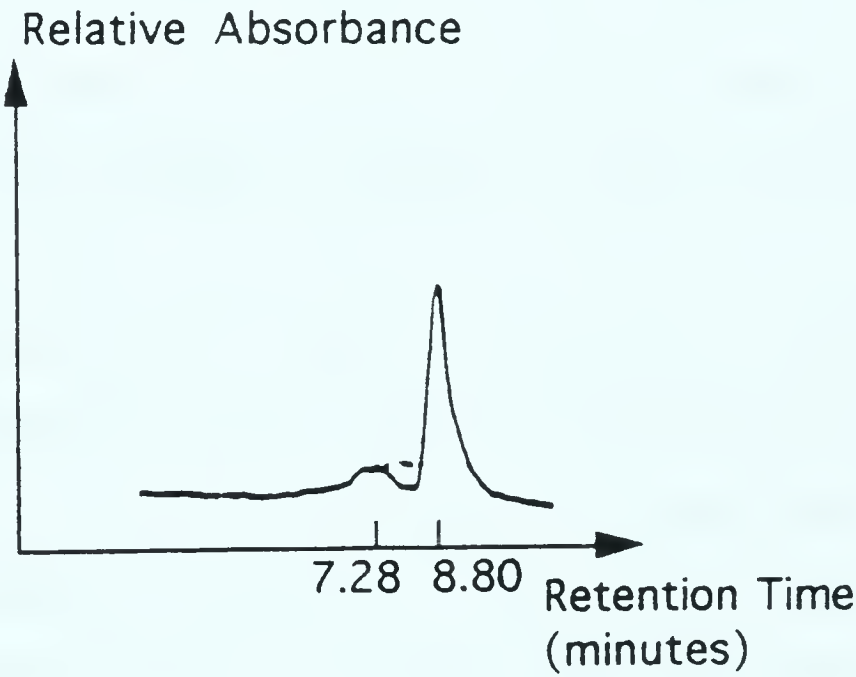


Table 26 Percent Aggregates of Conjugates
Purified by G-50

Reaction Ratio(BCPDA:MAb)	% Aggregates
1:1	(n=2) 9±3
5:1	(n=2) 42±2
10:1	(n=1) 46

Contrary to what was observed when HSA, or as reported in the literature (2) BSA was conjugated to BCPDA, a high degree of crosslinking appears to have occurred when BCPDA was conjugated to MAb B43. Since one BCPDA molecule has two sulfonyl chloride groups it can theoretically react with two protein molecules. Therefore, during the conjugation reaction, as there is an excess of BCPDA molecules present, crosslinking of proteins can occur that could ultimately lead to the formation of polymers or protein aggregates. It is also quite obvious that G-50 size exclusion chromatography is not a suitable method of purifying monomer conjugates from polymeric conjugates. These results (Table 26) are not unexpected since G-50 has a maximum separation range of only 50,000 M.W. Therefore, monoclonal antibodies which have a molecular weight of 150,000, and aggregates which obviously have much larger molecular weights than 150,000, would be eluted together in the void volume.

(4.6.1) Immunoreactivity of G-50 Purified Conjugates

The results of the inhibition radioimmunoassay performed on various samples of MAb B43-BCPDA conjugates are given in Table 27. The results are expressed as the concentration of the protein conjugate at which the tracer MAb B43 is inhibited by 50% (IC₅₀).

Sample #1	= control 0.3mg/mL pure antibody
Sample # 2	= control 0.3 mg/mL pure antibody + 10% EtOH
Sample # 3	= control 0.3 mg/mL pure antibody +10% EtOH and passed through G-50
Sample #4	= MAb : BCPDA 1 :1
Sample # 5	= MAb : BCPDA 1 : 5
Sample # 6	= MAb : BCPDA 1 : 10

All samples were in acetate buffer of pH 6

Table 27 Immunoreactivity MAb B43 Conjugates PurifiedBy G-50

Sample #	IC ₅₀
1	18.75ng
2	20.00ng
3	21.25ng
4	28.75ng
5	No Immunoreactivity
6	No Immunoreactivity

This assay is based on the ability of an antibody to compete with a radiolabeled, unmodified or a standard antibody, for a limited number of antigen sites. It is very important that one should know the accurate concentrations of the standard and the test antibody because the competition for the antigen by the two antibodies must be compared at equal concentrations. It is clear from the results given above (Table 27) that, apart from the 1:1 conjugate, both the other conjugates have completely lost their ability to compete with the standard radiolabeled MAb B43 for the antigen. The three control samples (unmodified or standard) utilized in this experiment have IC₅₀ values of an average of 20 ng. On the other hand, the 1:1 conjugate needs 28 ng to achieve the same % of inhibition. This would imply that more of the 1:1 conjugate relative to the

unmodified antibody is needed to achieve the same % inhibition or in other words to compete with the standard radiolabeled antibody bound to the antigen. The other two conjugates were unable to compete with the standard radiolabeled antibody even at very much higher concentrations. This loss in the ability of the modified antibodies or the conjugates to compete with the standard radiolabeled antibody relative to the controls is a reflection of a decrease in their immunoreactivities. From this experiment one might conclude that the BCPDA to antibody ratio should not exceed 1 : 1.

(4.6.2) Factors Affecting the Percentage of Aggregates

(1) Immunoglobulins (IgG) versus albumins.

The HPLC results of the conjugates prepared by the reaction of BCPDA with HSA or with human IgG are presented in Tables 28 and 29.

Table 28 Effect of Conjugation Ratio on the Crosslinking
of HSA

Conjugation ratio HSA:BCPDA	% Cross linked protein
1:10	not visible
1:20	not visible

Table 29 Effect of Conjugation Ratio on the Crosslinking
of Human IgG

Conjugation ratio IgG:BCPDA	% cross linked protein (n=1)
1:1	4
1:3	6
1:12	21

These preliminary results tend to indicate that no significant concentrations of cross linked proteins are formed when albumin is reacted with BCPDA, an observation that is supported in the literature by Evangelista and by Diamandis (2,33). In their studies, when BCPDA was conjugated to BSA, no cross linked proteins were visible. However, we observed a considerable degree of aggregate formation when IgG was allowed to react with BCPDA. (Figures 13 to

15). From these experiments, one tends to conclude that the formation of aggregates, when BCPDA is conjugated to proteins appears to be limited to both human IgG and MAb B43 only.

Figure 13 A HPLC Chromatogram of IgG

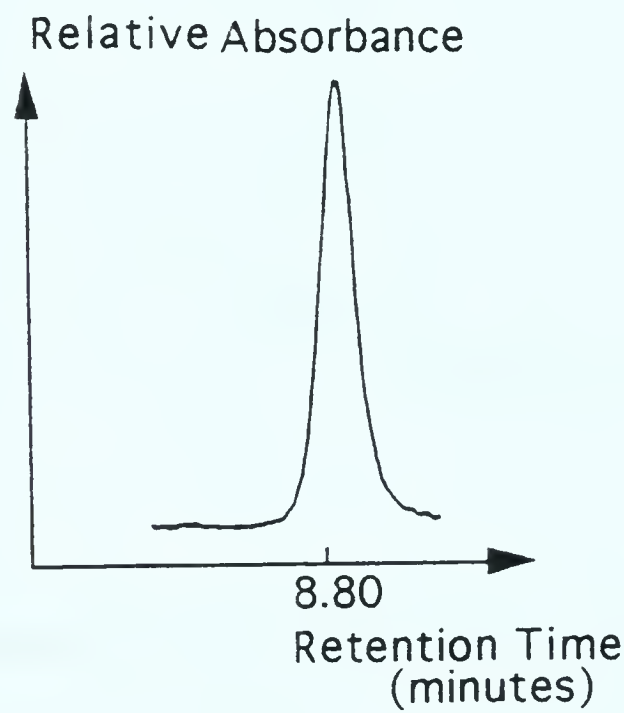


Figure 14 A HPLC Chromatogram of IgG and BCPDA at a 1 : 1 Mole Ratio

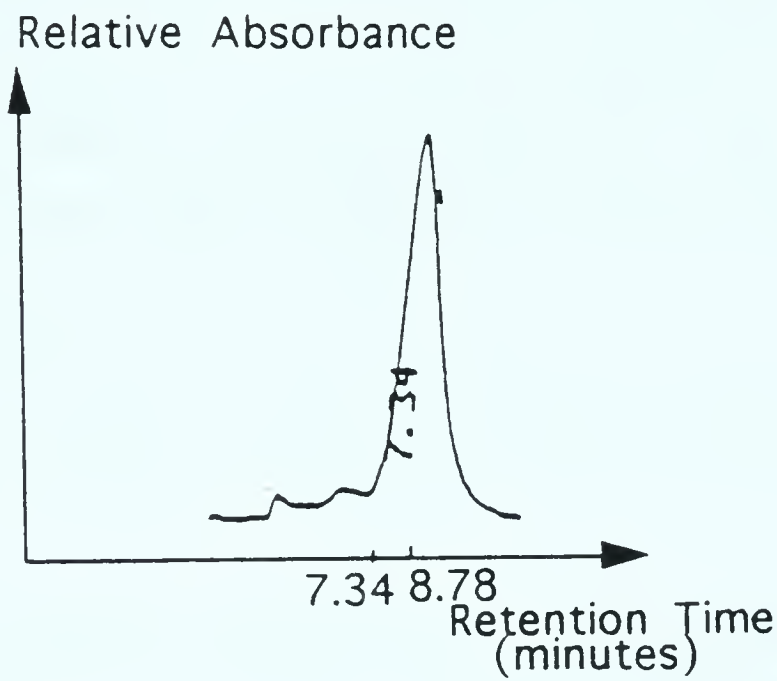
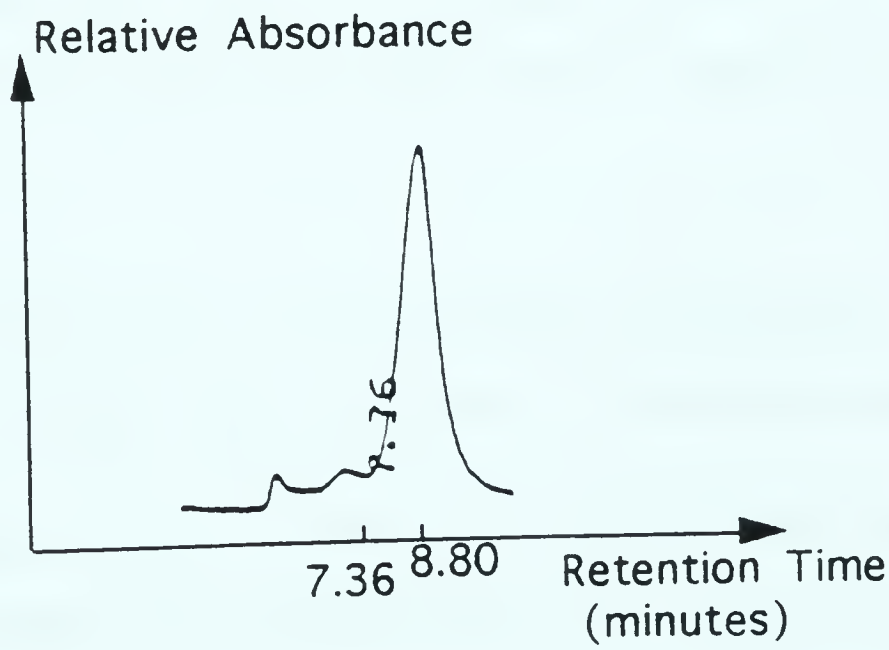


Figure 15 A HPLC Chromatogram of IgG and BCPDA at a 1 : 3 Mole Ratio



(2) Rate of addition of BCPDA

When 50 μ L of BCPDA in ethanol (1mg/mL) were added to 1mL of MAb B43(2mg/mL, 5:1 mole ratio) over a period of 10 minutes and analysed by HPLC the results obtained for the % of cross linked proteins was approximately the same (48%) as when all of the BCPDA solution was added at the same time (42%). Therefore, the rate of addition of BCPDA does not appear to affect or influence the degree of cross linking.

(3) The effect of the concentration of MAb on the percent aggregates.

There was no significant difference in the % aggregates when a concentration of 1mg/mL of antibody was used (43%) relative to when a concentration of 2mg/mL of antibody was used, at a conjugation ratio of 5:1 (42%). But when the concentration of antibody was further reduced to 0.5 mg/mL, the % aggregates decreased to about 30%. This is not unusual since the reactivity between any two molecules decreases when the concentration decreases.

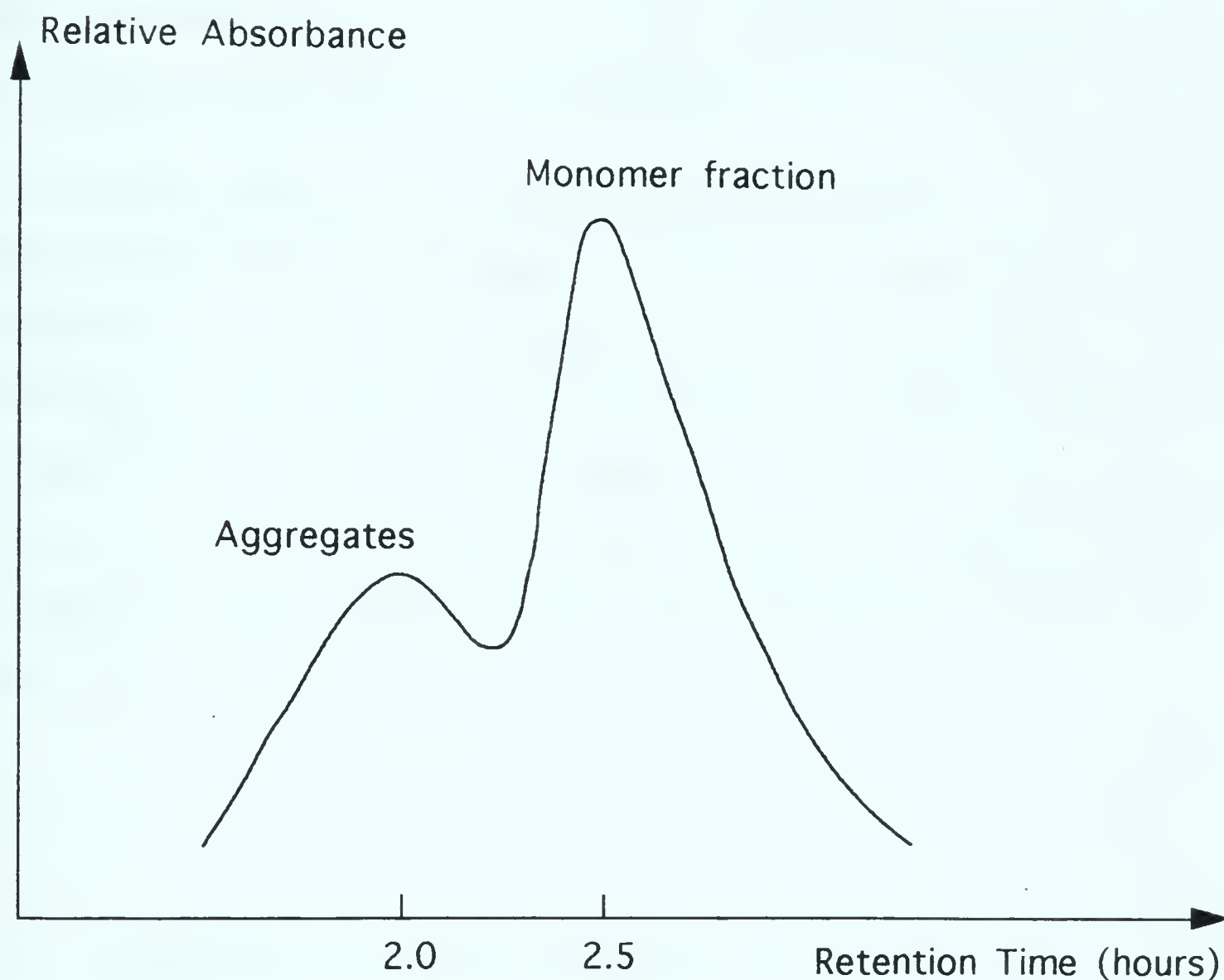
(4.6.3) Purification of MAb-BCPDA Conjugates By Sephacryl S-300 Size Exclusion Chromatography

Since it was unknown whether the reduced immunoreactivity of these purified MAb B43 conjugates was due to the number of

chelates on the antibody or whether it was due to the presence of cross linked proteins that resulted in the formation of aggregates, the conjugates resulting from the reaction of BCPDA with MAb B43 were first purified from the aggregates by S-300 size exclusion chromatography (Figure 16). As can be observed, Sephacryl S-300 does separate the aggregates from monomer forms of the conjugate.

A further examination of the nature of the purified monomeric conjugates (1 : 1,1 : 5, 1 : 10) by HPLC clearly indicated, that the percentage of aggregates in all three purified conjugates was less than 10%. Therefore it is safe to assume that these conjugates consist mainly of monomer conjugates.

Figure 16 A S-300 Chromatogram of MAb-BCPDA Conjugate



(4.6.4) Determination of the Degree of Conjugation of BCPDA to MAb B43

The absorbances at 280nm and at 324nm were measured for a series of BCPDA solutions of various concentrations. The ratios of the absorbances at these two wavelengths in all cases were determined to be equal to 1.7 (280nm : 324nm). This was done in

order to measure the contribution from the BCPDA to the absorbance at 280nm, when the absorbance of the conjugate was measured at the same wavelength. This would also enable one to calculate the concentration of the protein in the conjugates.

As already stated, it was assumed that there was no significant absorbance of the protein at 324nm, which was the characteristic wavelength used in the computation of the BCPDA concentration of the conjugates. Molar absorptivity of MAb B43 was then determined by measuring the absorbance at 280 nm of MAb solutions at various concentrations. Table 30 shows the results of this experiment which indicate that the molar absorptivity of MAb B43 was $2.8 \times 10^5 \text{ mol}^{-1} \text{ L cm}^{-1}$.

Calculation of the Molar Absorptivity

$$[\text{MAb}] = 4 \times 10^{-6} \text{ M}$$

$$\text{molar absorptivity} = \frac{A}{bc}$$

$$\begin{aligned} &= \frac{1.10}{1 \times 4 \times 10^{-6}} \\ &= 2.8 \times 10^5 \text{ mol}^{-1} \text{ L cm}^{-1} \end{aligned}$$

$$[\text{MAb}] = 2 \times 10^{-6} \text{ M}$$

$$\begin{aligned} \text{molar absorptivity} &= \frac{0.55}{1 \times 2 \times 10^{-6}} \\ &= 2.8 \times 10^5 \text{ mol}^{-1} \text{Lcm}^{-1} \end{aligned}$$

Table 30 Molar Absorptivity MAb B43

Sample	Concentration of MAb	Absorbance at 280nm
1	0.6 mg/mL(4x10 ⁻⁶ M)	1.08
2	0.6 mg/mL	1.12
3	0.6mg/mL	1.11
4	0.3mg/mL(2x10 ⁻⁶ M)	0.55

UV spectra of each of the three fractions assumed to correspond to the monomer conjugates were obtained. A typical calculation of the number of moles ligand (BCPDA) per mole of protein is shown below.

Let us, for example, consider the conjugate prepared by the reaction between BCPDA and MAb at a 1:1 mole ratio.

Volume of the monomer fraction collected from the S-300 column was 5mL. The absorbances at 324nm and 280 nm were determined to be 0.061 and 1.084 respectively. The molar absorptivity of BCPDA at 324 nm is given in the literature (2) as

$$1.52 \times 10^4 \text{ mol}^{-1} \text{Lcm}^{-1}$$

$$\text{The [BCPDA]} = \frac{0.061}{1.52 \times 10^4}$$

$$= 4 \times 10^{-6} \text{M}$$

$$\text{BCPDA moles in 5 mL} = 2 \times 10^{-8}$$

Contribution of BCPDA absorbance to

$$280 \text{ nm} = 1.7 \times 0.061$$

$$= 0.104$$

Therefore, absorbance at 280 nm. due to

$$\text{MAb alone} = 1.084 - 0.104 = 0.98$$

$$\text{Therefore, [MAb]} = \frac{0.98}{2.7 \times 10^5}$$

$$= 3.36 \times 10^{-6} \text{M}$$

$$\text{MAB moles in 5 mL} = 1.815 \times 10^{-8}$$

$$\text{Therefore MAb : BCPDA in conjugate} = 1 : 1$$

Similarly the ratio of BCPDA : MAb in the other two preparations were determined to be 1 : 3.2 and 1: 6.9 respectively. The concentrations of the MAb in these three samples were calculated to be as follows (1) 54 μg per 100 μL , (2) 32 μg per 100 μL , and (3) 13.6 μg per 100 μL . The concentrations of BCPDA were computed to be (1) $4 \times 10^{-6} \text{M}$, (2) $7 \times 10^{-6} \text{M}$, and (3) $6.3 \times 10^{-6} \text{M}$ respectively.

(4.6.5) Immunoreactivity of MAb B43-BCPDA Conjugates Purified by S-300 Chromatography

The results of the radioimmunoassay of the three conjugates after purification on Sephacryl S-300 are given in Table 31.

When one compares the IC-50 values of the two control samples, it should be quite apparent that the addition of 10% EtOH does not appear to affect the immunoreactivity of the antibody (47.6ng and 47.0ng) significantly. It is also quite obvious that a gradual decrease in immunoreactivity of the conjugates have occurred with an increase in the number of chelates bonded to the antibody. The decrease in immunoreactivity of the conjugates is reflected by an increase in the values of IC₅₀, when the number of chelates per mole of antibody is increased from 1 to 6.9. When these results are compared to the values obtained prior to the purification of conjugates by the S-300 column, it is clear that a significant improvement in the immunoreactivities of conjugates has occurred between any two conjugates prepared by the same conjugation ratio. Therefore, one can assume that the reason for such an improvement is the absence of aggregates. However, the immunoreactivities continue to decrease as the number of ligands on the antibody increase, possibly due to ligands binding at antigen binding sites of the antibodies.

Table 31 IC-50 Values of the Purified Conjugates

Sample #	(BCPDA : MAb) conjugate	IC-50
1	1 : 1	52.5 ng
2	3.2 : 1	60.2 ng
3	6.9 : 1	70.7 ng
4	control-MAb (60µg/100µL) in acetate buffer	47.6 ng
5	control- MAb+10%EtOH [MAb] as above	47.0 ng

(4.6.6) Radiolabeling MAb-BCPDA Conjugates with ¹⁵³Sm

(1) Radiolabeling with Low Specific Activity ¹⁵³Sm
(3.7x10⁷Bq/mg)

The conjugates used in this experiment were those that contained 3.2 and 6.9 moles of BCPDA per mole of antibody. The percent complexation was determined by cation exchange chromatography after the reactions had proceeded for 16 hours in glass vials. Percent labeling or complexation have so far been

computed using the total activity of the wash and on the column. In most cases discussed so far, the residual activity in the vial was equal to or less than 10%. In these experiments the % complexation was calculated as before, and the residual activity of the vials were also determined.

From Table 32 it appears that as observed before, conjugates having similar ligand concentrations are labeled approximately to the same degree, but nearly 30% of the total activity was associated with the vial.

Table 32 Labeling Efficiencies of Conjugates with Sm at
16 hours in Glass Vials

Moles BCPDA per mole of antibody	Concentration of BCPDA	Mole ratio BCPDA:Sm	%Sm complexed of wash+column activity (n=2)	% Activity in vial of total activity (n=2)
3.2	$7 \times 10^{-6} \text{M}$	10:1	93 ± 5	29 ± 0
6.9	$6 \times 10^{-6} \text{M}$	10:1	94 ± 1	30 ± 1

(2) Labeling MAb-BCPDA Conjugates with High Specific Activity ^{153}Sm

Here all three conjugates were allowed to react with Sm for about 16 hours in Teflon vials. At the end of 16 hours, complexation yields of the conjugates were determined by cation exchange chromatography. Further, one of the conjugates that was diluted by a factor of 10 before labeling, was also complexed with Sm for the same period of time and analysed by cation exchange chromatography. The results are given below, in Table 33.

Table 33 Labeling Efficiencies of Conjugates at 16 hours
With Sm in Teflon Vials

Moles BCPDA per mole of antibody	Concentration of BCPDA	% complexation of wash + column activity (n=2)	% Activity in vial of total activity (n=2)
1	$4 \times 10^{-6}\text{M}$	84 ± 3	19 ± 3
3.2	$7 \times 10^{-6}\text{M}$	79 ± 4	14 ± 3
6.9	$6 \times 10^{-6}\text{M}$	87 ± 3	16 ± 2
(diluted) 3.2	$7 \times 10^{-7}\text{M}$	49 ± 4	44 ± 1

The data in Tables 32 and 33 indicate that when the conjugates are allowed to react with Sm for long periods of time a considerable amount of Sm appears to bind to the vial material. This effect was more pronounced when glass vials were used. Teflon vials were chosen on the assumption that they would have the least interaction with Sm. When the concentration of the conjugate was decreased, the percent of Sm binding to the vial appeared to increase significantly (Table 33).

An experiment was performed with the aim of determining the % complexation, when a particular conjugate is labeled with high specific activity Sm for 1 hour. This is important since it is known that when antibodies are labeled for long periods of time radiolysis of the antibodies could occur (114), and lead to erroneous results during *in vivo* experiments. Therefore, if maximum labeling can be achieved in one hour, this conjugate, when radiolabeled with Sm, could be used as a potential radioimmunotherapeutic agent. The % complexation was determined as stated in the experimental methods section by TLC and by cation exchange chromatography. The results obtained are given in Table 34. The data given in this Table clearly demonstrate the fact that this conjugate can be labeled in one hour to achieve the maximum % labeling yield. Another factor that should be apparent is that under the present experimental conditions, TLC and cation exchange chromatography appear to give similar results. It was also observed in this experiment that only about 7% of the total activity remained in the Teflon vial.

Table 34 Labeling Efficiencies Obtained For a 3:1
Conjugate in One Hour with Sm

Run #	% Yields obtained by TLC	% yields obtained by Cation exchange chromatography
1	87.0	88.0
2	82.0	86.0
3	88.0	80.0
Average yield	86.0±3.2	85.0±4.2

When one considers the fact that only about 7 % Sm activity was bound to the vial when the reaction was allowed to proceed for 1 hour, it can be concluded that labeling or the complexation of the conjugates should be completed in about 1 hour and if the mixture remains in contact with the vial, a gradual transfer of the metal from the complex to the vial occurs. This effect appeared to be more pronounced when the concentration of the conjugated chelate was decreased. Therefore, it is not prudent to measure complexing yields of such ligands under these conditions, because the vial material appears to compete for Sm with these ligands quite successfully. Therefore the results obtained as percent complexation yields would not be the true yields for these particular ligands. These would be net yields after the metal has transchelated to the vial. The only

complexation yields that can be considered for such ligands are yields obtained at shorter times, when the % activity associated with the vial material is at a minimum.

To determine what effect dilution would have on the rate of dissociation of the radiolabeled conjugate, the original labeled conjugate, which was diluted by a factor of 100 in the wash during the above experiment, was reanalysed by cation exchange chromatography at various time intervals. The results of which are presented in Table 35.

Table 35 The Effect of Dilution On the Rate of
Dissociation of the Radiolabeled MAb Conjugate

Dilution factor	Time of dilution	% Labeling yield (n=2)
100	20 minutes	81±1
100	1 hour	81±1
100	3 hours	82±4

The results of this experiment indicate that dilutions up to a factor of 100 do not appear to affect the stability of the metal ligand complex to any significant degree even after 3 hours. Therefore, if 100 μ L of the original labeled conjugate is injected into an animal which has about 3mL of blood, one would not expect

to observe a rapid dissociation of the metal ligand complex *in vivo* due to dilution effects.

To confirm the nature of the vial-bound radioactivity, an experiment was conducted to determine if a protein-bound structure was indeed the source of vial-associated radioactivity.

Radioiodinated MAb B43 at various concentrations was allowed to remain in these Teflon vials for about 24 hours and then removed. The % radioiodine activity bound to the unwashed empty vials was then determined. The results of this experiment are as follows (Table 36).

Table 36 Concentration of Iodinated MAb Versus %
Activity Bound to Vial

Concentration of MAb	% iodine bound to vial (n=2)
$1.3 \times 10^{-5} \text{M}$	1 ± 1
$2 \times 10^{-6} \text{M}$	5 ± 1
10^{-6}M	4 ± 0
10^{-7}M	5 ± 1

These data confirm the fact that the vial bound activity was not due to the adsorption of the antibody, but possibly an adsorption of free Sm or complexed Sm to the vial. A similar experiment to

determine the relationship between the concentration of free Sm and % Sm activity bound to the vial was performed by adding various concentrations of Sm to the vial, and measuring the activity of the vial after removing the metal solution from the vial and washing the vial once with 1 mL of acetate buffer. Results of this experiment are given in Table 37.

As the concentration of the Sm decreases there is a corresponding increase in the percentage of Sm that is bound to the vial. In this experiment the concentration of the "complexing ligand", that is, the number of active sites of the vial, is assumed to be held constant as the concentration of the metal is decreased. Therefore an increasing percentage of the total added metal can be adsorbed by the vial.

Table 37 Concentration of Sm Versus % activity Bound to
Vial

Concentration of Sm	% activity (n=2)
$7 \times 10^{-6} \text{M}$	36 ± 1
10^{-6}M	30 ± 8
$5 \times 10^{-7} \text{M}$	49 ± 6
10^{-7}M	80 ± 1

The % recovery of MAb from the cation exchange column was

determined by measuring the absorbance at 280 nm of an aliquot of a (MAb + Sm) sample of known concentration, before and after eluting the sample with 10 mL of saline, as described in section (3.5).

Although 70% of the Sm activity remained in the vial, the UV results indicated 100% recovery of the antibody. This experiment further confirms that the residual activity remaining in the vial is due only to free Sm.

(4.6.7) Non-Specific Binding of Sm to MAb in the Presence of BCPDA

When the sample mixtures were eluted on G-50 columns, one could observe two peaks for the antibody in both sample mixtures where one was a large peak and the other a comparatively smaller peak (see Figure 17). Of the two peaks which are associated with the antibody, the retention time of the larger peak corresponded to the retention time of protein molecules which have molecular weights larger than 50,000. These included proteins such as HSA and MAb B43 samples that were analysed before this experiment. The smaller peak had a retention time that was longer than the first peak but shorter than the retention time of the chelate peaks. Greater than 90% of the recovered Sm activity was associated with the two protein peaks (Table 38). When the same experiment was performed using DTPA instead of BCPDA as the chelate, the result obtained was the same as when BCPDA was used (Table 38). A similar pattern of

two peaks were seen when the MAb was analysed by HPLC. (Figure 18). When a standard mixture of proteins of different molecular weights was analysed by HPLC, and retention times of these protein standards were compared to the retention time of the smaller of the two peaks, it corresponded to a protein standard which had a molecular weight of 50,000. It was assumed at this stage that the smaller of the two protein peaks was due to a fragment of the MAb B43 or a protein of low molecular weight. The MAb, DTPA and Sm mixture was then analysed by cellulose TLC. The results of this experiment are presented in Table 39. As one can see, most of the activity is predominantly associated with the protein fractions.

Table 38 Analysis of a Solution Mixture of Sm, Chelate, and MAb B43 by G-50 Chromatography

Chelate	% Activity in large peak (n=2)	% Activity in small peak (n=2)	% Activity in BCPDA peak (n=2)
BCPDA	14±0	82±4	4±4
DTPA	23±0	77±0	0±0

Figure 17 A G-50 Chromatogram of MAb B43

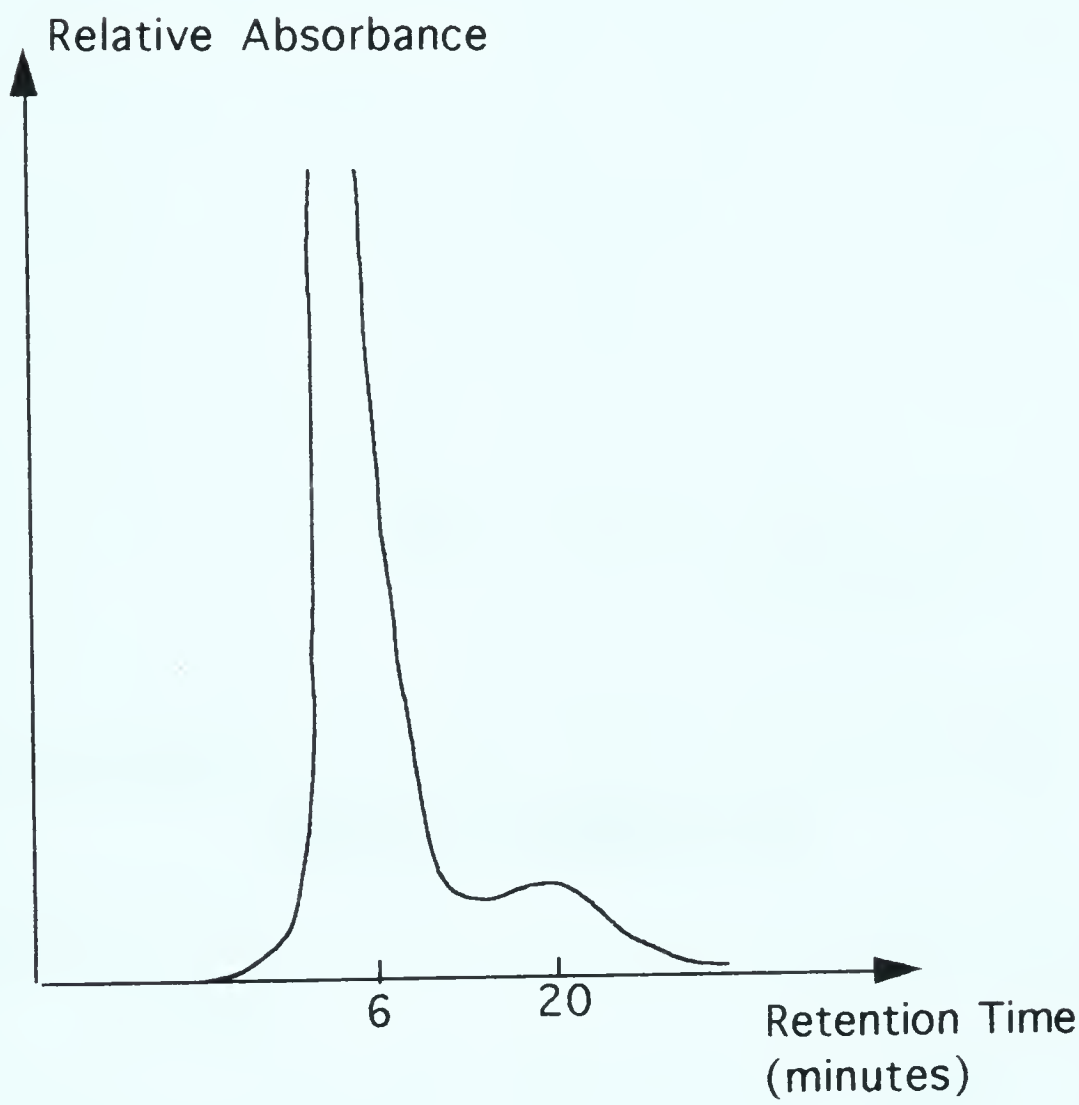


Figure 18 A HPLC Chromatogram of MAb B43

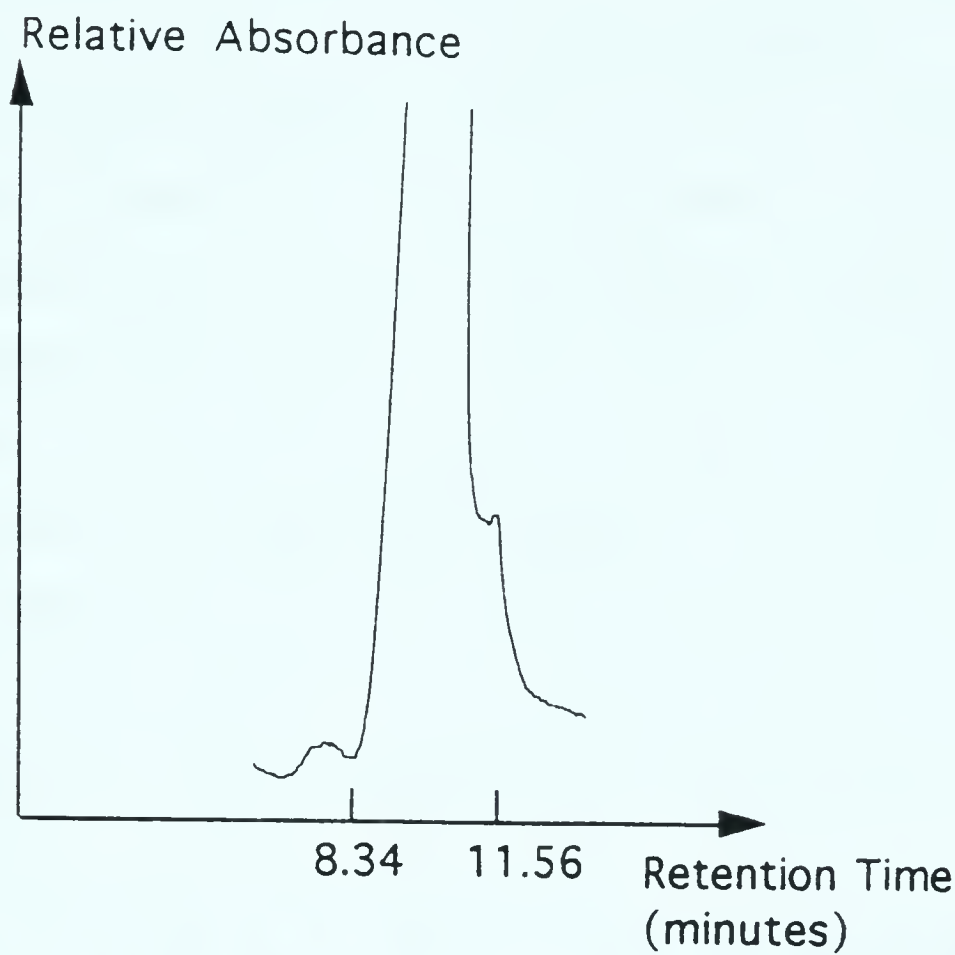


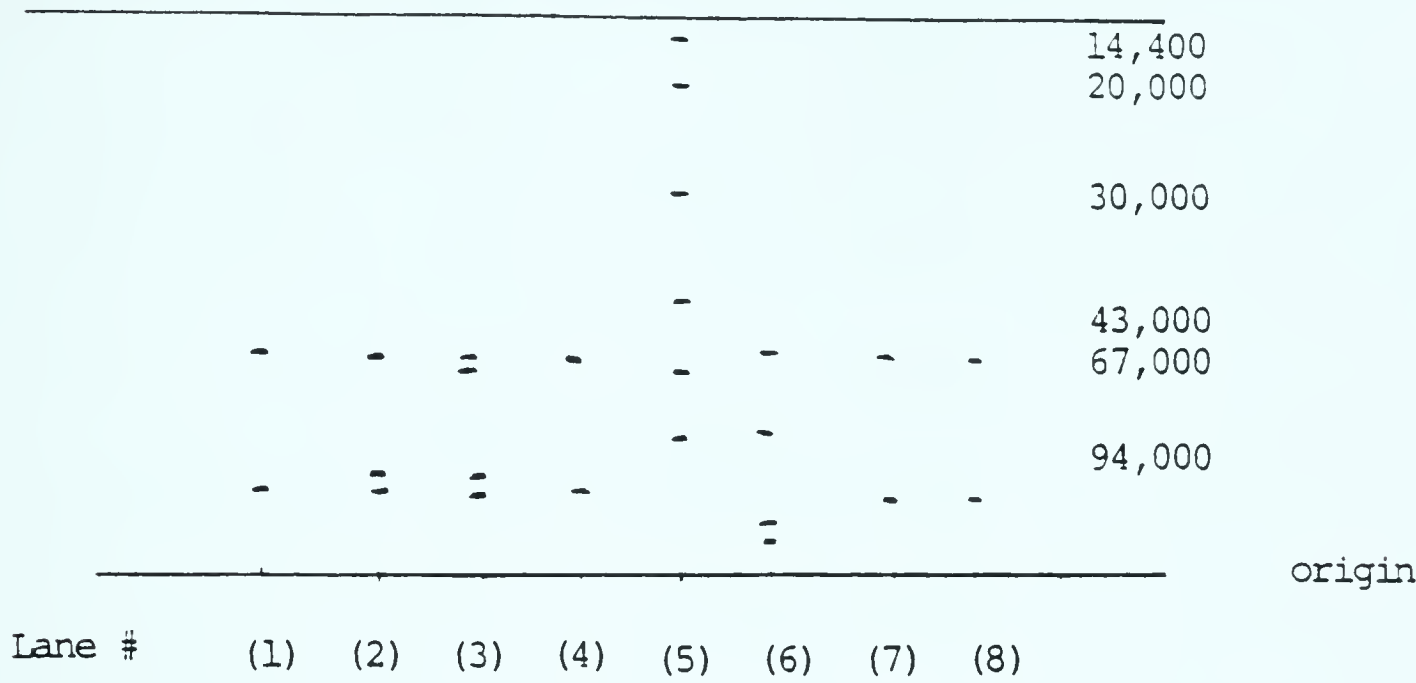
Table 39 Analysis of a Solution Mixture of Sm DTPA and MAb B43 by Cellulose TLC

Sample	% Activity at the origin (n=2)
SmCl ₃ (control)	4±3
¹²⁵ I-MAb (control)	100 (¹²⁵ I)±0
Sm+DTPA	7±4
Sm+DTPA+MAb	67±5

When the large peak was reanalysed by G-50 only one large peak,

corresponding to the MAb, was seen. To further confirm the purity, these MAb samples were analysed by electrophoresis, (SDS-PAGE) under non reducing conditions (Figures 19 and 20). It is quite obvious that when the distances traveled by each of these protein samples were compared to the distances traveled by the standard proteins, the fragment protein band of the original or the unpurified MAb sample corresponded to a protein having a molecular weight between 67,000 and 43,000 (Figures 19 and 20). Two other important results observed during the electrophoresis experiment were (1) the G-50 purified MAb sample did not appear to contain the fragment, which as already mentioned was confirmed by the reanalysis of this purified sample by G-50, and (2) there did not appear to be any difference between an unused sample stored at 4 °C and a sample that had been used and stored at room temperature for a few months. The only conclusion that can be made is that the original MAb sample that was used in the experiments has gradually denatured with time, even when stored at a temperature of 4 °C.

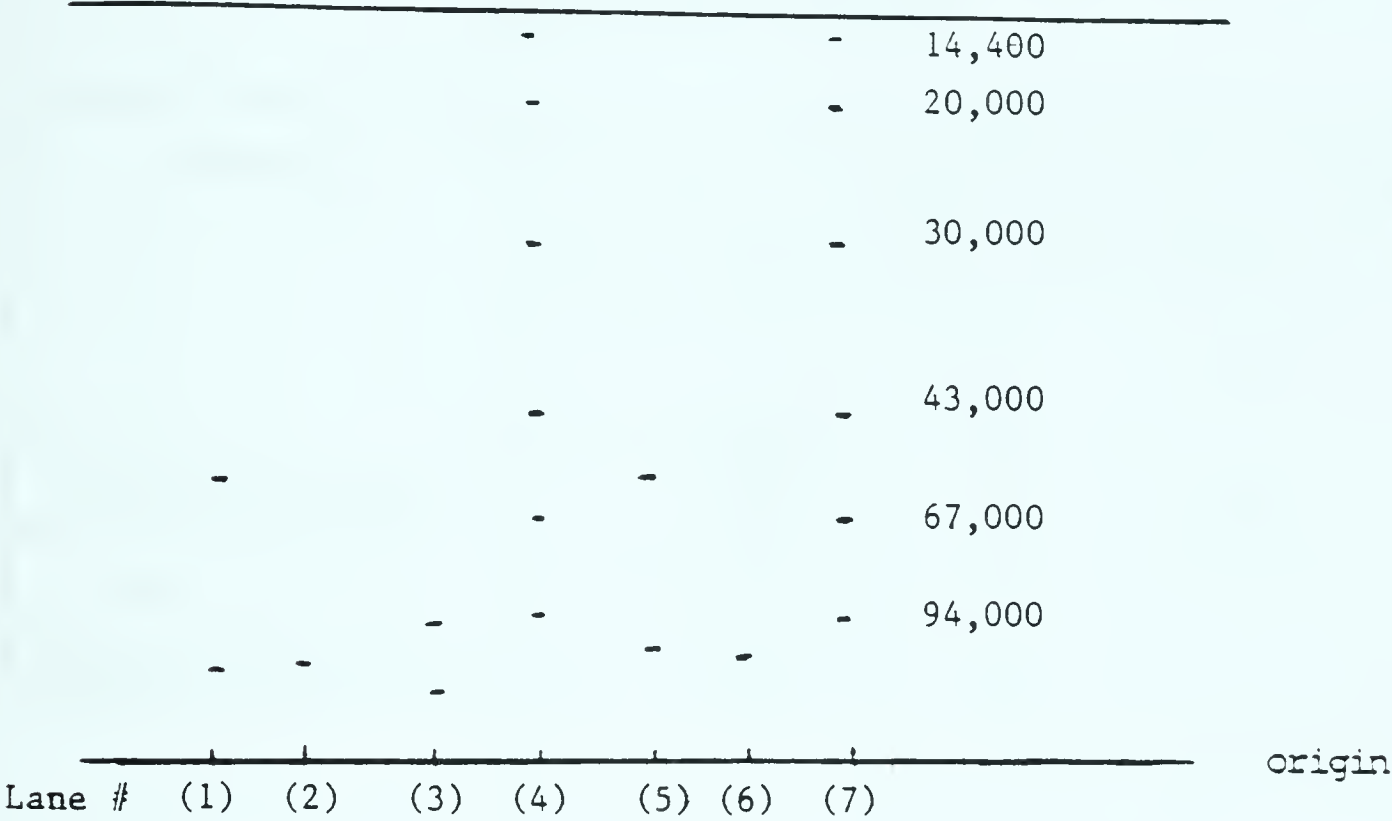
Figure 19 Gel Electrophoresis (SDS-PAGE) Of Unpurified MAb B43



Lane #

- (1) MAb B43 in PBS (used, stored at 4° C, 1.5 mg/mL)
- (2) MAb B43 in Tris (used, stored at 4° C, 1.5 mg/mL)
- (3) MAb B43 in PBS (unused, 4° C, 1.5 mg/mL)
- (4) MAb B43 in Tris (used, 22° C, 1.5 mg/mL)
- (5) Protein standards : MW. 14,400-94000
- (6) Pretinned MAb-174 (frozen)
- (7) Repeat of (1)
- (8) Repeat of (3)

Figure 20 Gel Electrophoresis (SDS-PAGE) of Unpurified and



Lane #

- (1), and (5) Unpurified MAb B43
- (2), and (6) Purified MAb B43
- (3) Human IgG
- (4), and (7) Protein standards

The G-50 purified MAb sample was then used to perform the original experiment discussed at the beginning of this section. The results of which are presented in the following Table 40.

Table 40 Determination of Non Specific Binding of Sm
With Purified Antibody

Sample	% activity of Chelate (0.5 cm above origin) determined by TLC (n=2)	% activity of chelate determined by G-50 (n=2)
MAB +BCPDA+Sm	76±3	93±1
MAB+ DTPA+Sm	87±1	-
BCPDA+Sm (control)	97±0	-

The above data indicate that most of the Sm is bound to the respective chelates in the presence of the purified antibody. These results provide further arguments that when the conjugate is labeled with Sm, it is the chelate conjugated to the antibody that is predominantly labeled with Sm. One can also conclude that during the previous experiment, where the antibody contained the fragment, even though Sm was complexing with the chelate, the fragment probably was interacting noncovalently with the complexed chelate. Therefore, one could postulate that most of the metal was bound to this protein fraction indirectly.

(4.7) Transchelation Experiments.

(4.7.1) Sm-BCPDA and Sm-DTPA complexes versus HSA

If 1 mg of the labeled conjugate, with approximately 3 chelate residues on a mole/mole basis, and where the concentration of the chelate is ten times greater than the metal ion concentration, is administered to a patient, the resulting *in vivo* concentrations of BCPDA, Sm, and HSA would be 4×10^{-9} M, 4×10^{-10} M, and 6×10^{-4} M respectively, assuming a total blood volume of 5 litres. This would be translated to the following mole ratios *in vivo* of BCPDA : Sm : HSA as 1 : 0.1 : 10^5 . Here the concentration of HSA is assumed to be 40mg/mL.

If the stability of the conjugated and the unconjugated chelate metal complexes are assumed to be the same, this transchelation experiment can be performed using the unconjugated chelate. Thus, by separating the protein fraction from the metal chelate complex on a cellulose TLC system, one can conveniently estimate the degree of transchelation from the metal complex to the protein fraction.

Once the metal ligand complexes were prepared, various volumes of this complex and of HSA were mixed so as to obtain different mole ratios that would have some clinical significance to the desired *in vivo* mole ratios and also have adequate amount of Sm activity in order for the sample mixtures to be analysed with sufficient sensitivity. The results of experiments (a) and (b) are

given in Tables 41 and 42. The pH of the medium in these experiments was 7.5 (Tris 0.05M).

Consider the results in Table 41. The concentration of the metal ligand complex used in this experiment was much higher than would be expected in an actual *in vivo* experiment, in order to obtain sufficient activity of Sm for the analysis by TLC. Therefore the concentration of the complex was held fairly constant throughout the experiment, while the concentration of the HSA was varied from an *in vivo* concentration to lower concentrations. When free Sm was added to HSA in the *absence of BCPDA* the % complexation of Sm with HSA was much lower than when Sm-BCPDA complex was added to HSA, *at the same concentrations of HSA and time durations*. Thus, if free Sm binds to HSA to a lesser extent than when Sm is complexed to BCPDA, as shown in Table 41, the only explanation for this is, under these experimental conditions, although no direct transchelation of Sm occurred from the complex to HSA, BCPDA may be interacting with HSA in a non-covalent nature. The BCPDA cannot form covalent bonds with HSA since the chelate had been hydrolysed. One could also postulate that at the low concentrations of Sm-BCPDA complex that are used under *in vivo* conditions, this interaction could be minimal.

Table 41 Transchelation of Sm from Sm-BCPDA Complex
to HSA

Final [HSA]	Final [BCPDA]	Final [Sm]	Time of reaction (minutes)	%Activity in HSA fraction (n=2)
$6 \times 10^{-4} \text{M}$	$2 \times 10^{-6} \text{M}$	-	15	84 ± 3
$6 \times 10^{-4} \text{M}$	$2 \times 10^{-6} \text{M}$	-	30	85 ± 4
$6 \times 10^{-4} \text{M}$ (control)	-	$2 \times 10^{-6} \text{M}$	30	33 ± 2 (by TLC and cation exchange)
$6 \times 10^{-5} \text{M}$ (control)	-	$2 \times 10^{-6} \text{M}$	30	7 ± 0 (by cation exchange)
$5 \times 10^{-5} \text{M}$	$4 \times 10^{-6} \text{M}$	-	30	24 ± 4
$3 \times 10^{-4} \text{M}$ (control)	-	$2 \times 10^{-6} \text{M}$	30	18 ± 0 (by cation exchange)
$3 \times 10^{-4} \text{M}$	$4 \times 10^{-6} \text{M}$	-	30	75 ± 1

Table 42 Transchelation of Sm from Sm-DTPA Complex to
HSA

Final [HSA]	Final [DTPA]	Time of reaction (minutes)	% Activity in HSA (n=2)
$5 \times 10^{-4} \text{M}$	$2 \times 10^{-6} \text{M}$	15	0 ± 0
$5 \times 10^{-4} \text{M}$	$2 \times 10^{-6} \text{M}$	120	0 ± 0
$5 \times 10^{-4} \text{M}$	$2 \times 10^{-6} \text{M}$	180	0 ± 0

The possibility that serum could be interacting with BCPDA has also been implied by Diamandis and his co-workers (115). In their immunoassay procedures where BCPDA -Eu complex is used as a fluorescent probe, measures had been taken to "prevent fluor - serum interactions " In a recent report published by Carter (116) it is stated that "generally, serum albumin has a greater affinity for small, negatively charged hydrophobic molecules." In this report the authors have elaborated the mechanism of binding of 2,3,5-triiodobenzoic acid with HSA. They have observed that the aromatic ring binds to certain amino acid residues via hydrophobic interactions, and the carboxylate group of the compound binds with amino acid residues such as arginine and lysine. Since BCPDA has a large hydrophobic moiety and two carboxylate groups, the above mentioned interactions are quite conceivable with HSA. On the other

hand the Sm-DTPA complex, under these conditions does not appear to interact with HSA, neither is Sm transchelated to HSA. However long the reaction was allowed to proceed, all of the Sm activity remained with DTPA (Table 42).

It has also been reported by Schomaker (113) that when Yb-Citrate complex is mixed with a sample of human serum, 95% of the Yb activity was observed to be associated with the HSA fraction. The reason that these authors have given for this observation is that "a ligand exchange reaction can be assumed between the citrate ligand and the albumin, if the lanthanides are applied as citrate complexes intravenously". The concentrations that these authors have used were 10^{-7}M as Yb and 10^{-5}M as the citrate concentration. As one knows, the HSA concentration *in vivo* is 10^{-4}M . If one were to calculate the theoretical yield of Yb that would be directly transchelated to HSA, based on the stability constants as reported by these same authors, for Yb-HSA and Yb-citrate, ($K = 10^{9.5}$ and $10^{12.5}$ respectively) and assuming that under these circumstances the predominant Yb citrate species is $\text{Yb}(\text{citrate})_2$, one would have to assume that the observed Yb association is due only to some interaction between the citrate and HSA or due to the formation of a mixed complex of the nature of HSA-Yb-Citrate.

(4.7.2) Interaction of Sm Complexes with Hydroxyapatite.

Since hydroxyapatite is a major component of the bone, and since it is known from various biodistribution studies performed, (Ref.85, p23) that Sm has a high affinity for the bone, it was decided to measure the stability of the Sm-BCPDA complex relative to the affinity of hydroxyapatite towards Sm. This was also compared to the stability of a Sm-DTPA complex to a similar hydroxyapatite preparation. Various quantities of the hydroxyapatite suspension in phosphate buffer were mixed with different concentrations of Sm-BCPDA or Sm-DTPA complexes in Tris buffer of pH 7.5, as described in the experimental methods section (3.24b). As the exact concentration of the hydroxyapatite in the bone was not available, arbitrary quantities of hydroxyapatite were used. The results of these experiments are given in the following two Tables (43 and 44).

As stated earlier, the concentration of the Sm-BCPDA and the Sm-DTPA complexes are much higher than would be expected in actual *in vivo* experiments. Even at these high concentrations of BCPDA, it appears that this chelate cannot compete with hydroxyapatite for Sm. This was true for all concentrations of hydroxyapatite, and the transchelation of Sm from BCPDA appeared to be very rapid.

Table 43 Transchelation of Sm from Sm-BCPDA Complex
to Hydroxyapatite

Quantity of hydroxyap- -atite (mg)	Volume of Sm- BCPDA complex	Moles of BCPDA in complex	Moles of free Sm	Time of reaction (minutes)	% Activity in hydroxyap- -atite (n=2)
75	20 μL	4×10^{-10}	-	30	100 ± 0
20	20 μL	4×10^{-10}	-	30	100 ± 0
20	40 μL	8×10^{-10}	-	15	100 ± 0
20	100 μL	2×10^{-9}	-	15	100 ± 0
75	-	-	10^{-11}	30	100 ± 0

Table 44 Transchelation of Sm from Sm-DTPA Complex to Hydroxyapatite

Quantity of hydroxyapatite (mg)	Volume of Sm-DTPA	Moles DTPA in complex	Time of reaction (minutes)	% Activity in hydroxyapatite (n=2)
20	20 μ L	2×10^{-10}	30	8 ± 1
20	20 μ L	2×10^{-10}	120	9 ± 2
20	20 μ L	2×10^{-10}	180	9 ± 0
85	20 μ L	2×10^{-10}	120	11 ± 3

Since free Sm also reacted rapidly with hydroxyapatite to the same degree as when Sm was complexed to BCPDA, it is not possible at this time to speculate whether the Sm interacts with the hydroxyapatite while it is still complexed to BCPDA or whether there is a replacement of the BCPDA by the hydroxyapatite. Whatever the case may be, it is apparent that there is a rapid uptake of Sm by the hydroxyapatite, when Sm-BCPDA is added.

Sm-DTPA appears to be very stable in the presence of hydroxyapatite, maintaining the Sm activity even up to 3 hours and in the presence of high concentrations of hydroxyapatite.

One can therefore conclude from all these *in vitro* transchelation experiments, that BCPDA may not be a suitable ligand to be used *in vivo*, due to the apparent instability of this complex in the presence of the various challenging compounds used so far. On the other hand the DTPA-Sm complex did not depict such instability under the same conditions. When one compares the stability constant reported in the literature of Sm-DTPA and the stability constant determined in this study for the Sm-BCPDA complex, (10^{22} and 10^7 respectively) it was not surprising to observe the results discussed in sections (4.7.1) and (4.7.2).

(4.8) Biodistribution Studies in Mice

The most obvious result of these experiments is the high % of activity that is localised in the liver. In all experiments, on the average, approximately 40% of the injected dose was in the liver and about 30% of the activity in the "residual" carcass, of which certain organs had been removed. Table 45 depicts the mean % of the injected dose per gram of tissue of some organs at each time interval.

Table 45 Biodistribution Studies of MAb B43-BCPDA-Sm

Time	Blood	Spleen	Liver	Kidney	Bone
6hrs.	0.11±0.02	1.41±0.19	30.40±3.25	3.88±0.49	6.93±1.65
24hrs.	0.03±0	1.50±0.21	35.0±4.2	3.55±0.66	8.88±1.73
48hrs.	0.02±0.01	1.84±0.03	29.34±6.58	2.64±0.44	8.89±0.53

It is quite apparent from the above results, that the liver has the highest affinity for Sm, followed by the bone and then by the kidney. There appears to be very little activity present in blood even at a very short time period after the administration of the radiolabeled conjugate (6hrs.). These results appear to be similar to those obtained by Boniface and co-workers (101) 6 days after the injection of another monoclonal antibody labeled with Sm via cyclic DTPA, into tumored rats. Their results indicate that the highest localisation of activity was in the kidney and the remainder of the activity distributed as follows (from the highest to the lowest % activity) : tumor, liver, bone, and spleen. The biodistribution of Sm-acetate in tumored rats also at 6 days (101), shows that the two organs with highest equal uptake of activity are the liver and spleen, followed by stomach, kidney and bone. The conclusion that can be derived from these results is that in the absence of a very stable Sm-chelate complex, Sm appears to transchelate or transcomplex rapidly to some unknown component in the liver, directly or

indirectly. This results in a high uptake of activity by that organ.

(5.0) SUMMARY OF RESULTS

(1) Synthesis of BCPDA

Although the procedure reported in the literature was adopted in the synthesis of the above compound, certain modifications as mentioned below had to be made in order to prepare a pure compound. (a) Seventeen hours were needed in this study for step one of this synthesis to be completed, compared to 6 hours that has been reported in the literature, (b) prior to the synthesis of the final compound (4), compound (3) had to be purified according to the procedure mentioned in the experimental methods section of this thesis. Literature claims that no purification step was needed in the synthesis of BCPDA, and (c) the colour of BCPDA obtained in the present synthesis was dark brown, whereas the literature reports the colour to be yellow.

(2) Fluorometric Studies Of Sm-BCPDA Complexes

Our studies indicate that pure BCPDA has a molecular emission at about 410 nm, when the excitation wavelength is approximately 320 nm. Metal ion emissions of the Sm-BCPDA complex were observed at 570 nm, and 610 nm at the same excitation wavelength. The stability constant of a 1 : 1 Sm-BCPDA complex which was determined utilizing the molecular fluorescence of BCPDA was

calculated to be 4.4×10^6 L/mole.

(3) Complexation Studies Of Sm-BCPDA

Most of the complexation studies involving BCPDA and DTPA were performed utilizing cation exchange chromatography. On a few occasions cellulose TLC was used to compare the complexation yields obtained by cation exchange chromatography, and when it was necessary to determine separately the complexation yields of Sm-BCPDA and other Sm-ligand complexes during the same experiment. It was observed that the experimentally determined % yields of Sm-BCPDA complexes were similar to the theoretical yields calculated using the stability constant obtained fluorometrically.

The complexation yields of HSA-BCPDA conjugates and MAb-BCPDA conjugates, obtained by the above methods indicate that yields are a function of the BCPDA concentration, and not on the number of chelates bound to the protein. It was also apparent that the longer the time of complexation, the greater the % of Sm that was non specifically bound to the vial. This effect was more pronounced when glass vials were used.

High complexation yields (~ 90%) were obtained for HSA-BCPDA and MAb-BCPDA conjugates at original concentrations within 1-2 hours of complexation.

It was also determined, both by TLC and G-50 size exclusion chromatography, that non specific binding of Sm to proteins was

minimal, when MAb-BCPDA and MAb-DTPA conjugates were allowed to complex with Sm.

(4) Conjugation Of BCPDA To HSA And BCPDA

The degree of conjugation increased with an increase in the BCPDA : protein reaction ratios for both HSA and MAb B43. The degree of conjugation between BCPDA and HSA was the same at pH 7 and 9, and the conjugation reaction was complete in 1/2 hour. No apparent aggregation was visible during HSA, BCPDA conjugations, but increasing amounts of aggregation were visible with increasing concentrations of BCPDA, during human IgG and MAb B43 conjugation reactions. The immunoreactivity of MAb decreased as the number of BCPDA molecules per protein molecule increased. This decrease in immunoreactivity was also seen as the % aggregates increased.

(5) Transchelation Studies

(a) The Effect of HSA

The percent ^{153}Sm activity that was associated with the HSA fraction, when *in vivo* concentrations of HSA were allowed to complex at specific time intervals with free Sm, was much less than when Sm-BCPDA complex was allowed to react with the same concentration of HSA and time period. Minimal ^{153}Sm activity was detected in the HSA fraction when Sm-DTPA complex was allowed to react with HSA under the same experimental conditions. This may be due to a non covalent interaction between BCPDA and HSA.

(b) The Effect of Hydroxyapatite

When the above experiment was performed under the same experimental conditions as above, with different quantities of hydroxyapatite instead of HSA, most of the ^{153}Sm activity was observed to be associated with the hydroxyapatite when Sm-BCPDA complex was used, and minimal ^{153}Sm activity was detected when Sm-DTPA was used. These results indicate that hydroxyapatite has a much higher affinity for Sm than BCPDA, whereas the affinity of DTPA for Sm, appears to be much higher than hydroxyapatite.

(6) Biodistribution Studies Of MAb-BCPDA-Sm

A high uptake of Sm by liver was observed within 6 hours when Sm labeled MAb-BCPDA conjugates were administered into mice. It appears that Sm transchelates rapidly to some unknown component in the liver directly or indirectly.

(6.0) CONCLUSION

Although BCPDA was found to be a chelate that can be conjugated to a monoclonal antibody with high efficiency, the absolute stability of the Sm-BCPDA complex and the relative stability of this complex in the presence of various "challenging compounds" was determined to be inadequate for the MAb-BCPDA- ^{153}Sm complex to be utilized as a potential radioimmunotherapeutic agent.

REFERENCES

- (1) Kozak, R.W., Waldmann, T.A., Atcher, R.W., Gansow, O.A., Trends In Biotechnology, 4, 259, 1986.
- (2) Evangelista, R.A., Pollak, A., Allore, B., Templeton, E.F., Morton, R.C., Diamandis, E.P., Clin. Biochem., 21, 173, 1988.
- (3) Adelstein, S.J., Kassis, A.I., Criteria For The Selection Of Nuclides For Radioimmunotherapy, in Radiolabeled Monoclonal Antibodies For Imaging And Therapy, Edited By Srivastava, S.C., p167, 1986.
- (4) Early, P.J., Razzak, M.A., Sodee, D.B., Text Book Of Nuclear Medicine Technology, p87, 1975.
- (5) Casarett, A.P., Radiation Biology, Prentice Hall Inc., p28, 1968.
- (6) Mausner, L.F., Straub, R.F., Srivastava, S.C., Production And Use Of Prospective Radionuclides For Radioimmunotherapy, In Radiolabeled Monoclonal Antibodies For Imaging And Therapy, Edited By Srivastava, S.C., Plenum Press p149, 1986.
- (7) Delmon-Moingen, L.I., Mahmood, A., Davison, A., Jones, A.G., J. Nucl. Biol. Med., 35, 50, 1991.
- (8) Humm, J.L., J.Nucl.Med., 27, 1490, 1986.
- (9) Yuanfang, L. and Chuanchu, W., Pure And Applied Chemistry, 63, 432, 1991.
- (10) Goldenberg, D.M., Horowitz, Jo Ann, Sharkey, R.M., et al., J.Clin.Oncol., 9, 548, 1991.

- (11) Bender, H., Takahashi, H., Adachi, K., et al., *Cancer Research*, 52, 121, 1992.
- (12) Pedley, R.B., Begent, R.H.J., Boden, J.A., et al., *Int.J.Cancer*, 47, 597, 1991.
- (13) Meredith, R.F., LoBuglior, A.F., Roger, W.E.P., et al., *J.N.M.*, 32, 1162, 1991.
- (14) Eary, J.F., Krohn, K.A., Kishore, R., Nelp, W.B., *Radiochemistry of Halogenated Antibodies*, in *Radiodiagnosis and Therapy*, Edited by Zalutsky, M.R., p83, 1989.
- (15) Fritzberg, A.R., Berninger, R.W., Hadley, S.W., Wester, D.W., *Pharmaceutical Research*, 5, 325, 1988.
- (16) Motta-Hennessy, C., Sharky, R.M., Goldenberg, D.M., *Appl.Radiat.Isot.*, 42, 421, 1991.
- (17) Mehta, M.P., Kubsad, S.S., Fowler, J.F., et al., *Int.J.Radiat.Oncol. and Biol.Phys.*, 19, 627, 1990.
- (18) Kosmas, C., Snook, D., Gooden, C.S., et al., *Cancer Research*, 52, 904, 1992.
- (19) Vriesendorp, H.M., Quadri, S.M., Stinson, R.L., et al., *Int.J.Rad.Oncol. and Biol.Phys.*, 22, 37, 1992.
- (20) Washburn, L.C., Lee, Y.C.C., Sun, T.T.H., et al., *Antibod.Immunocon. and Radiopharm.*, 4, 729, 1991.
- (21) Myers, M.J., *Quantitative Imaging and Internal Radiation Dosimetry in the Therapeutic Use of Labeled Monoclonal Antibodies in Radiolabeled Monoclonal Antibodies for Imaging and Therapy*, Edited by Srivastava, S.C., Plenum Press., p431, 1986.

- (22) Goldenberg, D.M., Blumenthal, R.D., Sharkey, R.M., *Seminars in Cancer Biology*, 1, 217, 1990.
- (23) Wessels, B.W., Rogus, R.D., *Med.Phys.*, 11, 638, 1984.
- (24) Zalutsky, M.R., *Antibody-Mediated Radiotherapy : Future Prospects*, in *Antibodies in Radiodiagnosis and Therapy*, CRC Pres Inc., p213, 1989.
- (25) Griffiths, G.L., Goldenberg, D.M., Knapp, F.F., et al., *Cancer Research*, 51, 4594, 1991.
- (26) Wolf, W., Jashovam, S., *Nucl.Med.Biol.*, 13, 319, 1986.
- (27) Wensel, T.G., Mears, C.F., *Bifunctional Chelating Agents for Binding Metal Ions to Proteins in Radioimmunoimaging and Radioimmunotherapy*, Edited By Burchiel, S.W., Rhodes, B.A., p185, 1983.
- (28) Yeh, S.M., Sherman, D.G., Mears, C.F., *Anal.Biochem.*, 100, 152, 1979.
- (29) Kozak, R.W., Raubitschek, A., Mirzadeh, S., et al., *Cancer Research*, 49, 2639, 1989.
- (30) Brinkley, M., *Bioconjugate Chemistry*, 3, 2, 1992.
- (31) Wong, S.S., *Chemistry of Protein Conjugation and Cross-Linking*, 7, 1991.
- (32) Brandt, K.D., Schnobrich, K.E., Johnson, D.K., *Bioconjugate Chemistry*, 2, 67, 1991.
- (33) Diamandis, E.P., Mortan, R.C., *J.Immun.Methods*, 112, 43, 1988.
- (34) Mears, C.F., McCall, M.J., Reardan, D.T., et al., *Anal.Biochem.*, 142, 68, 1984.

- (35) Hnatowich, D.J., Childs, R.L., Lanteigne, D., Najafi, A., J.Immunol.Methods, 65, 147, 1983.
- (36) Eckelman, W.C., Paik, C.H., Labeling Antibodies with Metals Using Bifunctional Chelates, in Antibodies in Radiodiagnosis and Therapy Edited By Zalutsky, M.R., CRC Press Inc., p103, 1989.
- (37) Hancock, R.D., Martell, A.E., Chem.Rev., 89, 1875,1989.
- (38) Bell, C.F., Principles and Applications of Metal Chelation, Clarendon Press, 1977.
- (39) Laitinen, H.A., Harris, W.E., Chemical Analysis, 2nd Edition, McGraw-Hill, p191, 1975.
- (40) Skoog, D.A., West, D.M., Holler, F.J., Fundamentals Of Analytical Chemistry, Saunders College Publishing, p261, 1988.
- (41) Brechbiel, M.W., Gansow, O., Atcher, R.W., et al., Inorg.Chem., 25, 2772, 1986.
- (42) Fawwaz, R.A., Wang, T.S.T., Srivastava, S.C., et al., J.Nucl.Med., 25, 796, 1984.
- (43) Lee, Y.C.C., Washburn, L.C., Sun, T.T.H., et al., Cancer Research, 50, 4546, 1990.
- (44) Moi, M.K., Mears, C.F., McCall, M.J., et al., Anal.Biochem., 148, 249, 1985.
- (45) Mears, C.F., Nucl.Med.Biol., 13, 311, 1986.
- (46) Deshpande, S.V., DeNardo, S.J., Kukis, D.L., et al., J.Nucl.Med., 31, 473, 1990.

- (47) Moi, M.K., Mears, C.F., DeNardo, S.J., J.Am.Chem.Soc., 110, 6266, 1988.
- (48) McMurry, T.J., Brechbiel, M., Kumar, K., Gansow, O.A., Biocon.Chem., 3, 108, 1992.
- (49) Griffiths, G.L., Goldenberg, D.M., Jones, A.L., Hansen, H.J., Bioconj.,Chem., 3, 91, 1992.
- (50) Fritzberg, A.R., Abrams, P.G., Beaumier, P.L., et al., Proc.Natl.Acad.Sci., 85, 4025, 1988.
- (51) Breitz, H.B., Weiden, P.L., Vanderheyden, J.L., et al., J.Nucl.Med., 33, 1099, 1992.
- (52) Najafi, A., Alauddin, M.M., Sosa, A., et al., Nucl.Med.Biol., 19, 205, 1992.
- (53) Tolman, G.L., Hadjian, R.A., Morelock, M.M., Drozynski, C.A., Cormier, T.A., J.Nucl.Med., 26, 438, 1985.
- (54) Hennessy, C.M., Eccles, S.A., Dean, C., Coghlan, G., Eur.J.Nucl.Med., 11, 240, 1985.
- (55) Burchiel, S.W., Hadjian, R.A., Hladik, W.B., et al., J.Nucl.Med., 27, 896, 1986.
- (56) Kagi, J.H.R., Kojima, Y., Chemistry and Biochemistry of Metallothionein, in *Experientia Supplementum*, 52, 25, 1987.
- (57) Goodwin, D.A., Antibody, Immunoconjugates, and Radiopharmaceuticals, 4, 427, 1991.
- (58) Sands, H., Gallagher, B.M., Physiological Pharmacological, and Immunological Aspects of Antibody Targetting, in *Antibodies in Radiodiagnosis and Therapy*, Edited By Zalutsky, M.R., CRC Press Inc., p129, 1989.

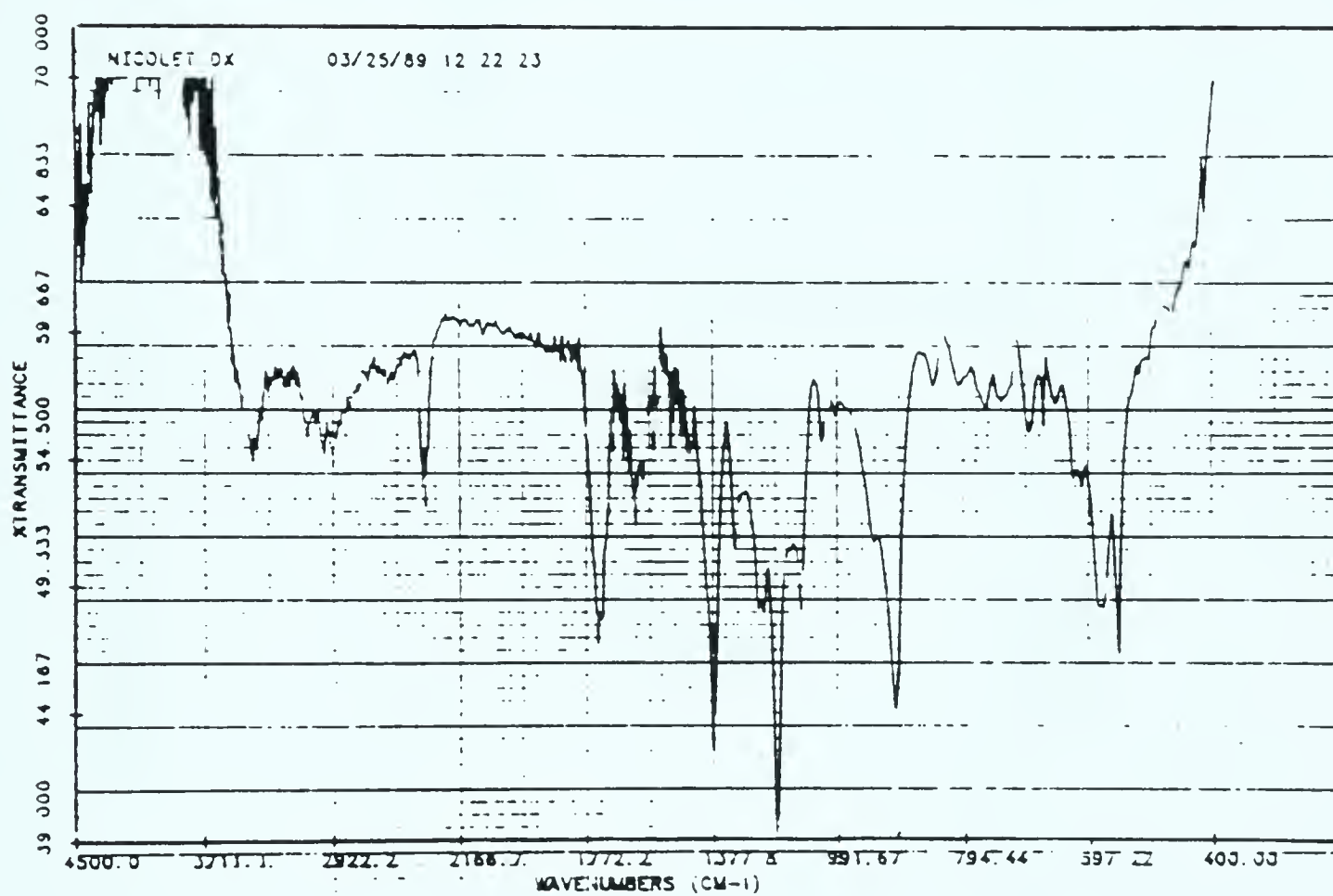
- (59) Buchsbaum, D.J., Lawrence, T.S., Targeted Diagnosis and Therapy, 3, 215, 1990.
- (60) Bosslet, K., Steinstraesser, A., Hermentin, P., et al., Br.J.Cancer, 63, 681, 1991.
- (61) Reardan, D.T., Mears, C.F., Goodwin, D.A., et al., Nature, 316, 265, 1985.
- (62) Bosslet, K., Hermentin, P., Kuhlmann, L., et al., Nucl.Med.Comm., 11, 704, 1990.
- (63) Goodwin, D.A., J.Nucl.Med., 28, 1358, 1987.
- (64) Paganelli, G., Malcovati, M., Fazio, F., Nucl.Med.Comm., 12, 211, 1991.
- (65) Kalofonos, H.P., Rusckowski, M., Siebecker, D.A., et al., J.Nucl.Med., 31, 1791, 1990.
- (66) Hnatowich, D.J., Virzi, F., Rusckowski, M., J.Nucl.Med., 28, 1294, 1987.
- (67) Maraveyas, A., Epenetos, A.A., Cancer Immunol.Immunother., 34, 71, 1991.
- (68) Rowlinson, G., Rusckowski, M., Gionet, M., et al., J.Nucl.Med., 29, 762, 1988.
- (69) Paganelli, G., Pervez, S., Siccardi, A.G., et al., Int.J.Cancer, 45, 1184, 1990.
- (70) Paganelli, G., Magnani, P., Zito, F., et al., Cancer Research, 51, 5960, 1991.
- (71) Pimm, M.V., Fells, H.F., Perkins, A.C., Baldwin, R.W., Nucl.Med.Comm., 9, 931, 1988.

- (72) Britton, K.E., Mather, S.J., Granowska, M., Nucl.Med.Comm., 12, 333, 1991.
- (73) Britton, K.E., Antibody, Immunoconjugates, and Radiopharmaceuticals, 4, 133, 1991.
- (74) Blumenthal, R.D., Sharkey, R.M., Goldenberg, D.M., Advanced Drug Delivery Reviews, 4, 279, 1990.
- (75) Sfakianakis, G.N., Garty, I.I., Serafini, A.N., Cancer Investigation, 8, 381, 1990.
- (76) Reilly, R.M., Clinical Pharmacy, 10, 359, 1991.
- (77) Ward, B.G., Mather, S.J., Hawkins, L.R., et al., Cancer Research, 47, 4719, 1987.
- (78) Ward, B.G., Wallace, K., Cancer Research, 47, 4719, 1987.
- (79) Chatal, J.F., Peltier, P., Bardies, M., et al., European J.of Nucl.Med., 19, 205, 1992.
- (80) Mosely, R.P., Davies, A.G., Richardson, R.B., et al., Br.J.Cancer, 62, 637, 1990.
- (81) Chatal, J.F., Saccavini, J.C., Gestin, J.F., et al., Cancer Research, 49, 3087, 1989.
- (82) Epenetos, A.A., The Practitioner, 228, 931, 1984.
- (83) Kalnicki, S., Bloomer, W.D., Antibody Radiotherapy : Current Status in Antibodies in Radiodiagnosis and Therapy, Edited by Zalutsky, M.R., CRC Press Inc., p201, 1989.
- (84) Alvarez, V.L., Lopez, A.D., Rodwell, J.D., McKearn, T.J., Stuart, F.P., Targeted Diagnosis and Therapy, 2, 99, 1989.

- (85) Tse, J., ^{153}Sm As a Potential Tumor Localizing Agent, Ph.D. Thesis, 1982.
- (86) Russel, P.J., Boniface, G.R., Izard, M.F., et al., Development of Animal Models to Assess Radioimmunoconjugates for the Treatment of Bladder Cancer, Unpublished Results.
- (87) Sinha, S.P., Complexes of the Rare Earths, Pergamon Press, 1966.
- (88) Moeller, T., The Chemistry of the Lanthanides, Reinhold Publishing Corporation, 1963.
- (89) Thompson, L.C., Complexes, in Handbook on the Physics and Chemistry of Rare Eaths, Edited by Gschneider, K.A., and Eyring, L., North-Holland Publishing Company, V3, p209, 1978.
- (90) Cotton, F.A., Wilkinson, G, Basic Inorganic Chemistry, John Wiley and Sons, p173, 1976.
- (91) Huheey, J.E., Inorganic Chemistry, Harper and Row Publishers, p804, 1983.
- (92) Stanley, E.C., Kinneberg, B.I., Varga, L.P., Anal.Chem., 38, 1362, 1966.
- (93) Sinha, A.P.B., Fluorescence and Laser Action in Rare Earth Chelates, in Spectroscopy in Inorganic Chemistry, Edited by Rao, R., p255, 1971.
- (94) Crosby, G.A., Whan, R.E., Alire, R.M., J. of Chem.Phys., 34, 743, 1961.
- (95) Crosby, G.a., Whan, R.E., Freeman, J.J., J.Phys.Chem., 66, 2493, 1962.
- (96) Alberti, G., Massucci, M.A., Anal.Chem., 38, 214, 1966.

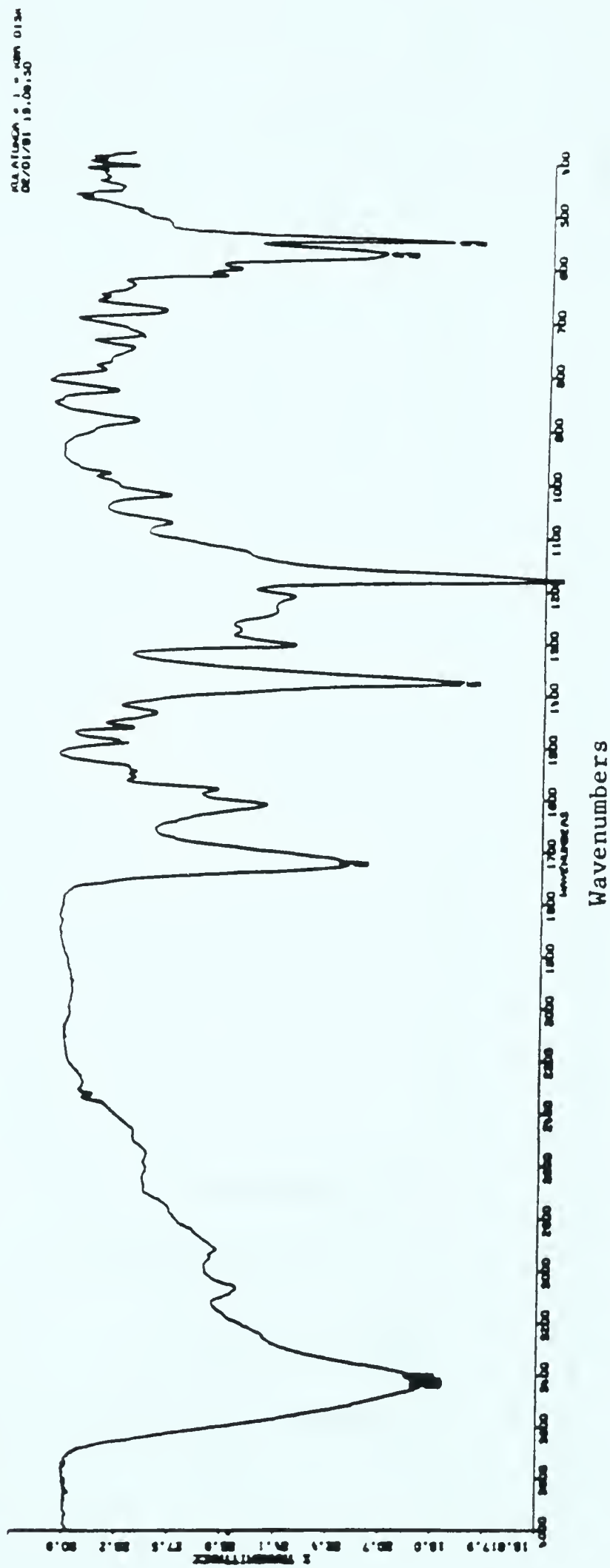
- (97) Haly, T.J., Toxicity, in Handbook on the Physics and Chemistry of Rare Earths, Edited by Gschneidner, K.A., Eyring, L., North-Holland Publishing Company, V4, p553, 1979.
- (98) Walker, K.Z., Boniface, G.R., Lightfoot, D.V., et al., Samarium-153 Labeled Monoclonal Antibody BCLA-38,
(1) Biodistribution Studies in a Nude Mouse Xenograft Model (unpublished results).
- (99) Lightfoot, D.V., Walker, K.Z., Boniface, G.R., et al., Samarium-153 Labeled Monoclonal Antibody BCLA-38,
(2) Therapeutic Studies in a Nude Mouse Xenograft Model (unpublished results).
- (100) Izard, M.E., Boniface, G.R., Hardiman, K.L., et al.,
Bioconjugate.Chem., 3, 346, 1992.
- (101) Boniface, G.R., Izard, M.E., Walker, K.Z., et al., J.Nucl.Med., 30, 683, 1989.
- (102) Goeckeler, W.F., Edwards, B., Volkert, W.A., Holmes, R.A., Simon, J., Wilson, D., J.Nucl.Med., 28, 495, 1987.
- (103) Goeckeler, W.F., Troutner, D.E., Volkert, W.A., Edwards, B., Simon, J., Wilson, D., Nucl.Med.Biol., 13, 479, 1986.
- (104) Turner, J.H., Martindale, A.A., Sorby, P., et al., Eur.J.Nucl.Med., 15, 784, 1989.
- (105) Lattimer, J.C., Corwin, L.A., Stapleton, J., et al., J.Nucl.Med., 31, 1316, 1990.
- (106) Lattimer, J.C., Corwin, L.A., Stapleton, J., et al., J.Nucl.Med., 31, 586, 1990.
- (107) Singh, A., Holmes, R.A., Farhangi, M., et al., J.Nucl.Med., 30, 1814, 1989.

- (108) Turner, C., A Comparative Study of Radiochelated and Radioiodinated Monoclonal Antibodies, M.Sc., Thesis, p44, 1986.
- (109) Schenk, G.H., Molecular Fluorescence and Phosphorescence, in Instrumental Analysis, Edited by Bauer, H.H., Christian, G.D., O'Reilly, J.E., Allyn and Bacon Inc., p228, 1978.
- (110) Kotrly, S., Sucha, L., Handbook of Chemical Equilibria in Analytical Chemistry, Ellis Horwood Limited, 1985.
- (111) Wheelwright, E.J., Spedding, F.H., Schwarzenbach, G., J.A.Chem.Soc., 75, 4196, 1953.
- (112) Critical Stability Constants, Edited by Martell, A.E., Smith, R.M., Plenum Press V3, p162, 1974.
- (113) Schomacker, K, Mocker, D., Munze, R., Beyer, G.J., Appl.Radiat.Isot., 39, 261, 1988.
- (114) Wahl, R.L., Wissing, J., Rosario, Renato del, Zasadny, K.R., J.Nucl.Med., 31, 84, 1990.
- (115) Reichstein, E., Shami, Y., Ramjeesingh, M., Diamandis, E.P., Anal.Chem., 60, 1069, 1988.
- (116) He, X.M., Carter, D.C., Nature, 358, 209, 1992.

Appendix (1)Spectrum 1IR Spectrum of Compound (4)- 1st Preparation

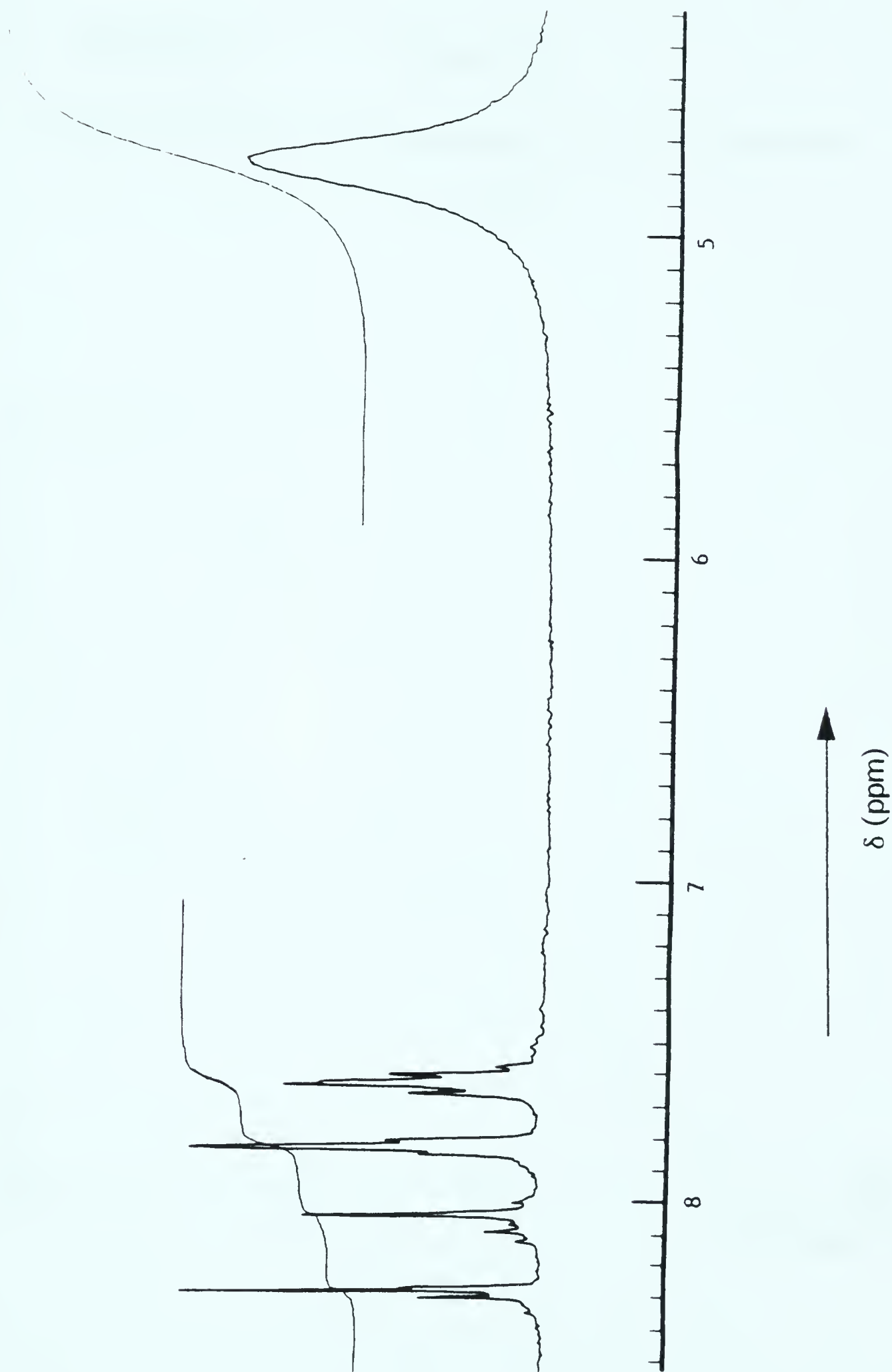
Appendix (1) Spectrum 2 IR Spectrum of Compound (4) 5th Preparation

% Transmittance



Appendix (1) Spectrum 3

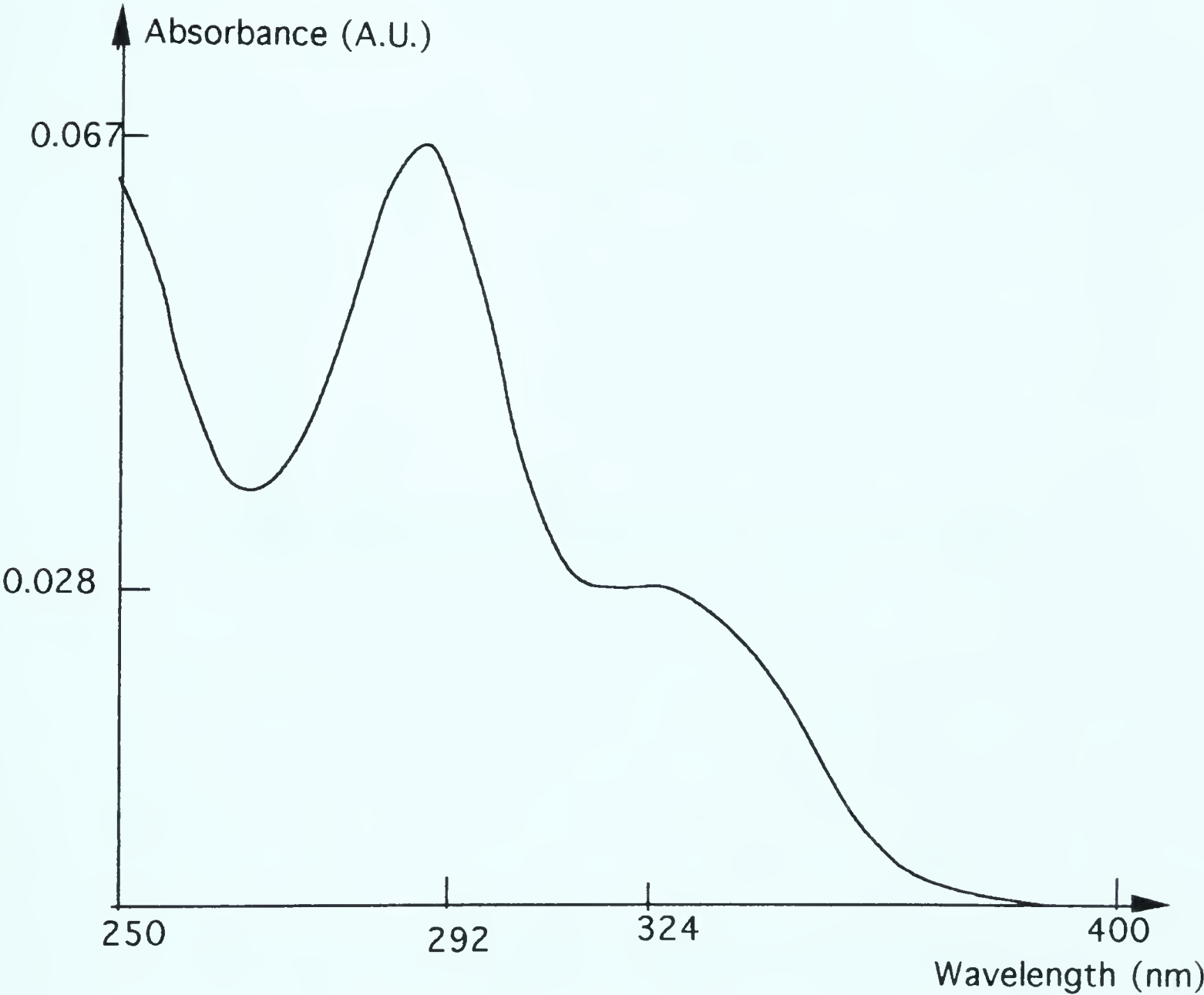
¹H NMR Spectrum of Compound (4)-5th Preparation

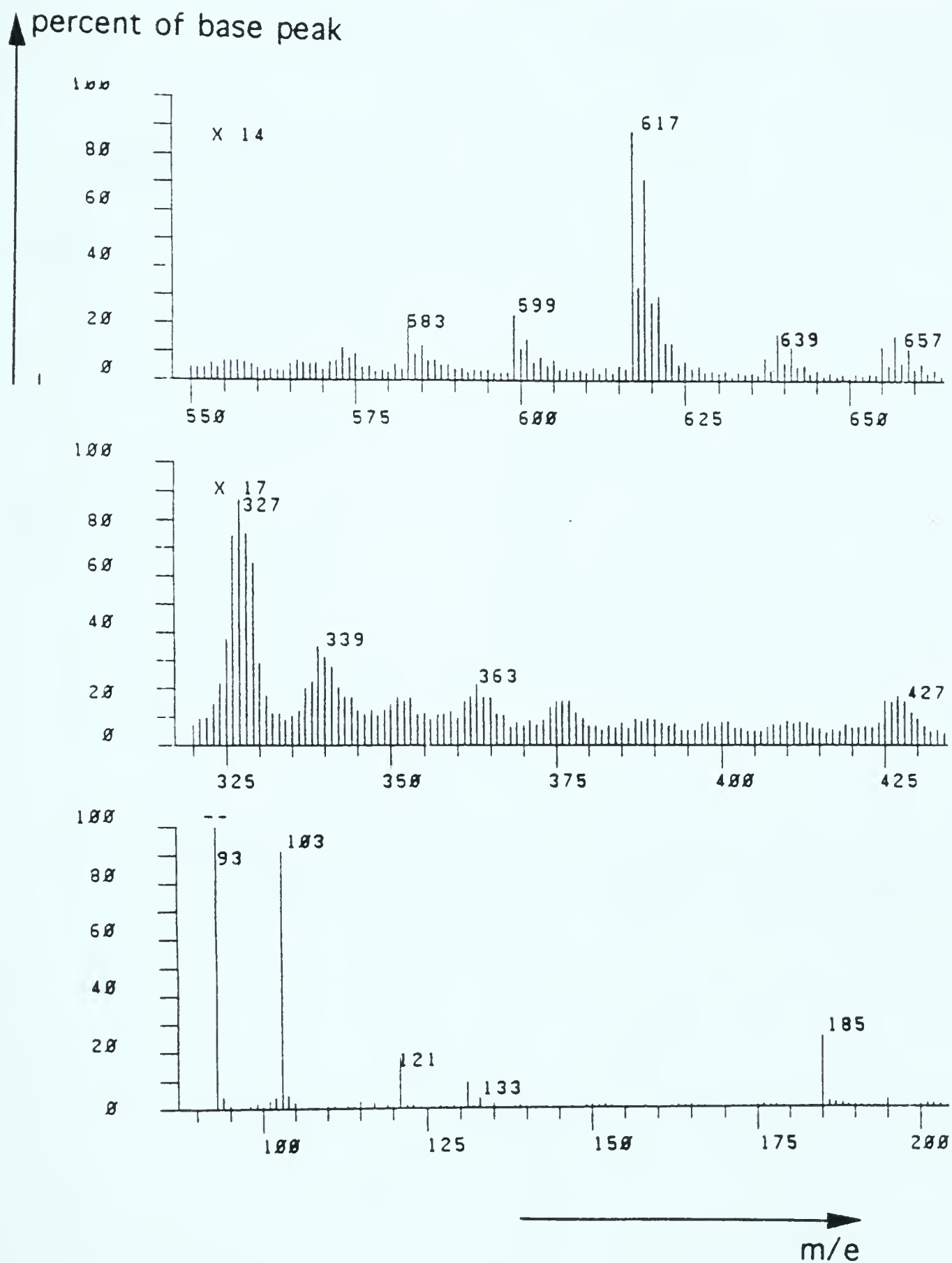


Appendix (1)

Spectrum 4

UV Spectrum of Hydrolysed Compound (4) - 5th Preparation
(10⁻⁶M in Tris Buffer)

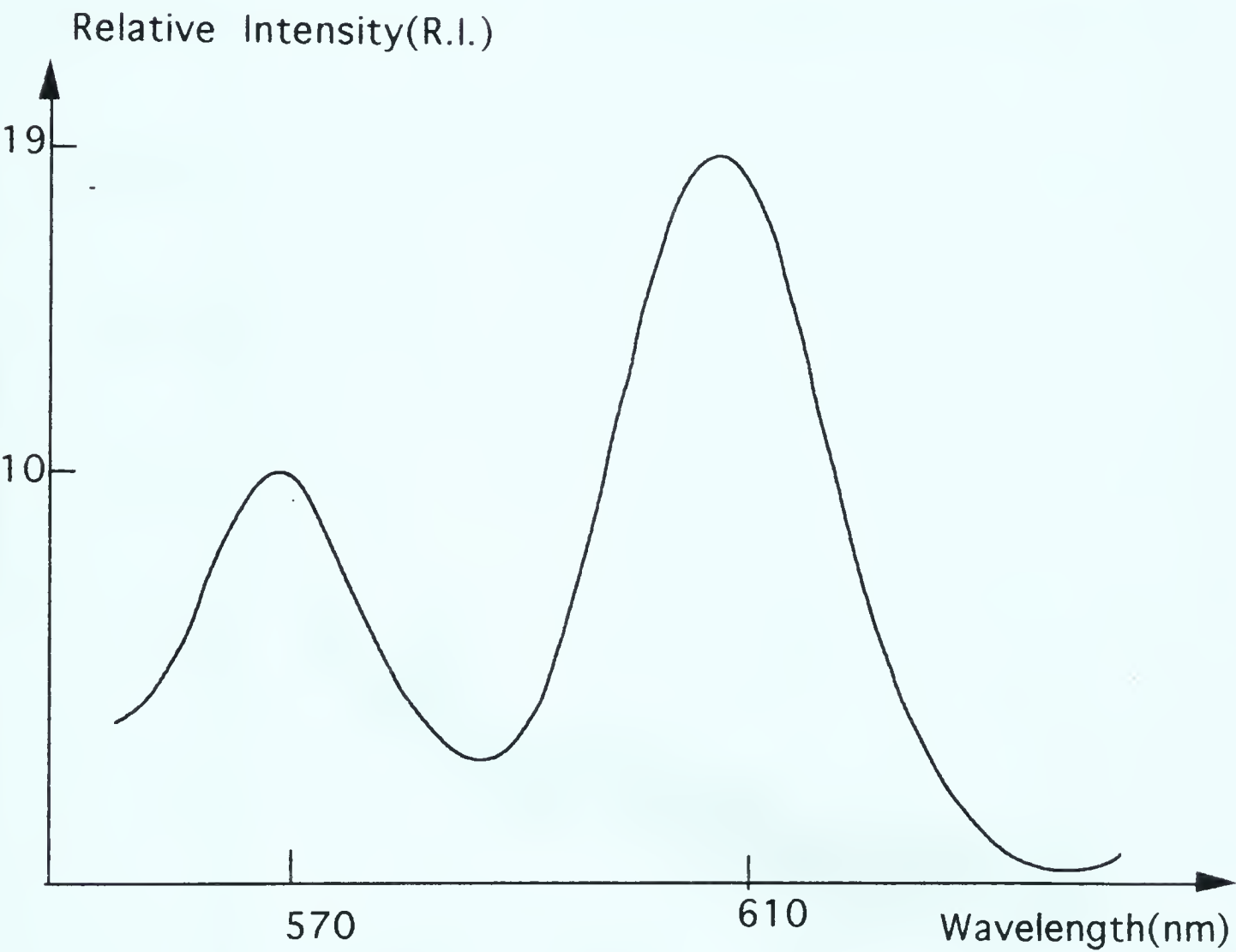


Appendix (1)Spectrum 5FAB Mass Spectrum of Compound (4)- 5th Preparation

Appendix (1)

Spectrum 6

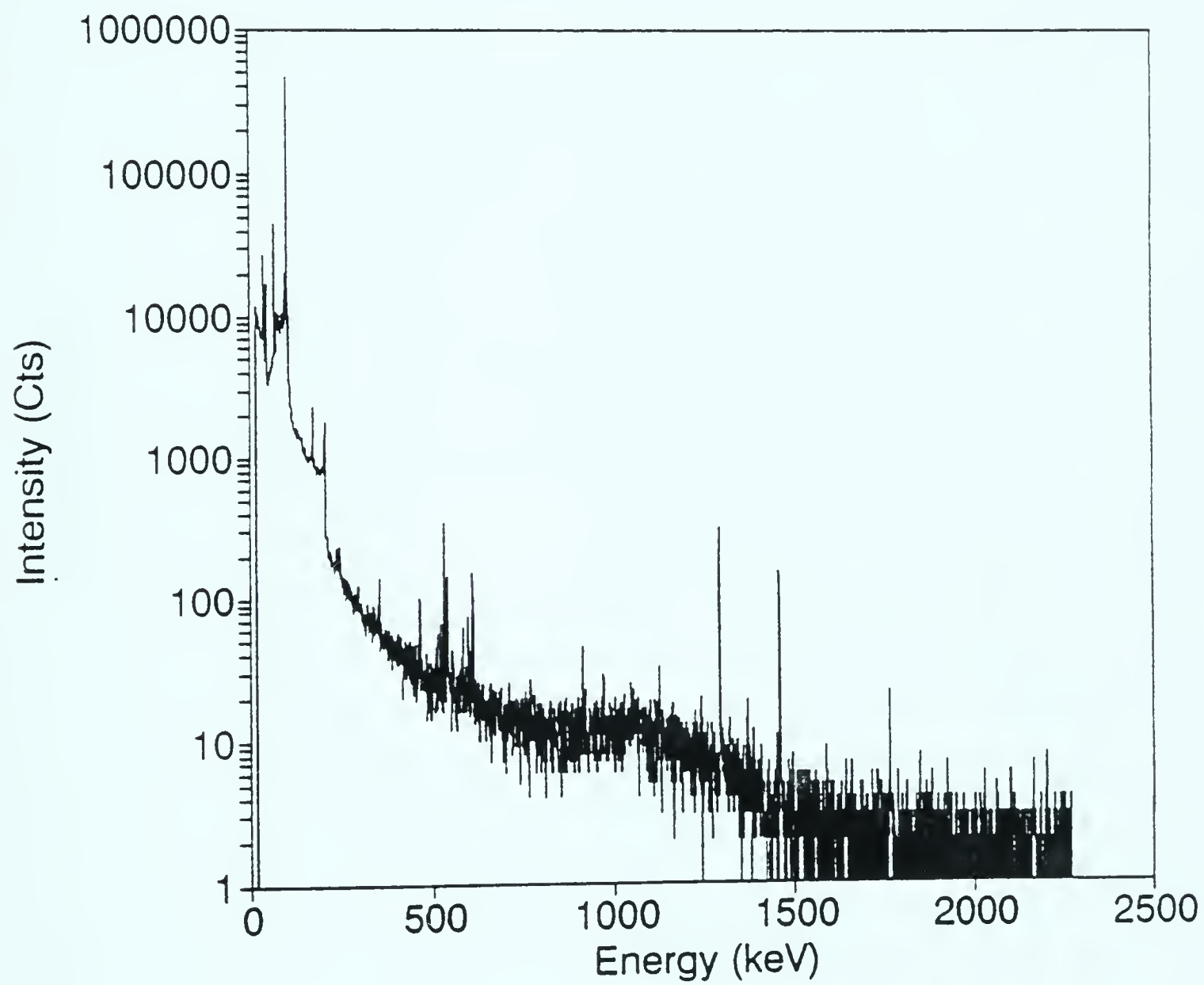
Fluorescence Spectrum of a Sm-BCPDA Complex (10^{-5} M) in Tris Buffer

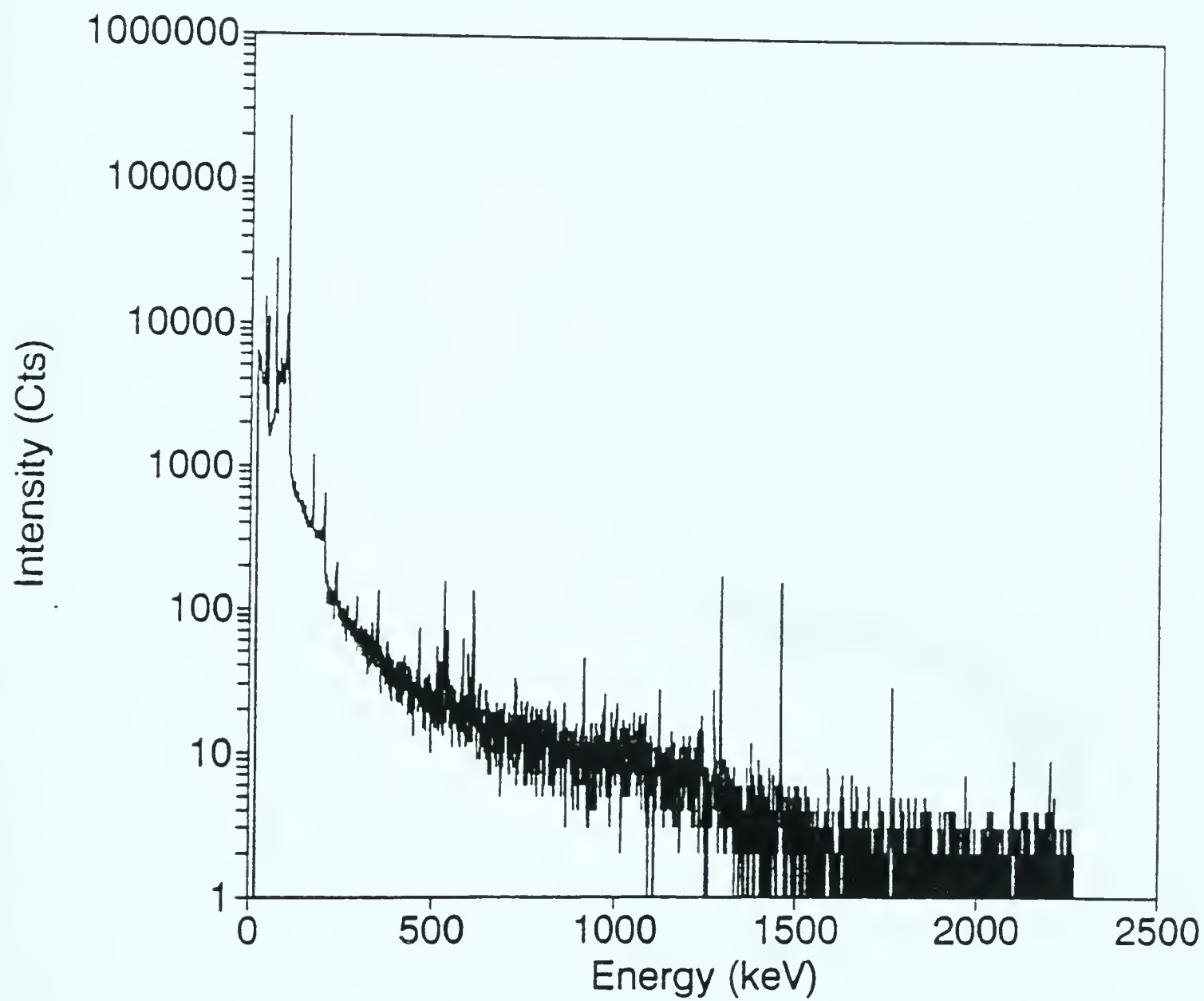


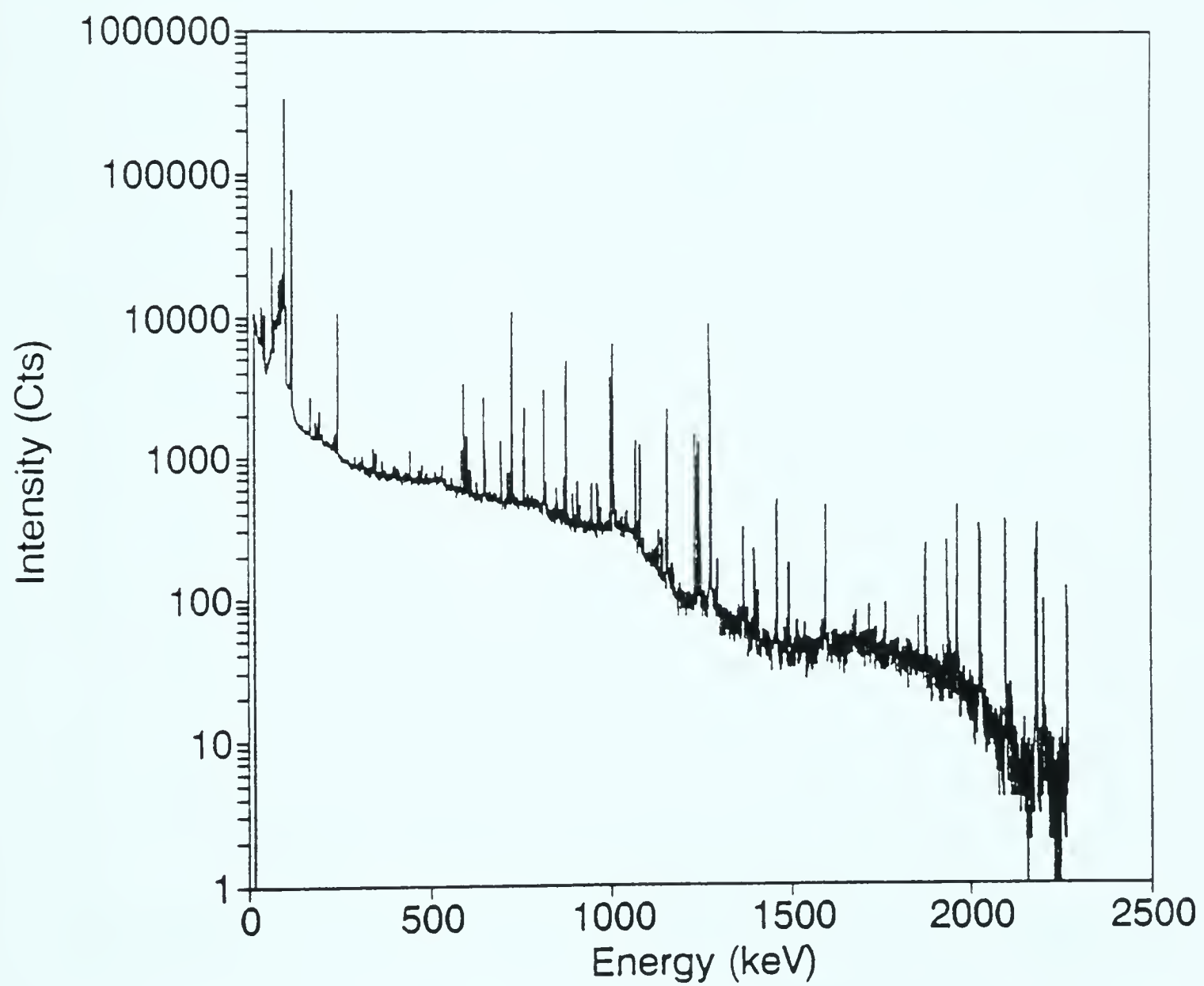
Appendix (1)

Spectrum 7

Gamma Spectrum of $^{153}\text{Sm}_2\text{O}_3$



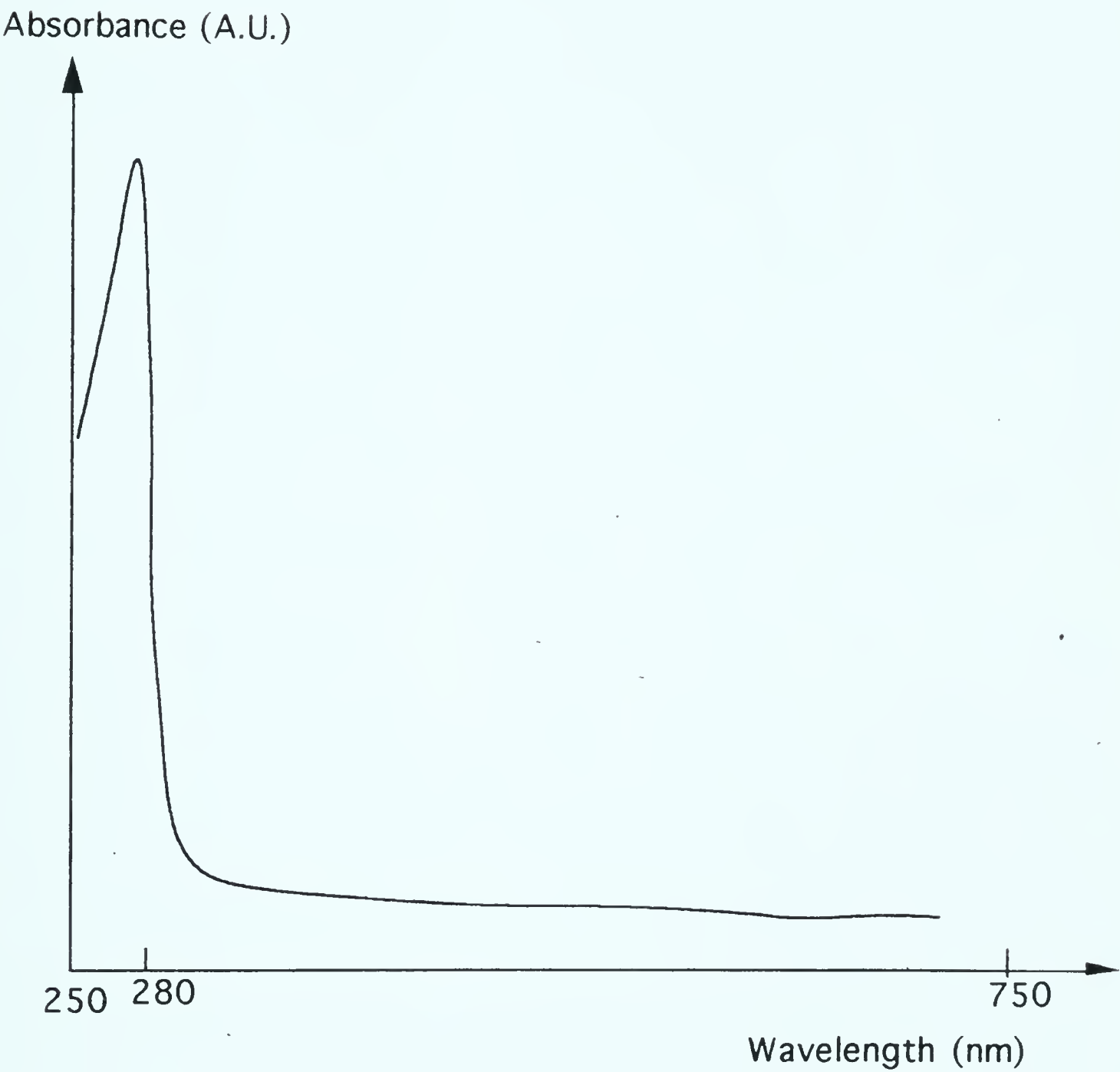
Appendix (1)Spectrum 8Gamma Spectrum of a New Sample of $^{153}\text{SmCl}_3$ 

Appendix (1)Spectrum 9Gamma Spectrum of an Old Sample of $^{153}\text{SmCl}_3$ 

Appendix (1)

Spectrum 10

UV Spectrum of HSA



University of Alberta Library



0 1620 0123 0810

B44940